

# Force transmission and fabric anisotropy

Farhang Radjai (DR CNRS)

Laboratoire de Mécanique et Génie Civil (LMGC)  
CNRS - Université Montpellier 2



# Outline

Introduction: granular disorder

Force distributions

Statistical models

Stress tensor

Fabric variables

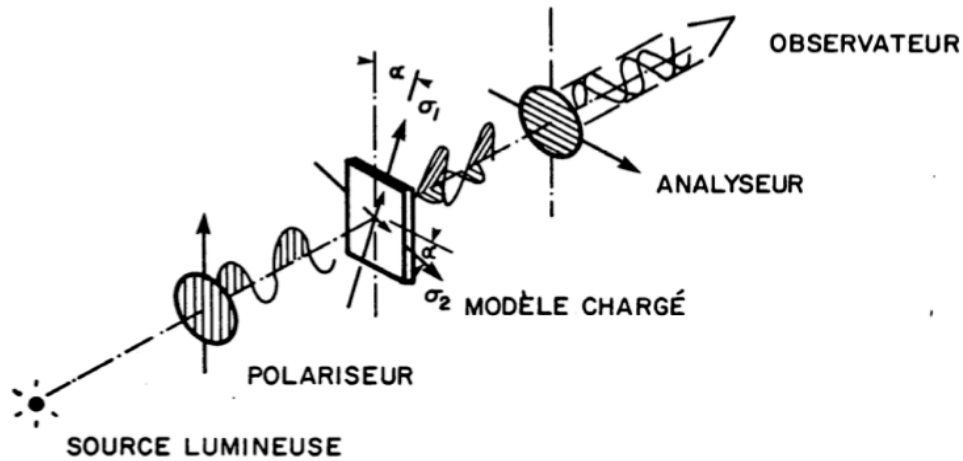
Harmonic decomposition

Bimodal nature of force networks

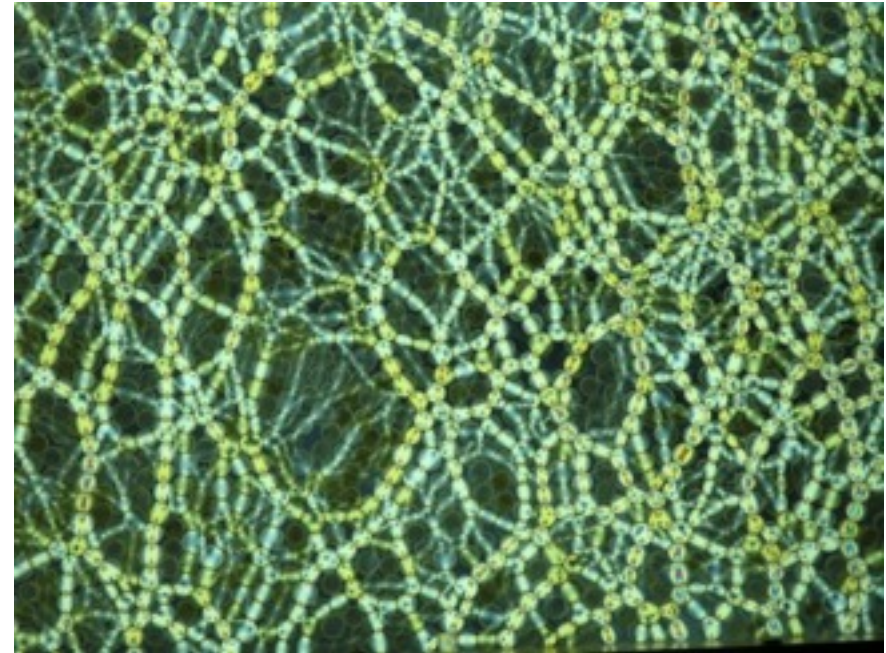
Concluding remarks

# Force distributions

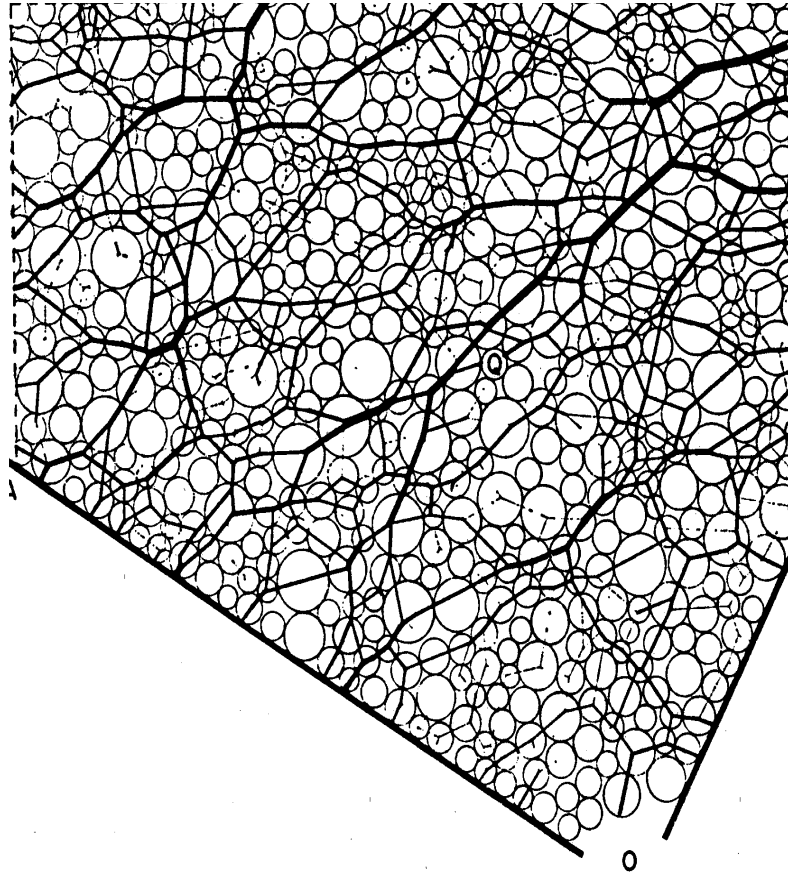
Dantu (1957)



Behringer et al. (1999)

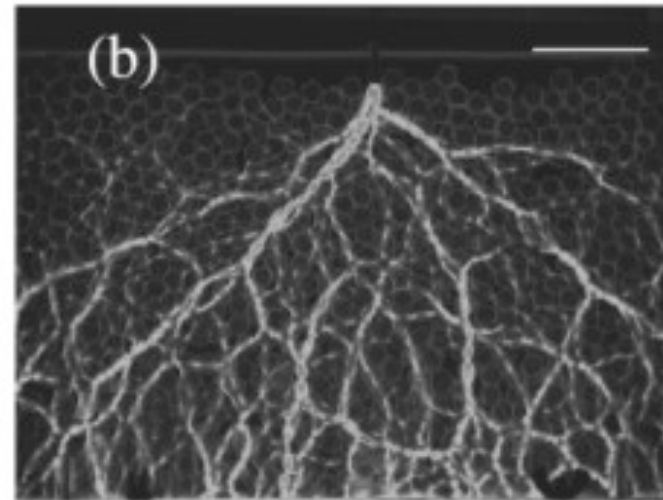
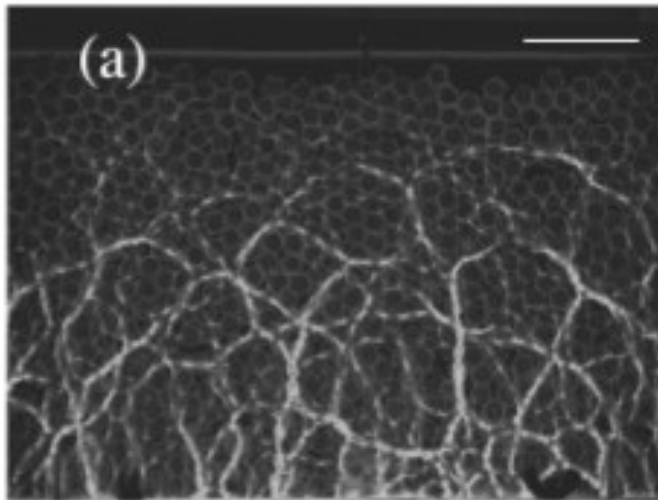


Photoelastic visualization of stressed particles.  
More loaded particles are brighter.



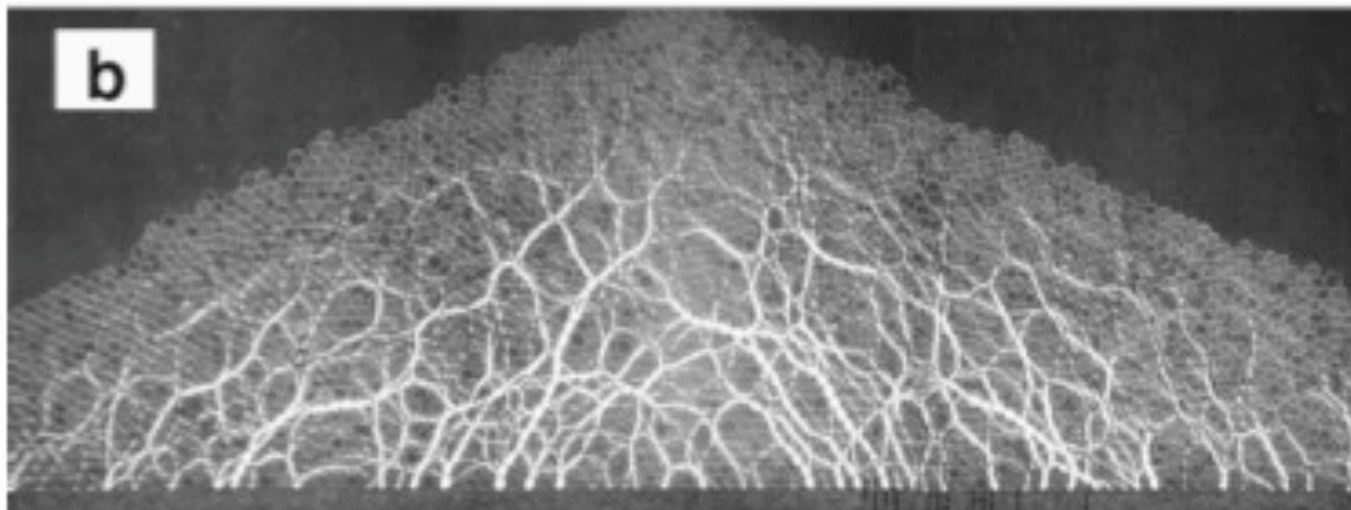
A. Drescher, G. de Josselin de Jong (1972)

The line width is proportional to the force.



Point load

E. Clément et al. (2002)

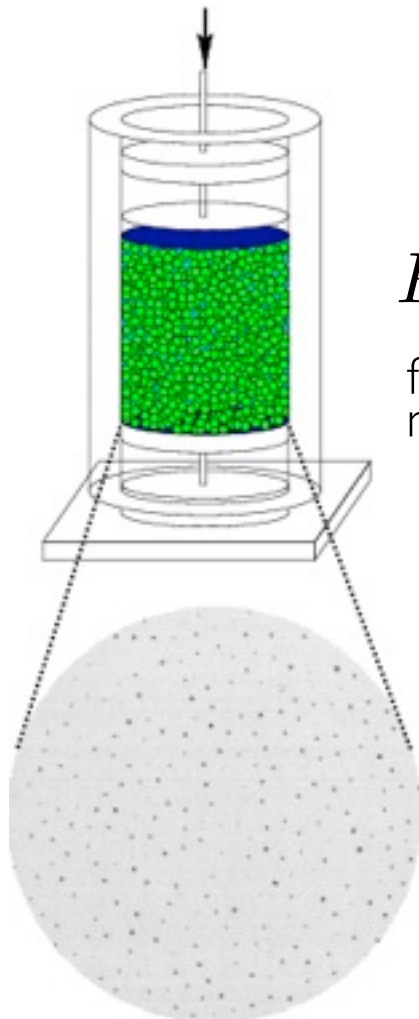


Pile

B. Behringer et al. (2002)

## Carbon-paper technique

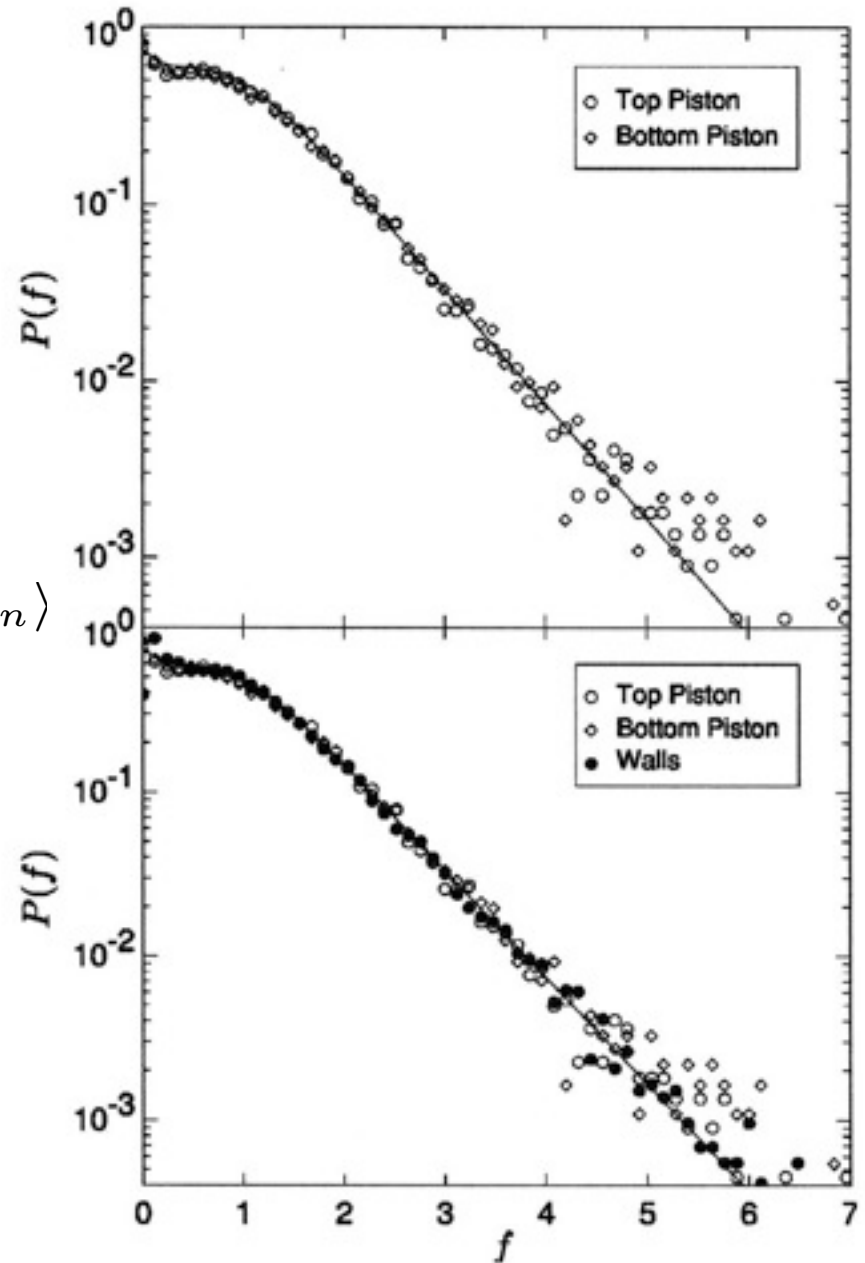
The trace left by a carbon paper interposed between a particle and a white paper is an increasing function of the magnitude of the contact force.



$$P_n(f_n) \propto e^{-\beta f_n / \langle f_n \rangle}$$

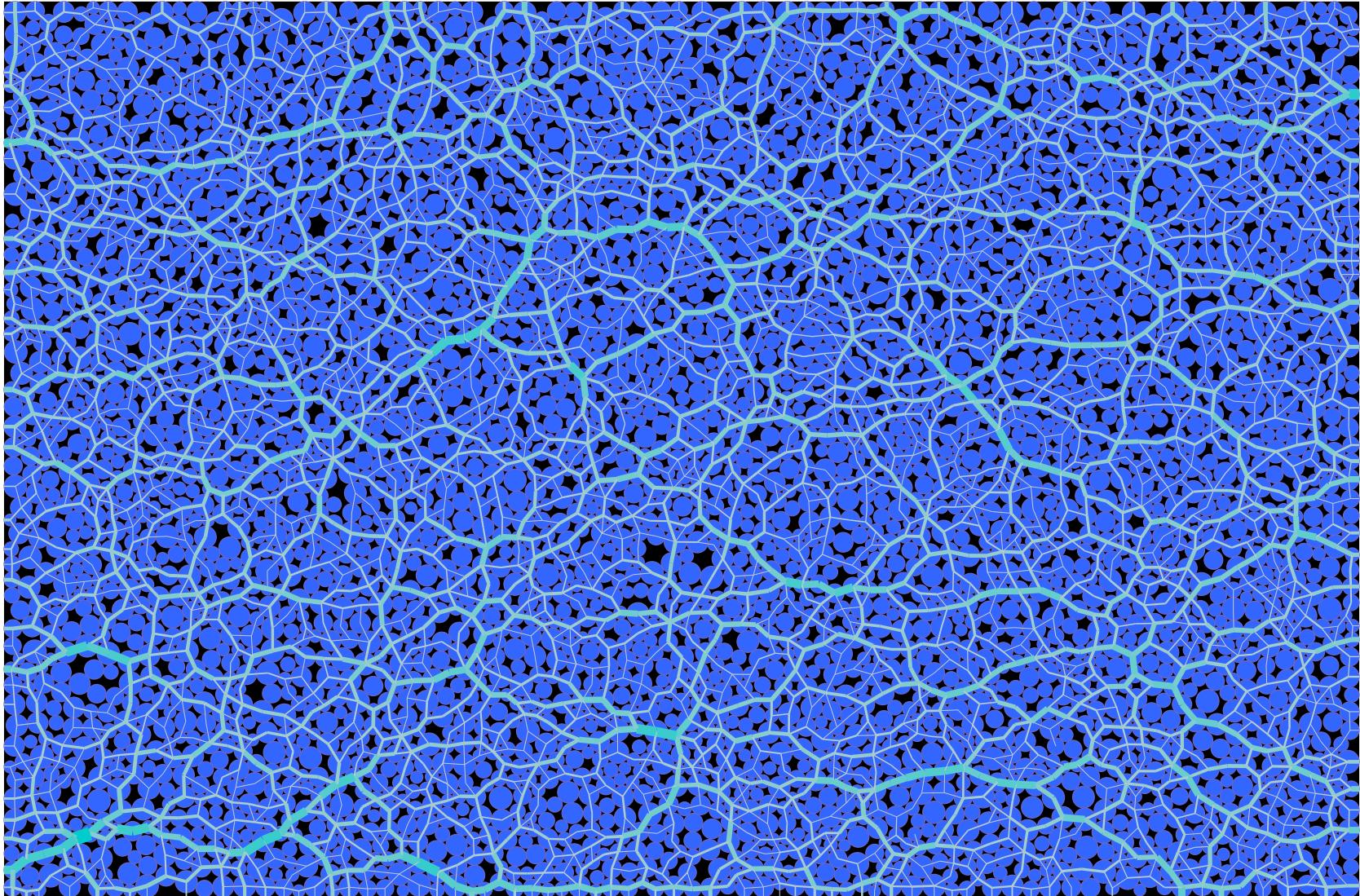
for forces above the mean force

Liu et al. (1995)

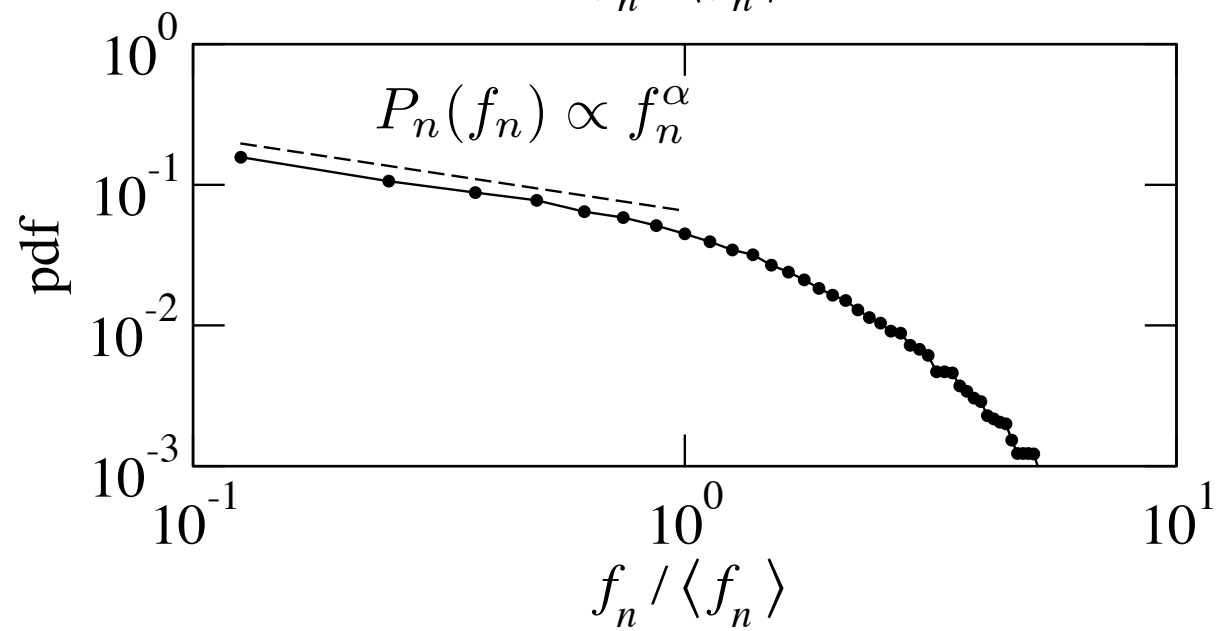
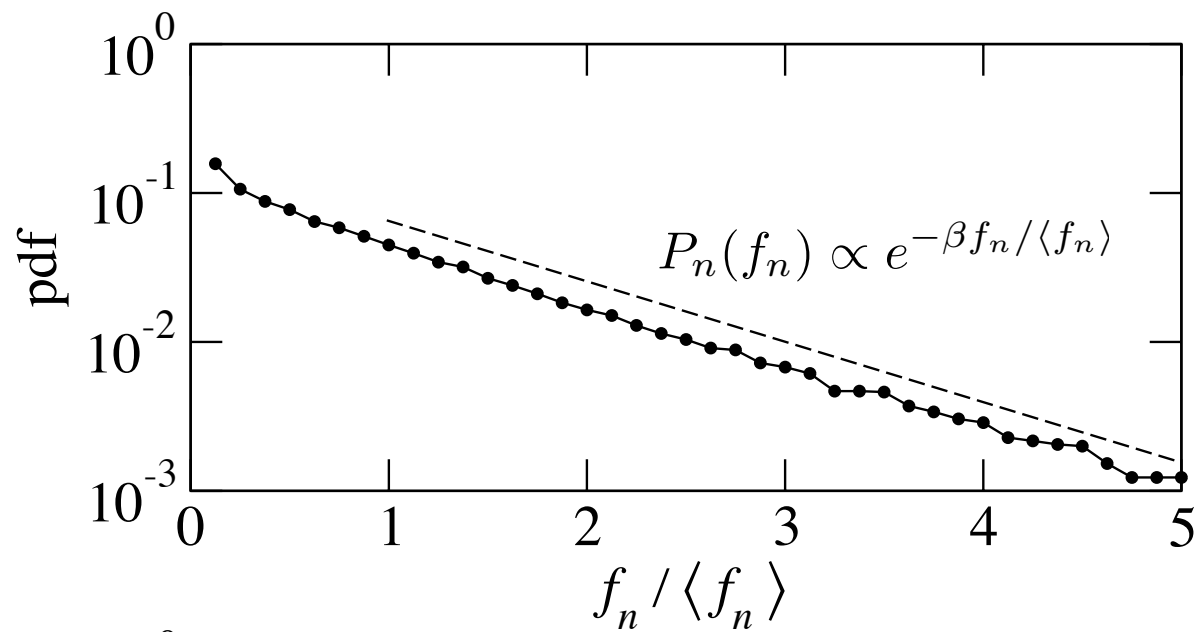


Mueth et al. (1998)

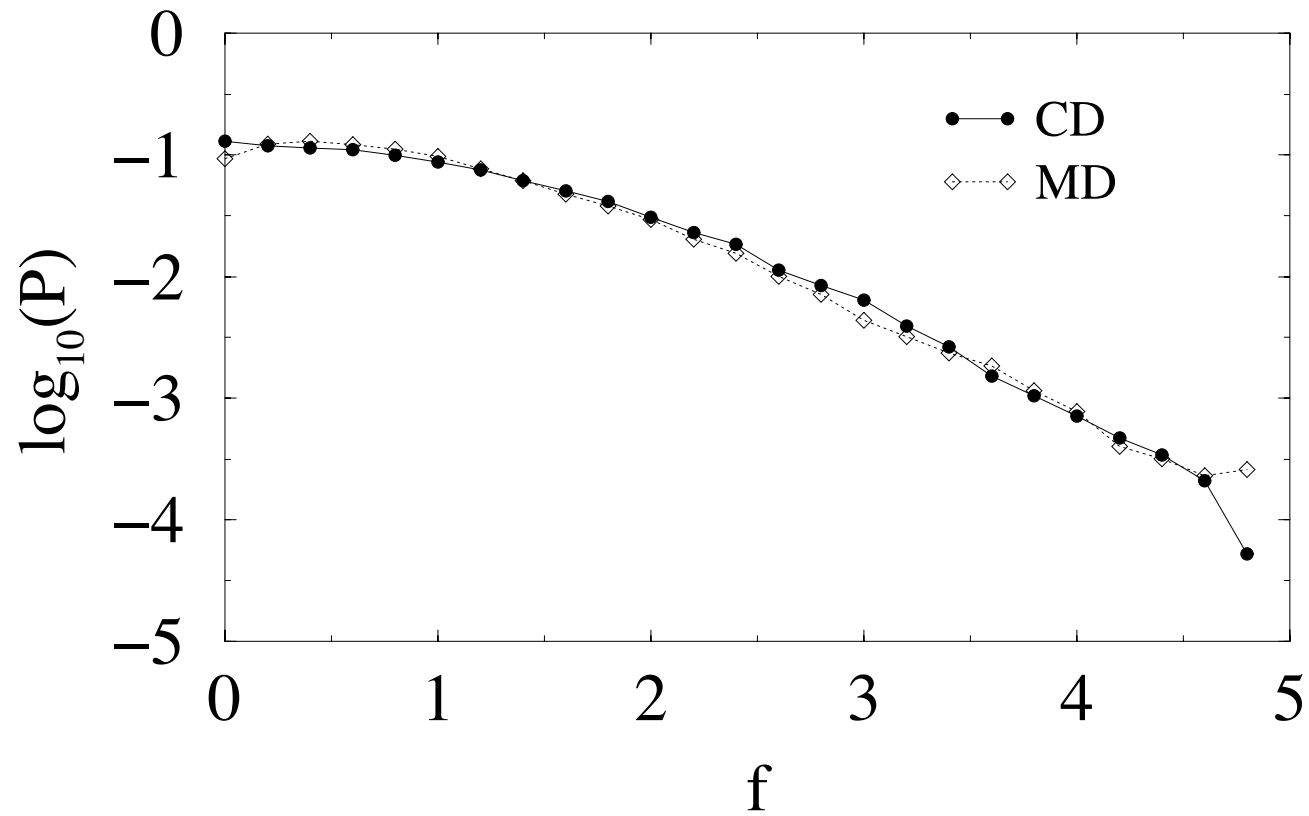
## Numerical simulations



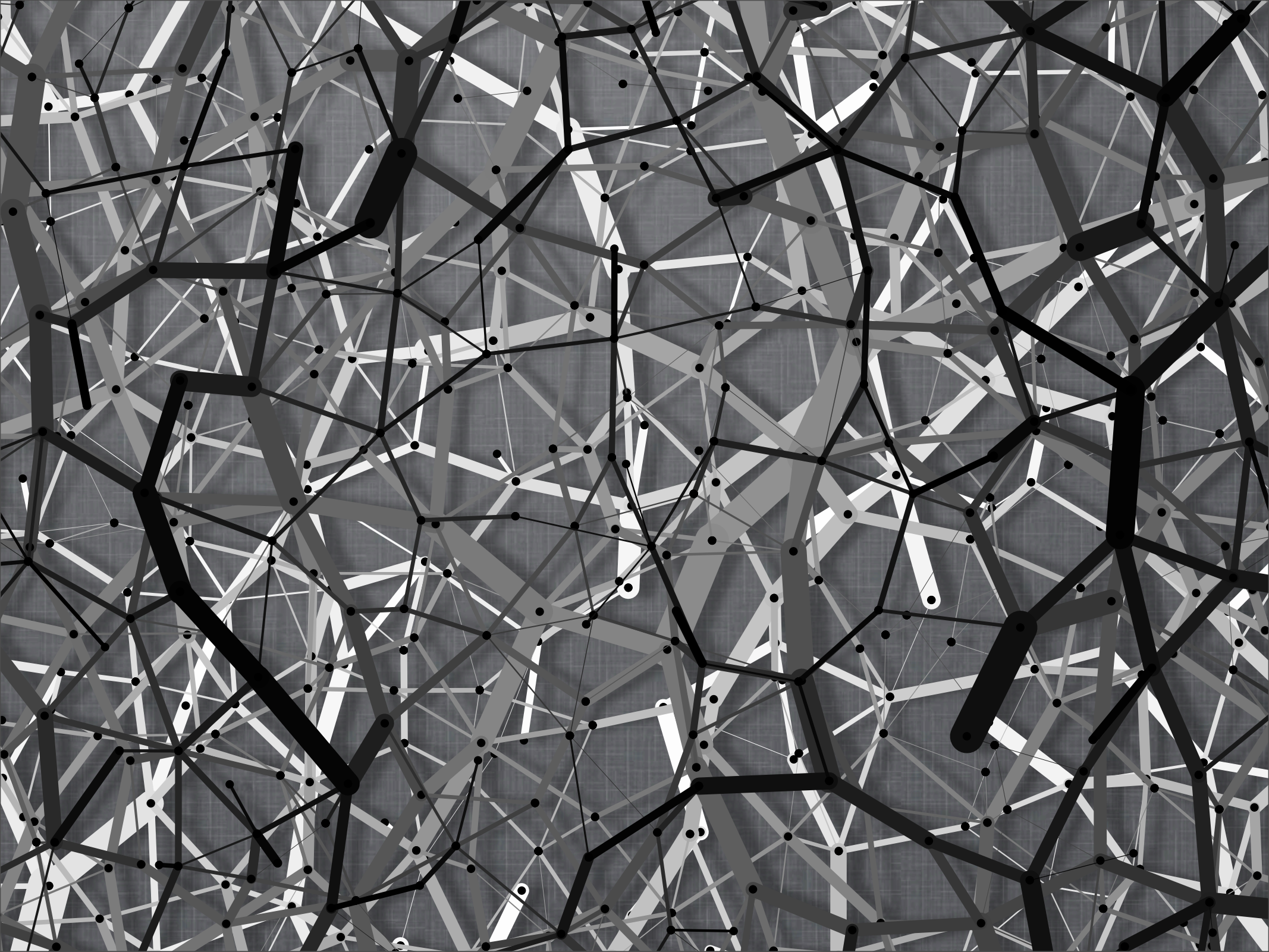
Radjai et al. (1995)



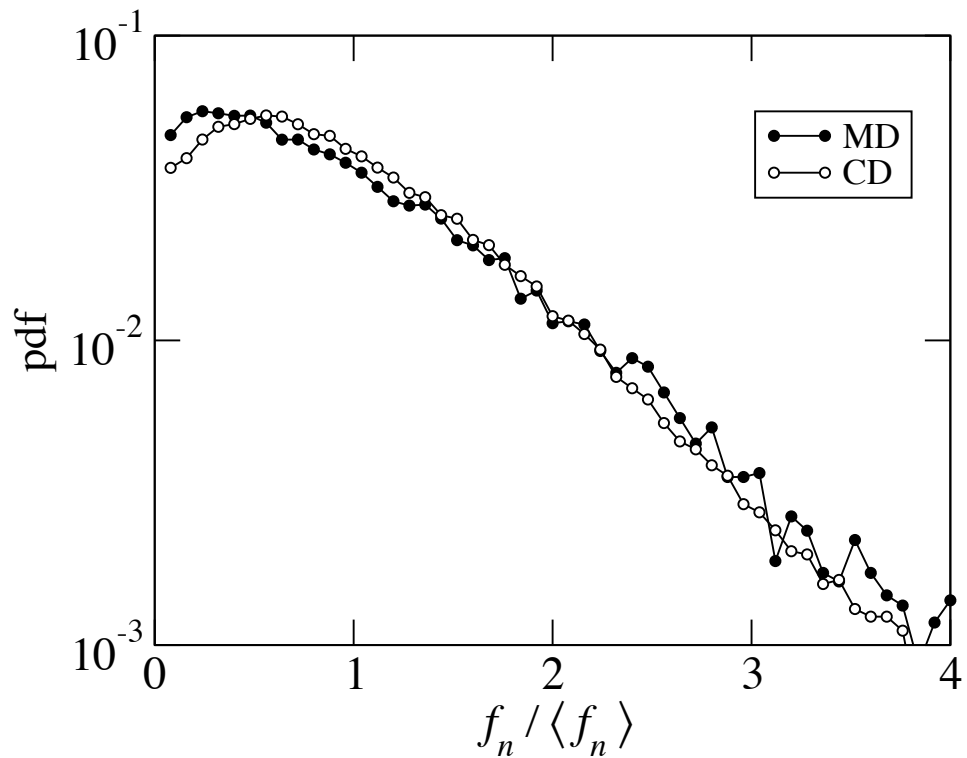




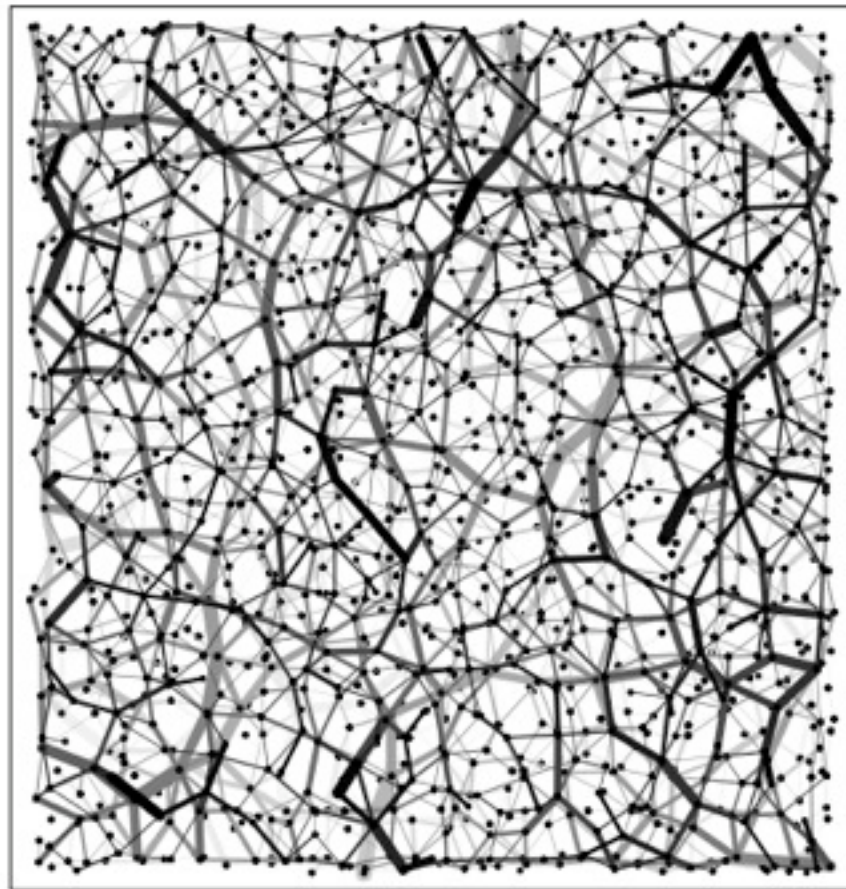
Force pdf by molecular dynamics and contact dynamics simulations.



3D



Richefeu et al. (2007)



Forces in a thin layer of a 3D packing.

Hybrid functional form:

$$h(x; \alpha, \beta) = A \begin{cases} x^{-\alpha} & x < 1 \\ e^{\beta(1-x)} & x > 1 \end{cases}$$

with  $\frac{1}{A} = \frac{1}{1-\alpha} + \frac{1}{\beta}$

$$\int_0^{\infty} h \, dx = 1 \qquad \int_0^{\infty} x h(x) dx = 1$$

$$\Rightarrow \beta^2 = (1-\alpha)(2-\alpha)$$

$$P_n(f_n) = h\left(\frac{f_n}{\langle f_n \rangle}; \alpha_n, \beta_n\right) \quad \langle f_n \rangle \quad \text{average normal force}$$

For an isotropic weakly polydisperse noncohesive system:

$$\alpha_n \simeq 0 \quad \beta_n = \sqrt{2} \simeq 1.4$$

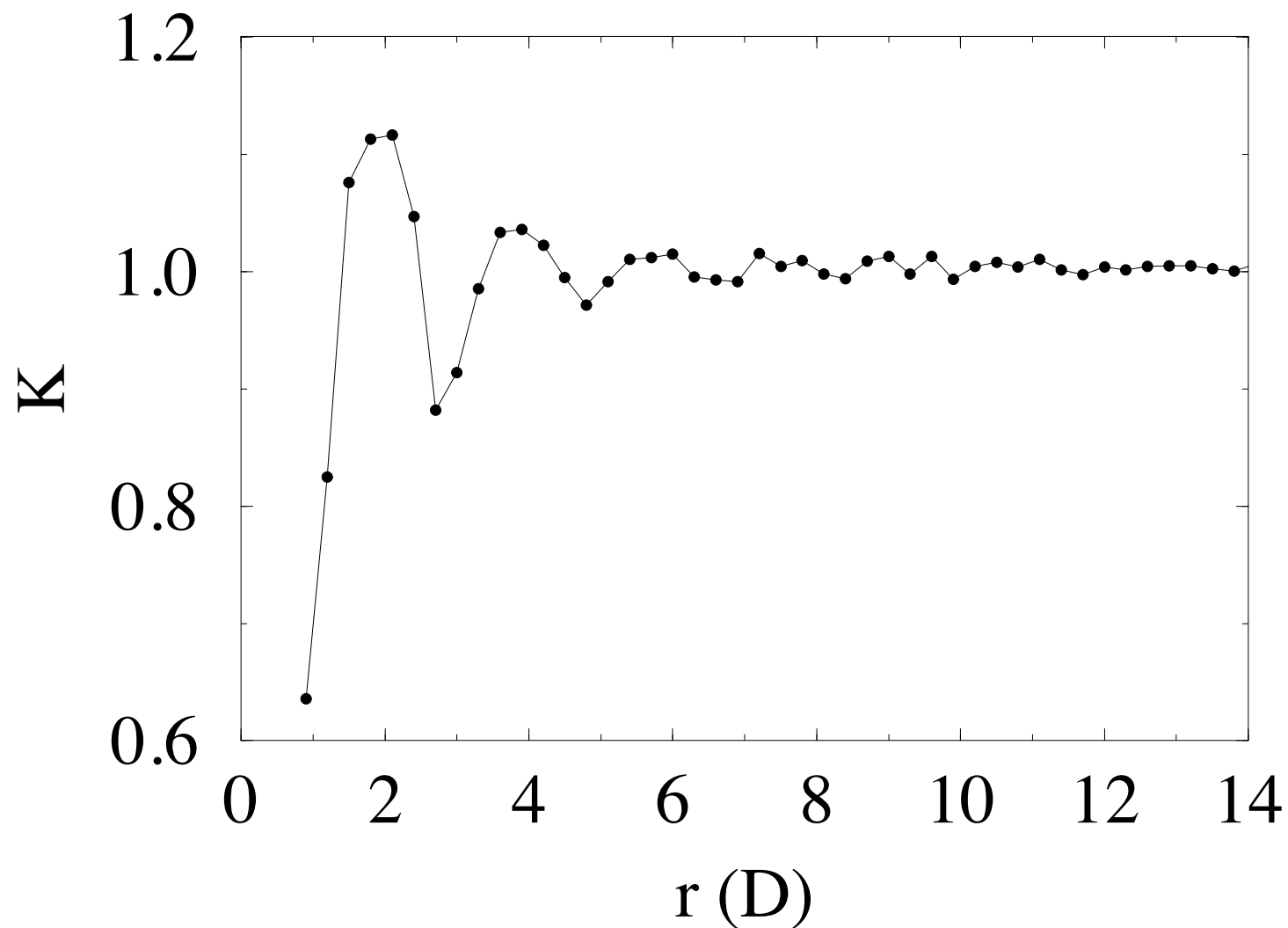
**Contribution of the weak network:**

$$h(x < 1) = \int_0^1 h(x) dx = \frac{1}{1 + \sqrt{\frac{1-\alpha}{2-\alpha}}}$$

$$\Rightarrow h(f_n < \langle f_n \rangle) \simeq 0.6$$

**60% of contacts have a force below the mean**

## Force-force correlations



$$K(r) = \frac{\langle f^i f^j \rangle_{\mathcal{S}}}{\langle f^2 \rangle}$$

$$\mathcal{S}(r) = \{i, j / (\vec{r}^i - \vec{r}^j)^2 = r^2\}$$

The forces below and above the mean force have different distributions. Most contact forces are below the mean force.

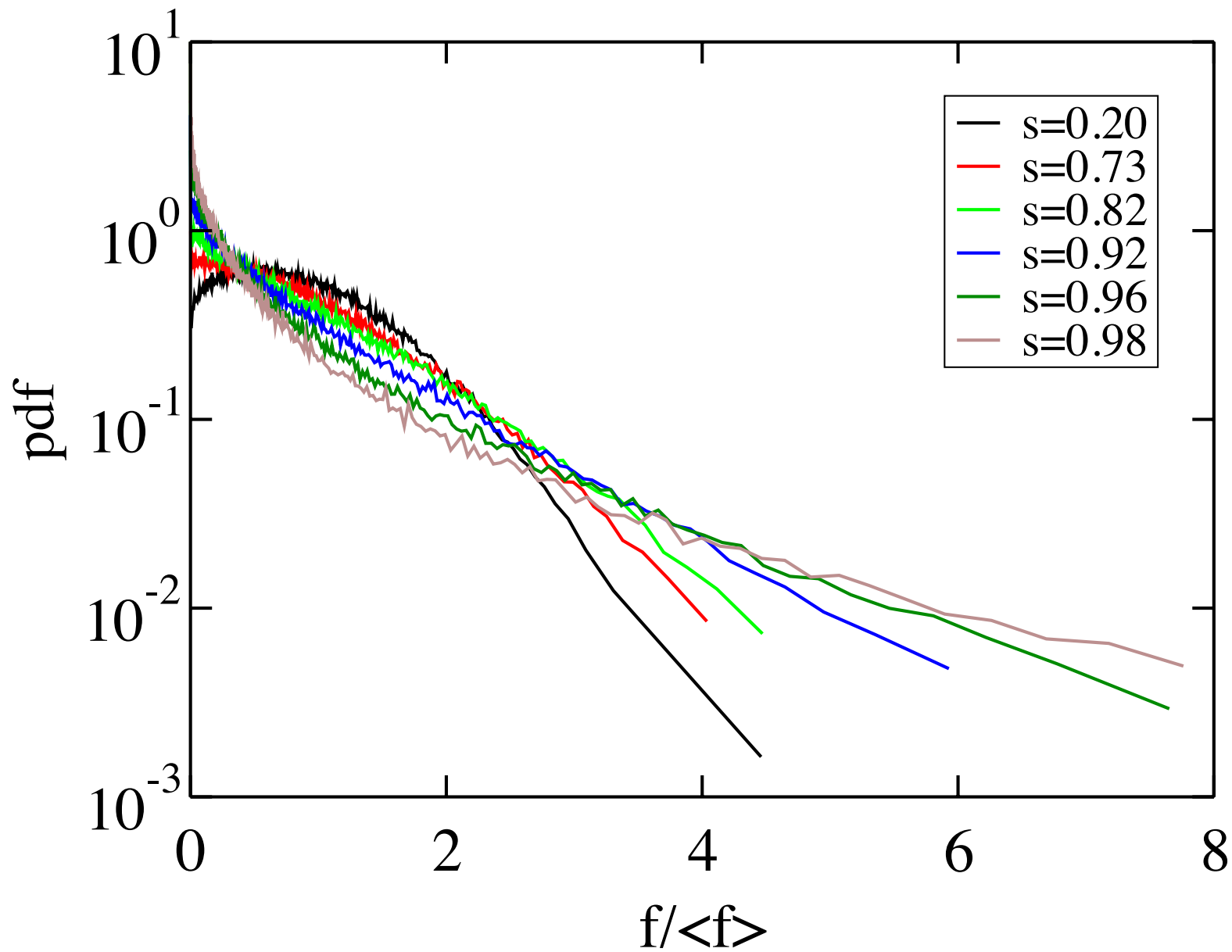
The force probability density does not tend to zero as the force declines to zero. The weak forces are as frequent as the forces around the mean.

The force distributions are exponentially broad and show no or weak central tendency.

The forces are correlated over several particle diameters (force chains).

How robust are the force distributions with respect to size polydispersity, particle shapes and cohesive interactions?

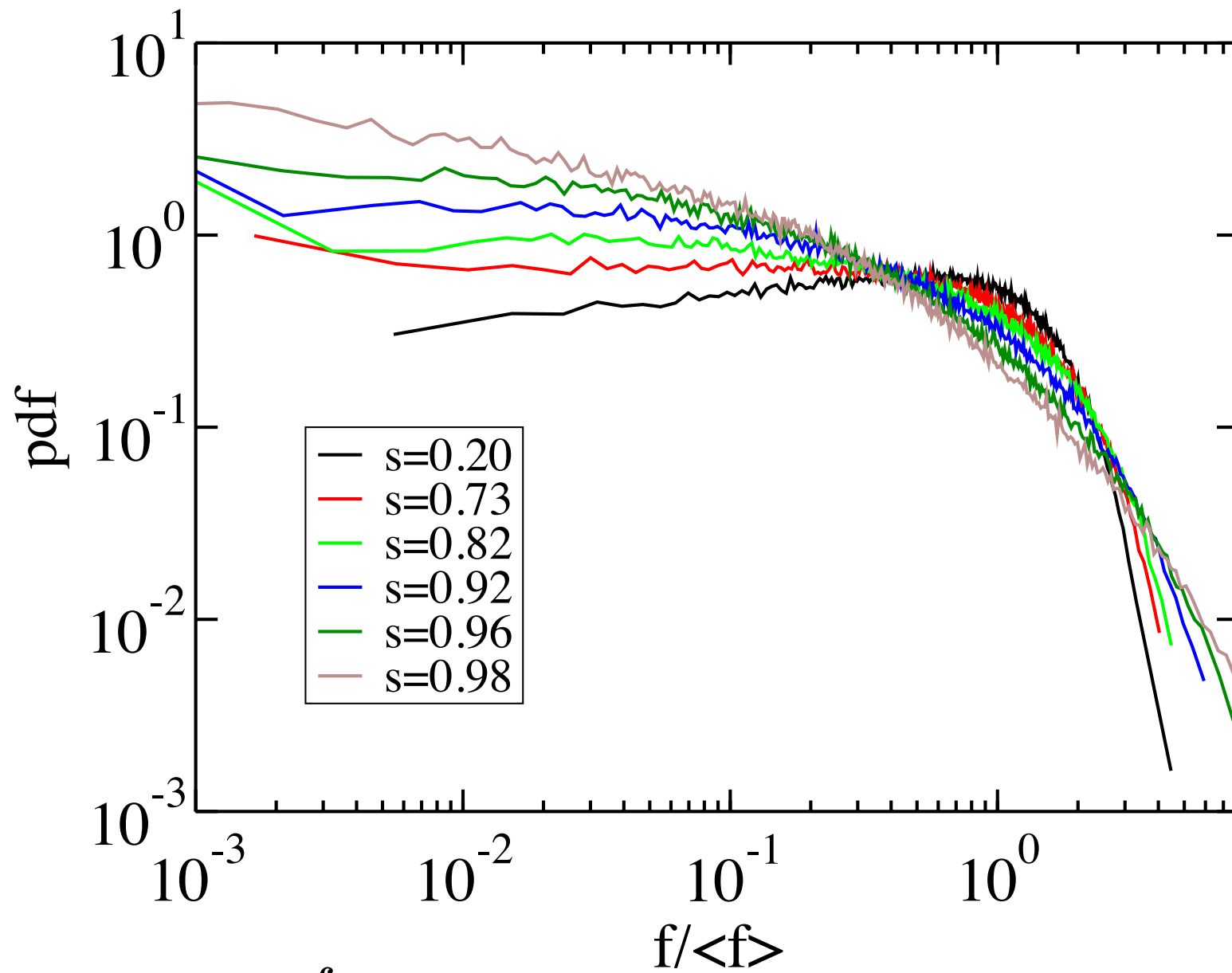
# Effect of size polydispersity



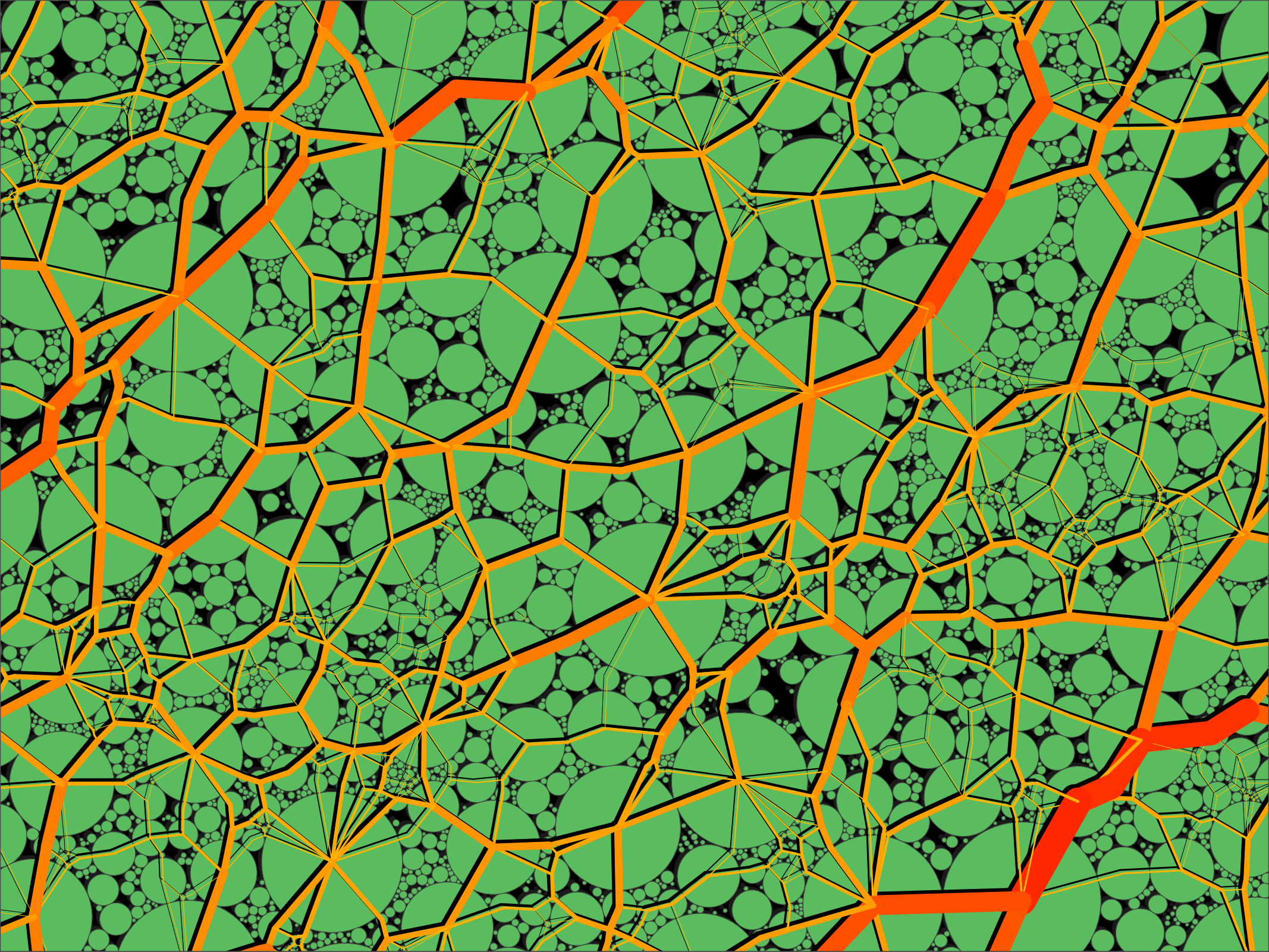
Voivret et al. (2008)

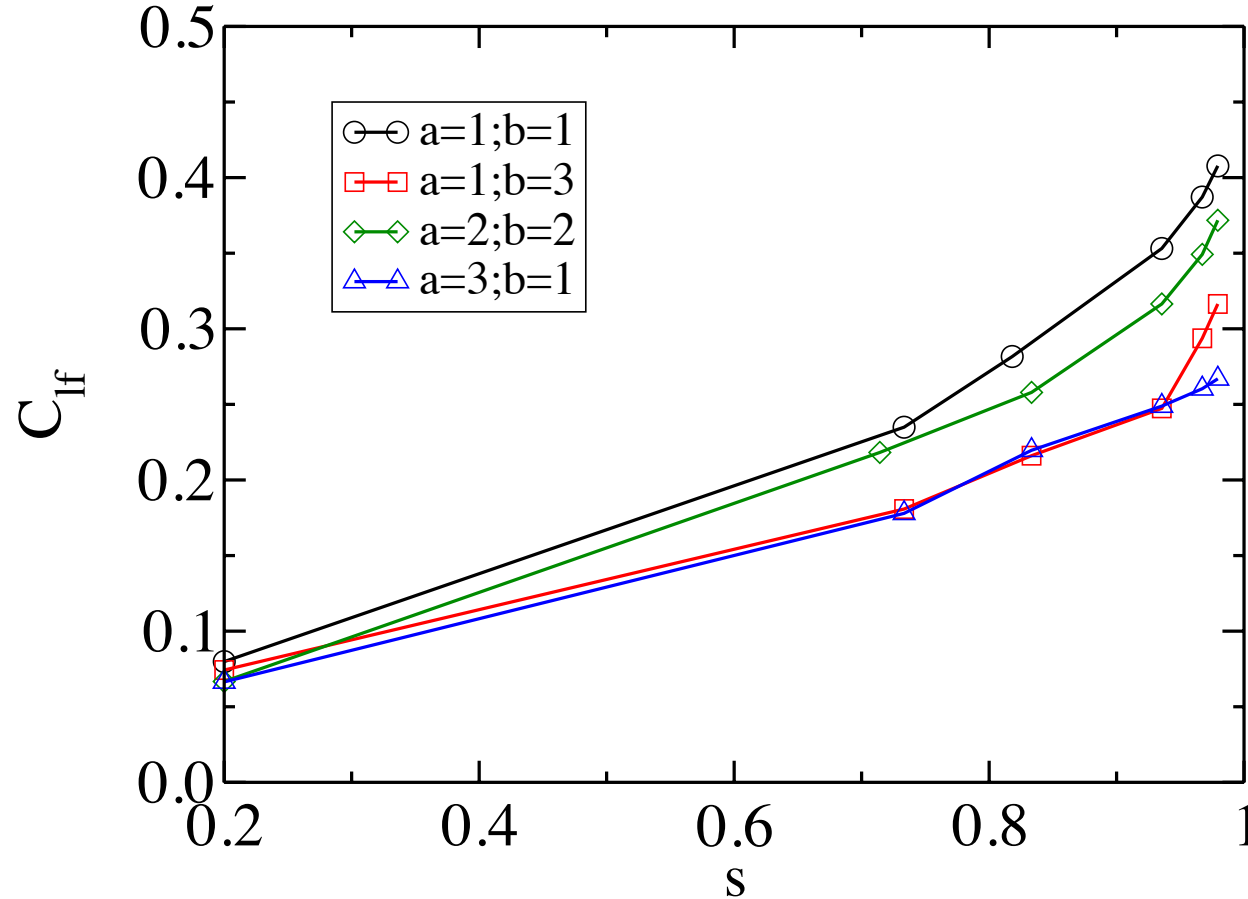
$$P(f_n) \propto e^{-\beta \frac{f_n}{\langle f_n \rangle}}$$





$$P(f_n) \propto \left( \frac{f_n}{\langle f_n \rangle} \right)^{-\alpha}$$

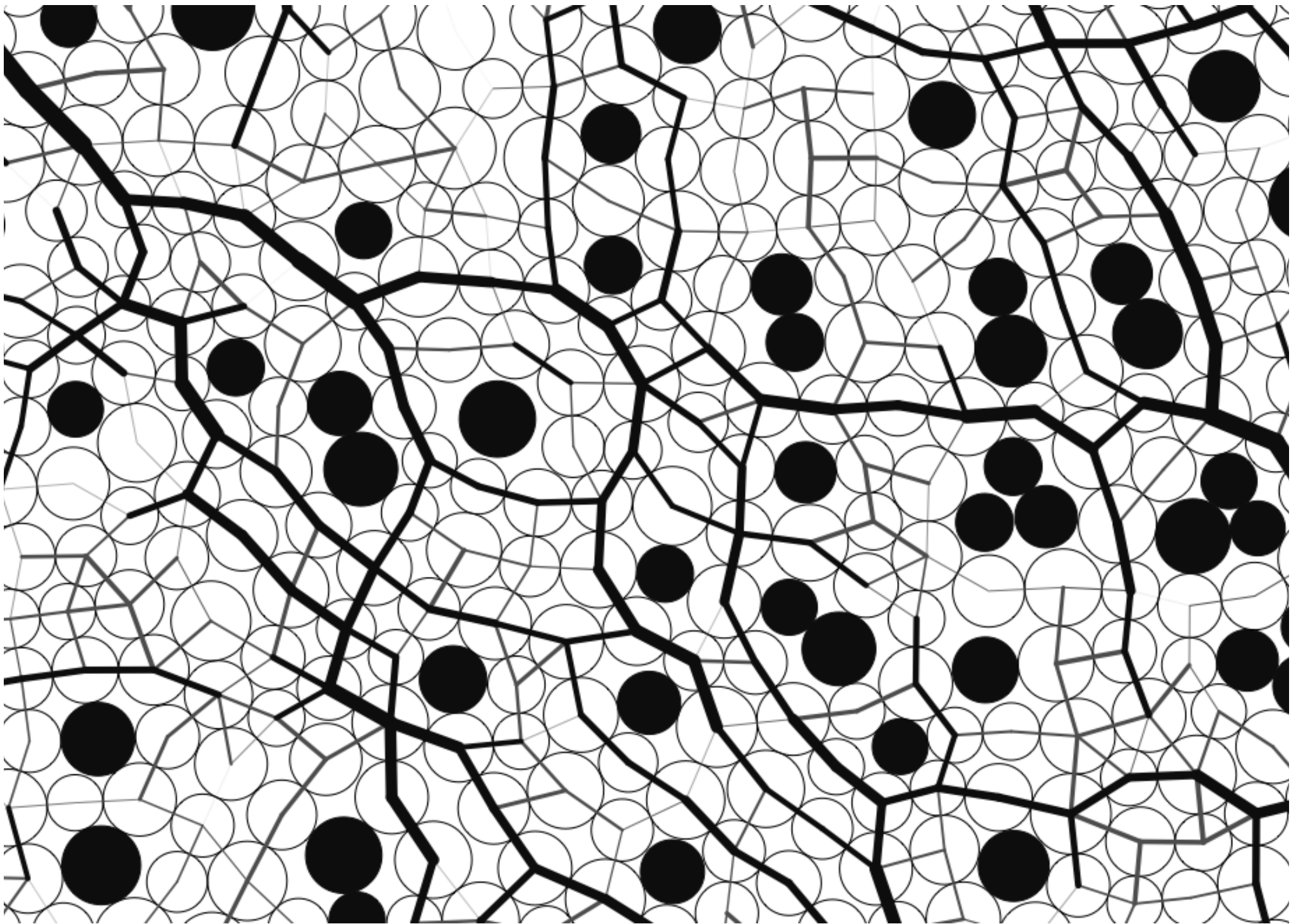




Force-size correlation as a function of size span for a uniform distribution by particle volumes.

$$C_{XY} = \frac{\langle XY \rangle}{\sqrt{\langle X^2 \rangle} \sqrt{\langle Y^2 \rangle}} \quad \begin{array}{l} X = x_i - \bar{x} \\ Y = y_i - \bar{y} \end{array}$$

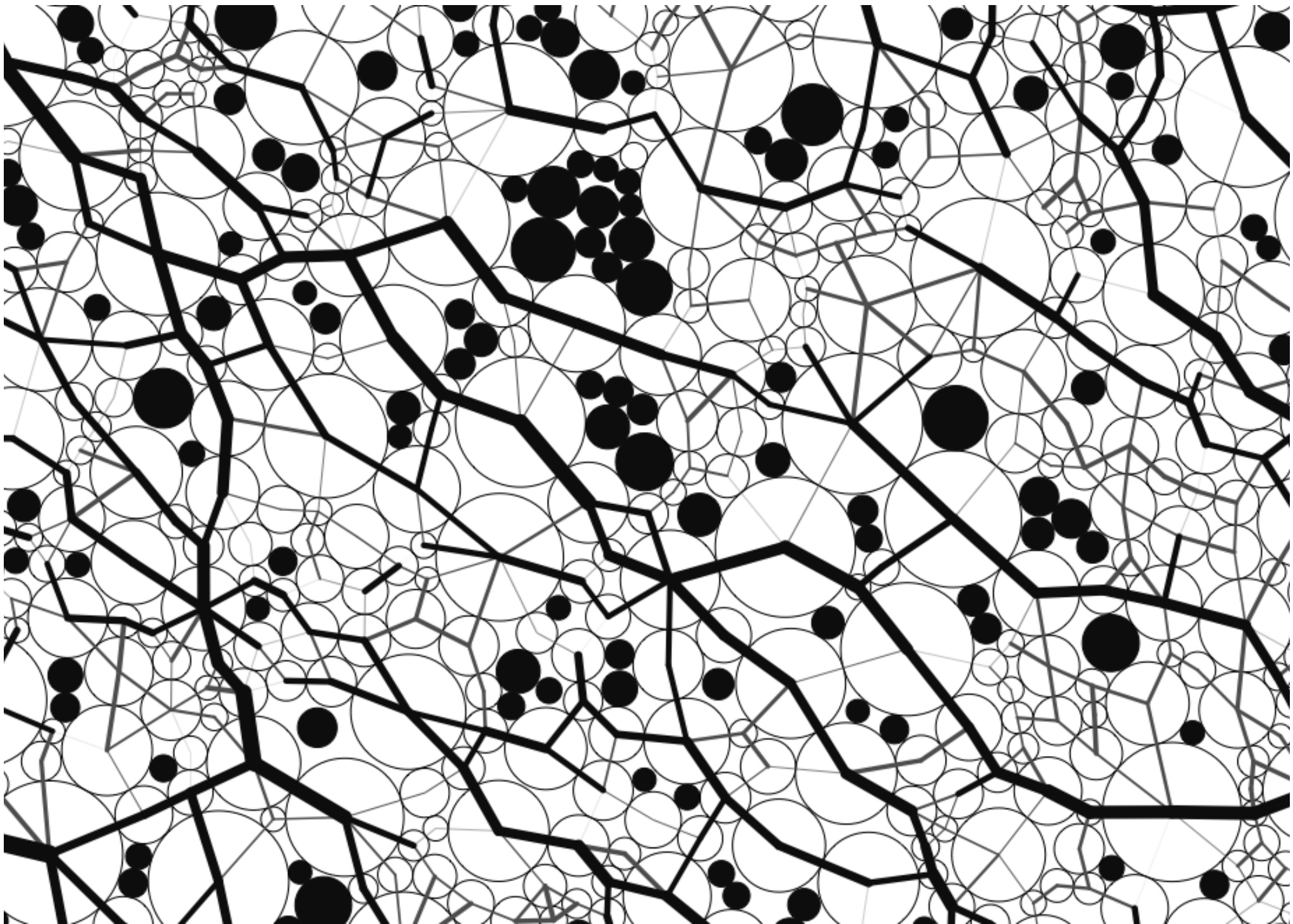
The force chains are captured by larger particles.



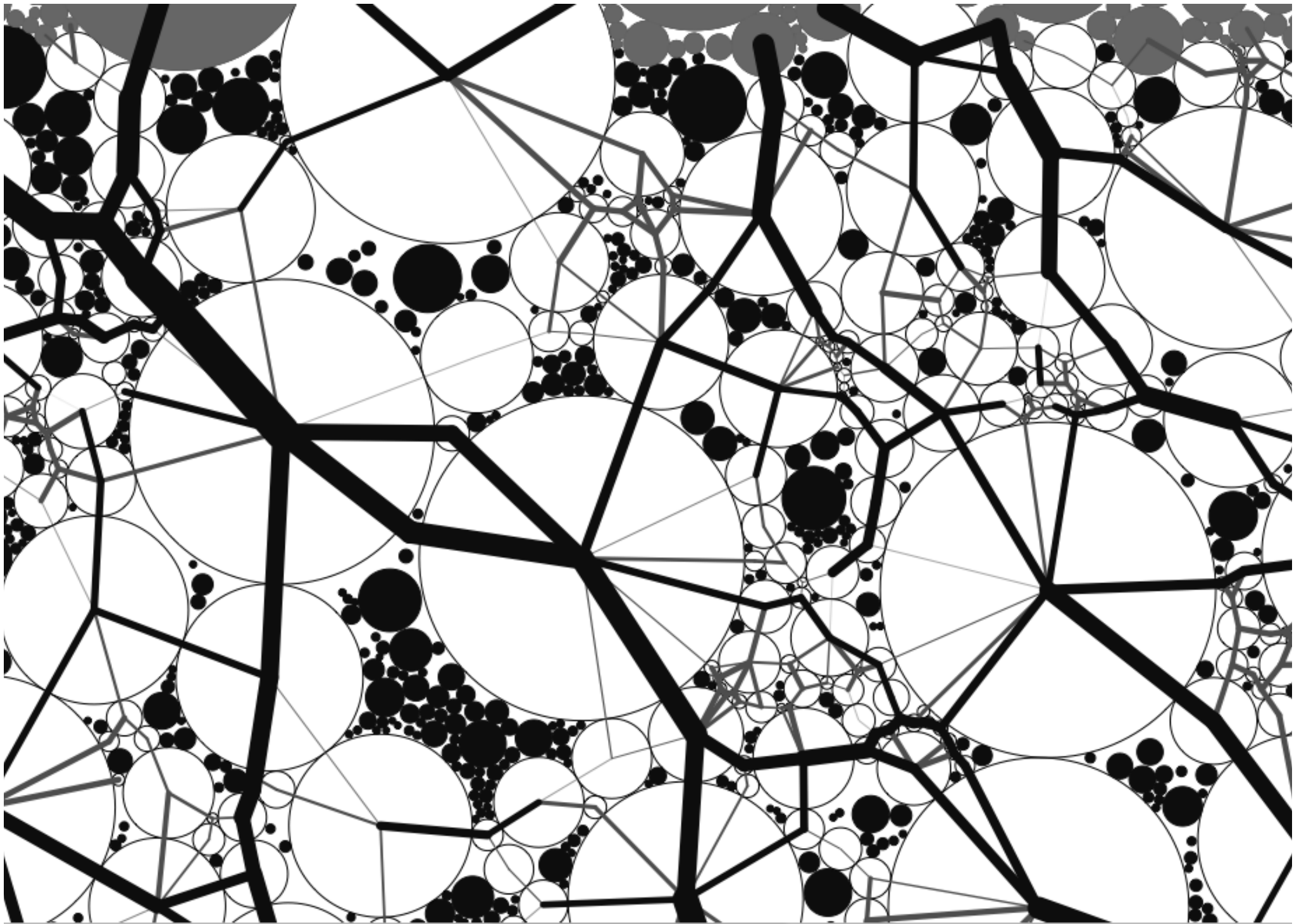
floating particles = particles with no force

$s = 0.2$

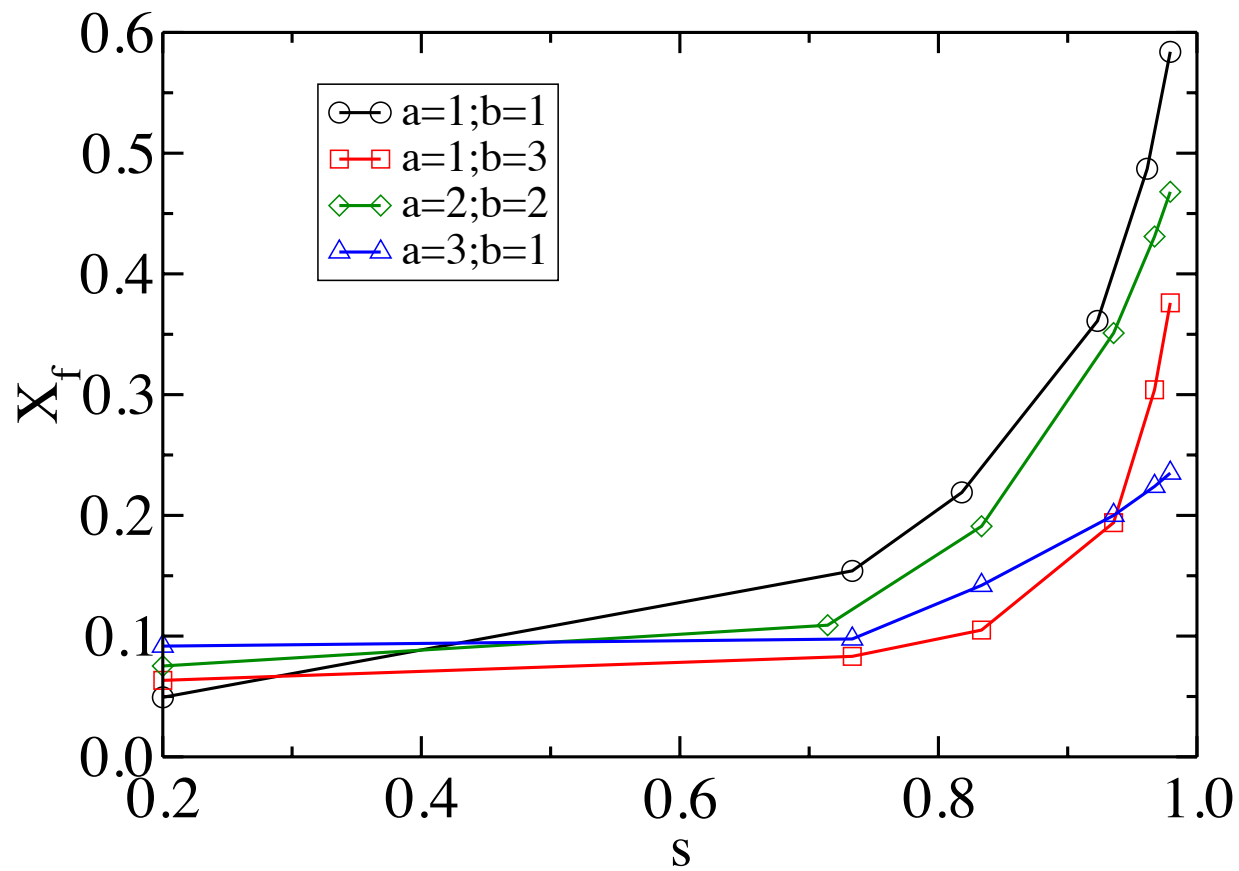
20



$s = 0.73$

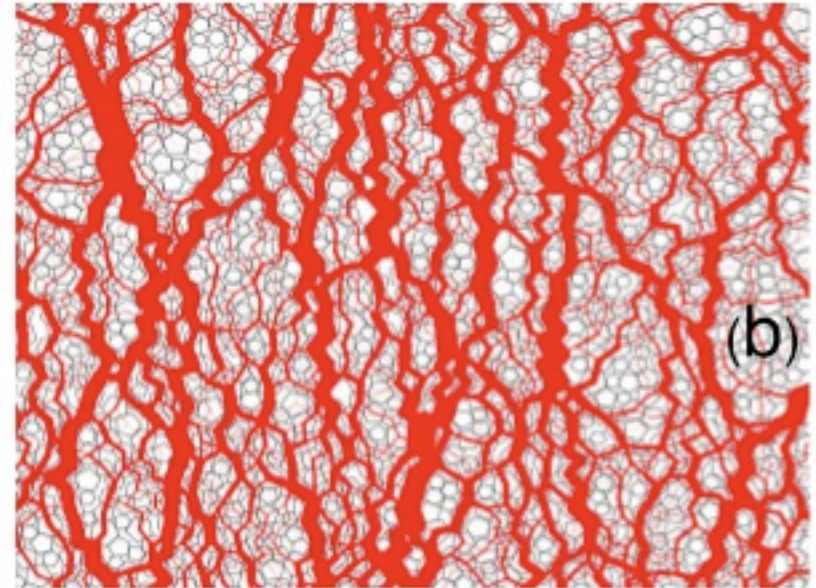
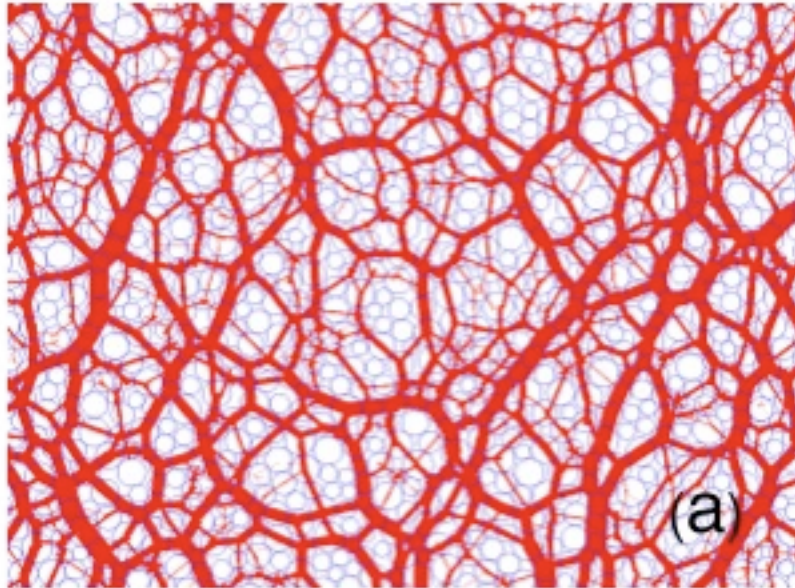


$s = 0.96$



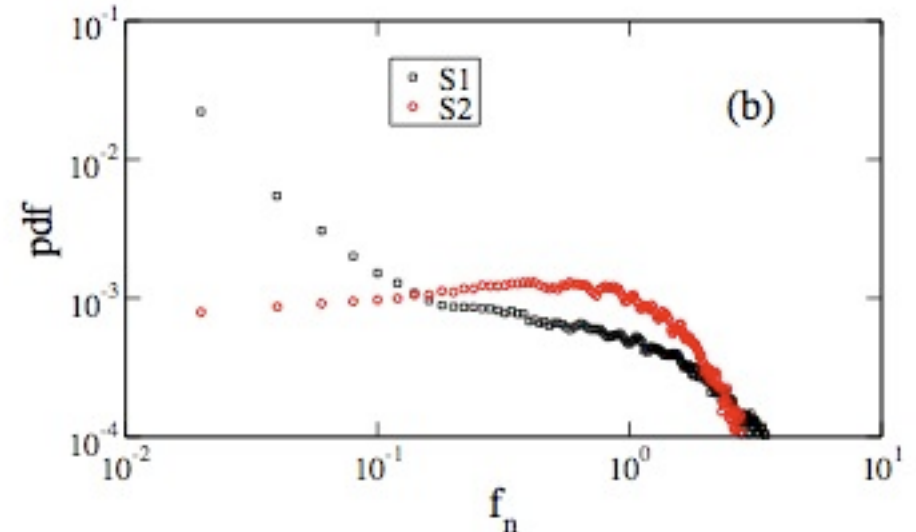
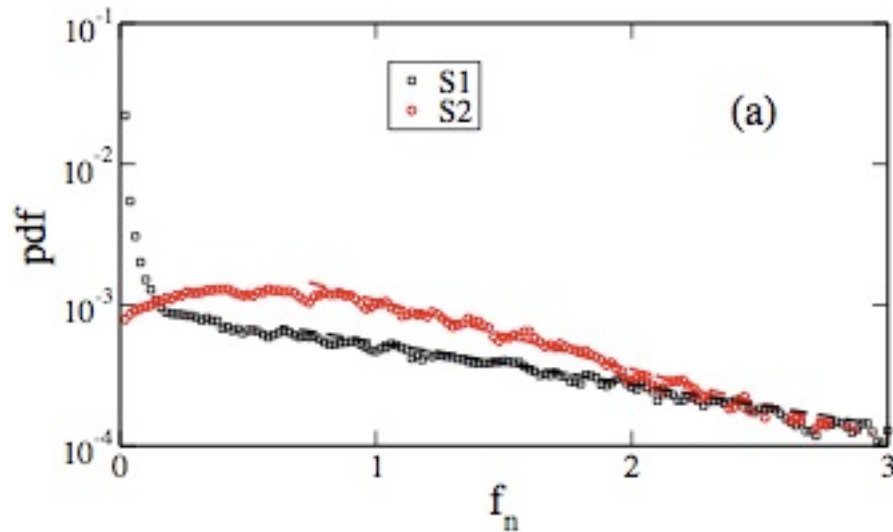
Proportion of floating particles as a function of size span for different particle size distributions.

## Effect of particle shape



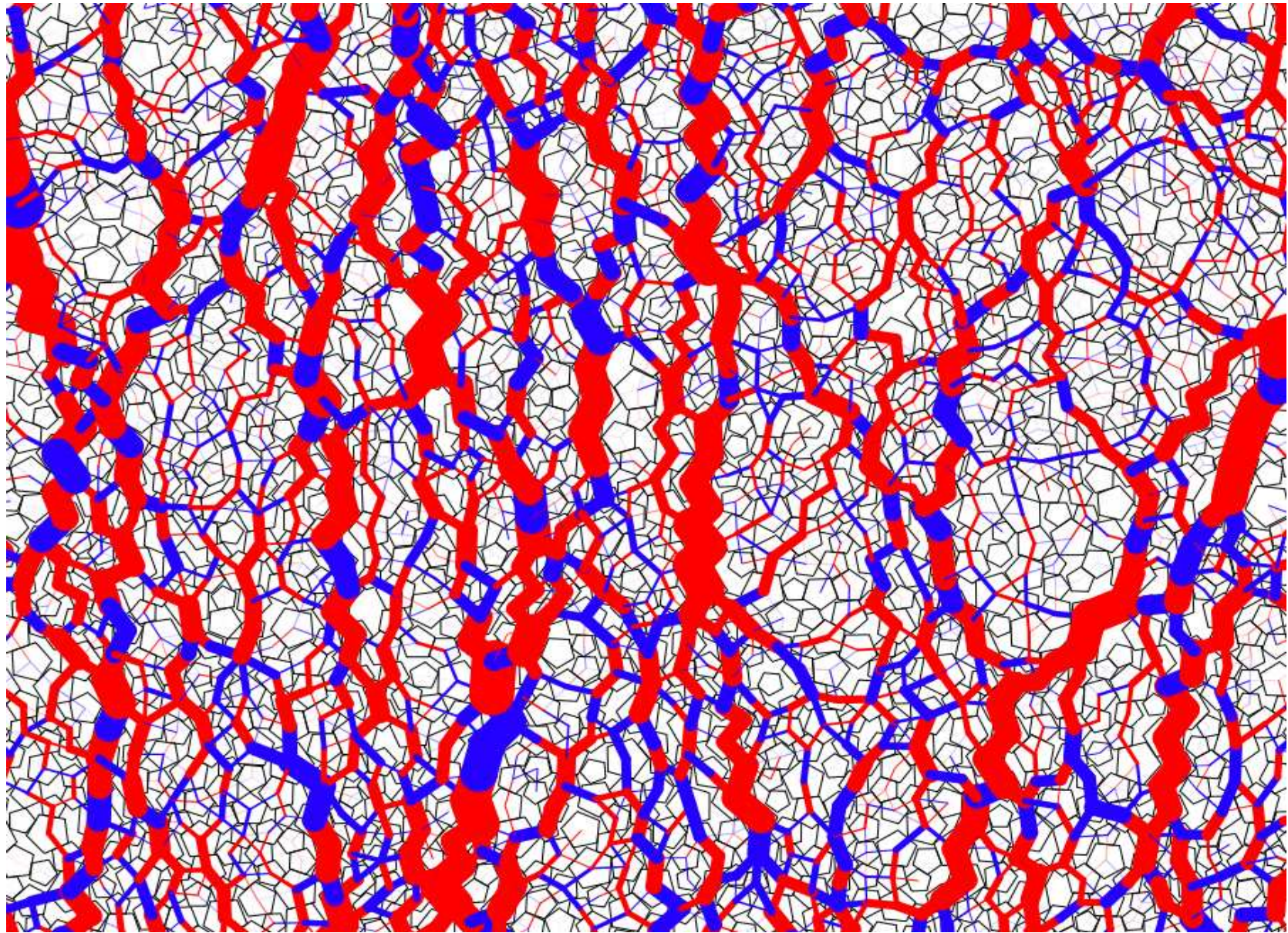
circular particles S2

polygonal particles S1



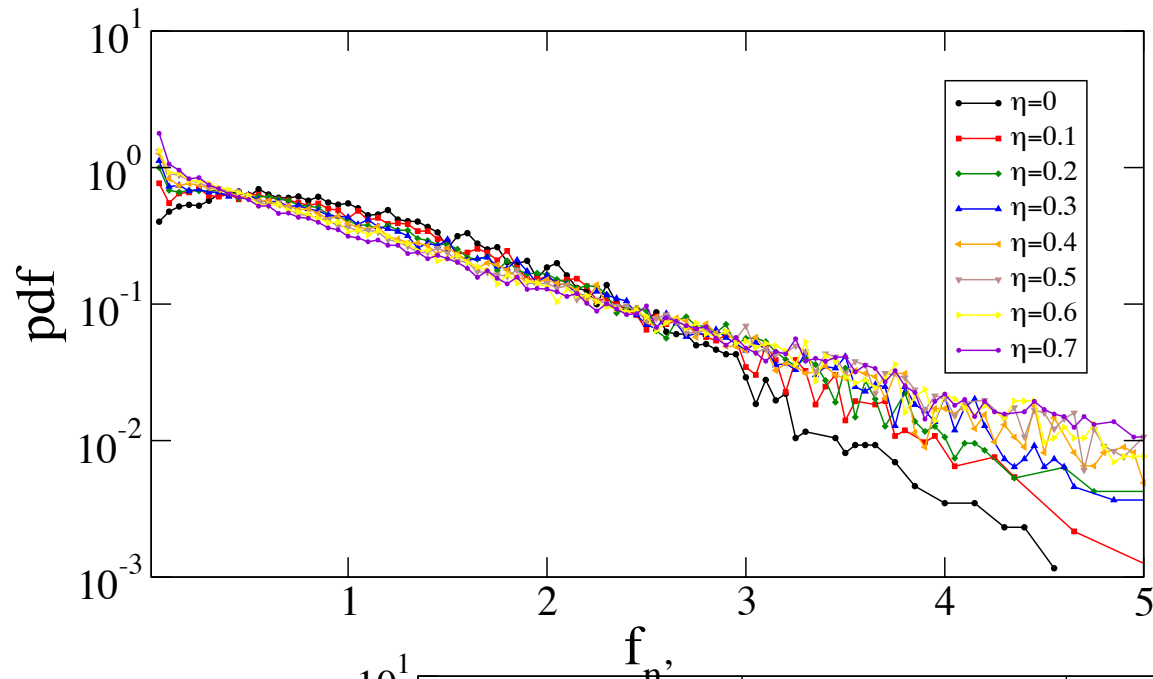
Azéma et al. (2007)



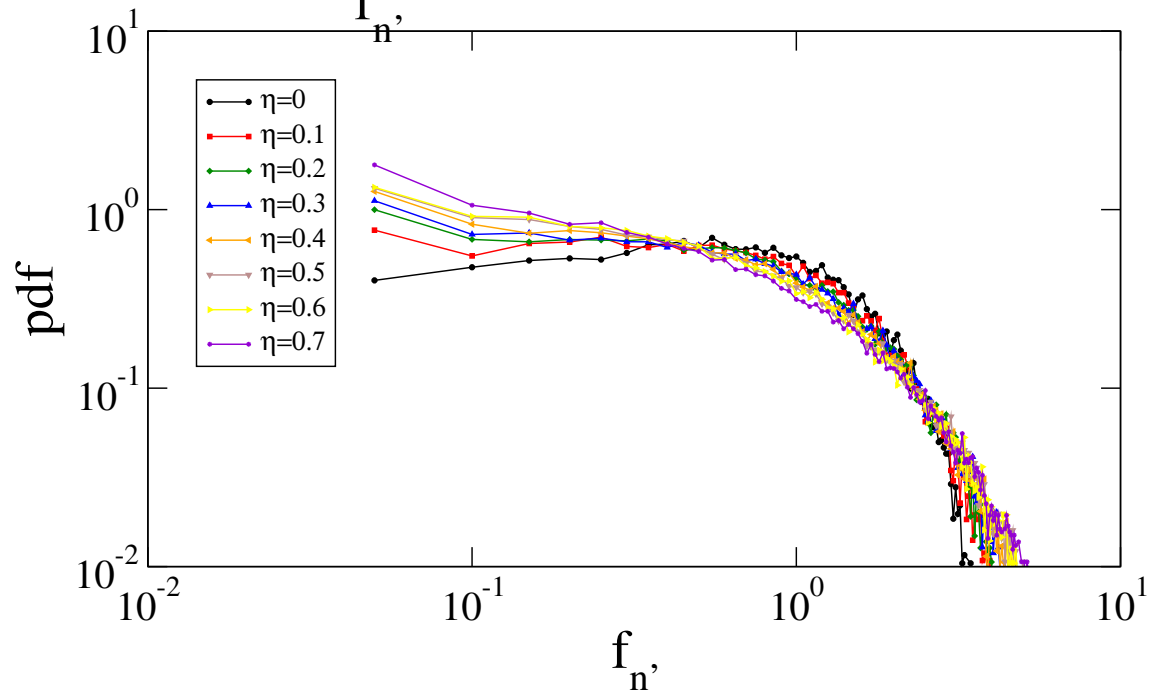


Side/side contacts (red) and vertex/side contacts (blue) in a packing of pentagonal particles.

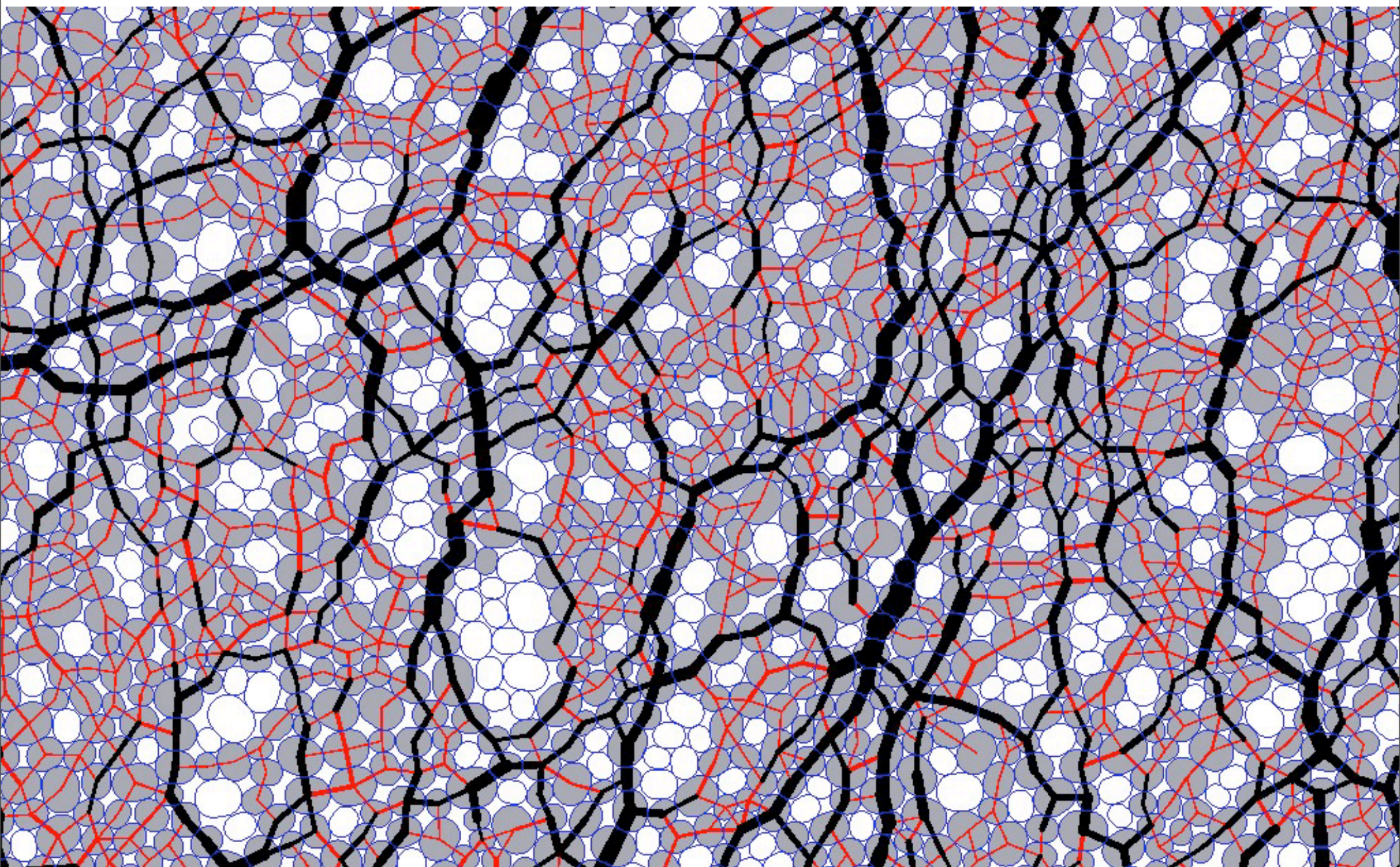
# elongated particles

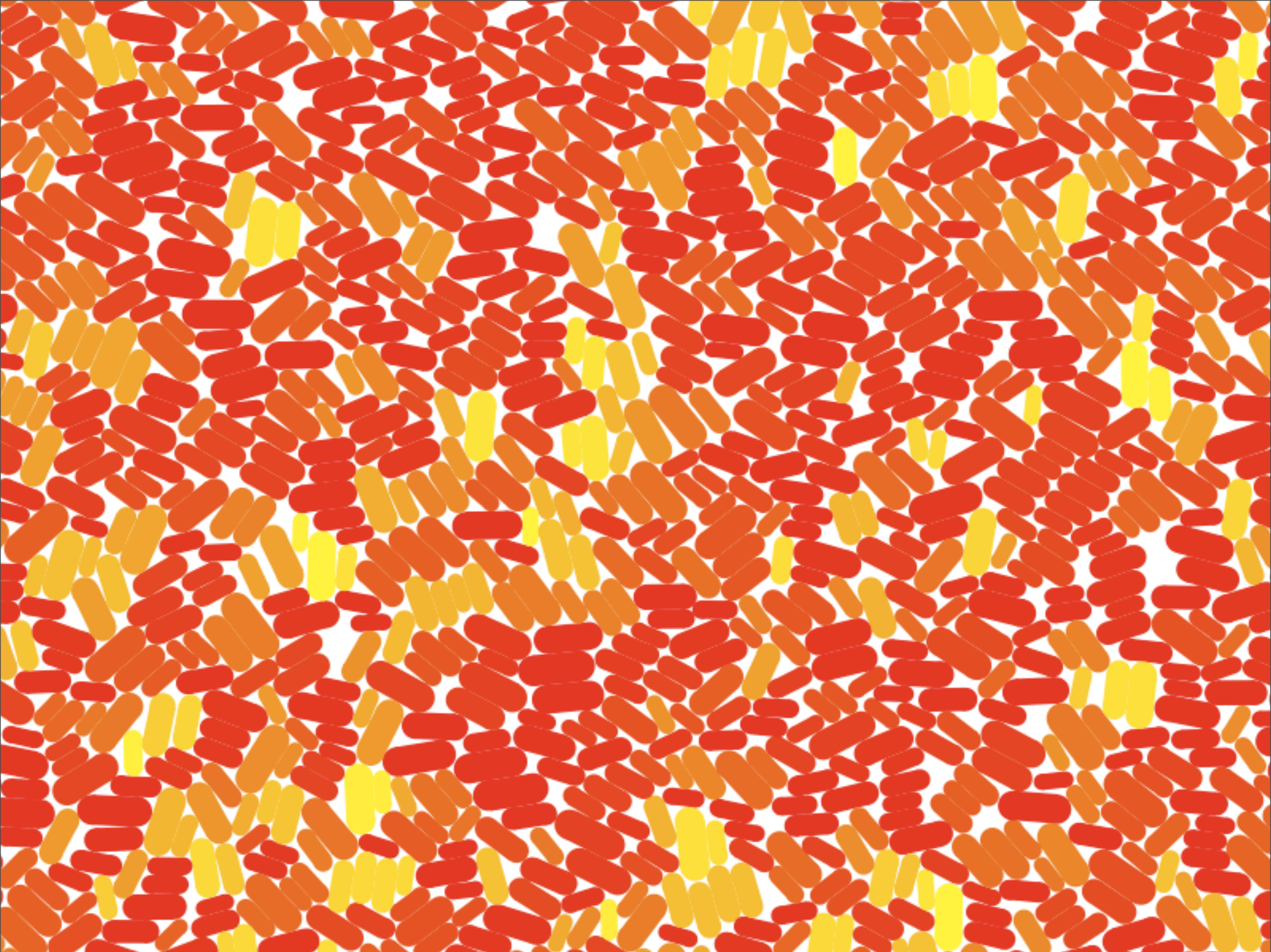


Force pdf's for increasing particle elongation.

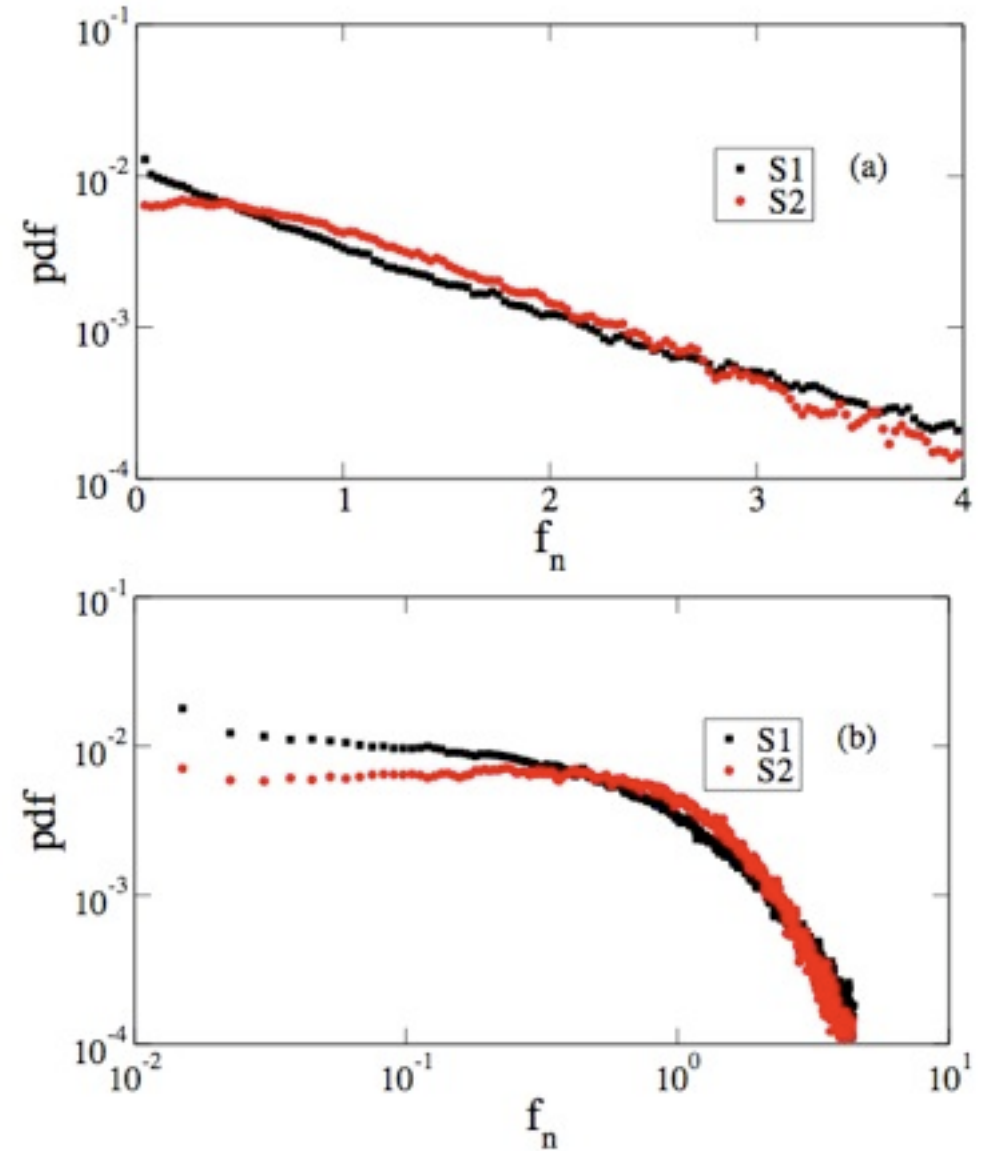
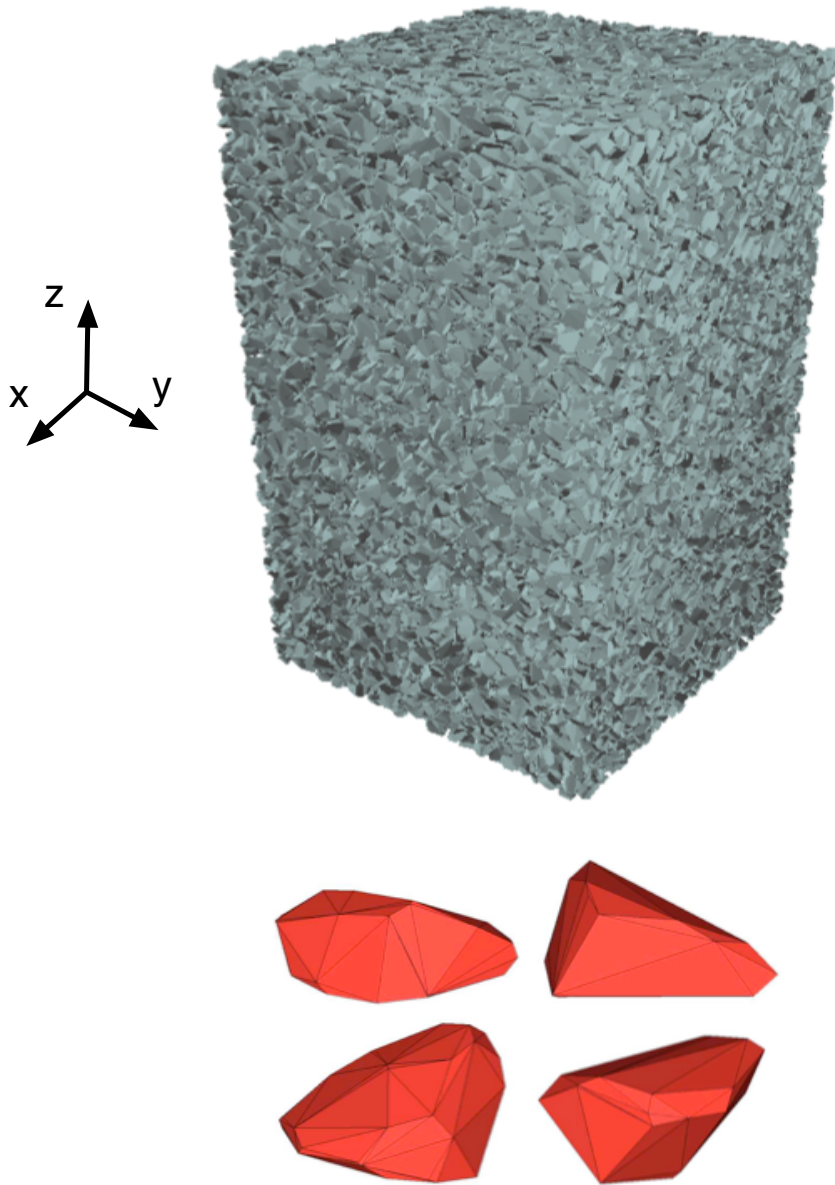


Azéma et al. (2010)

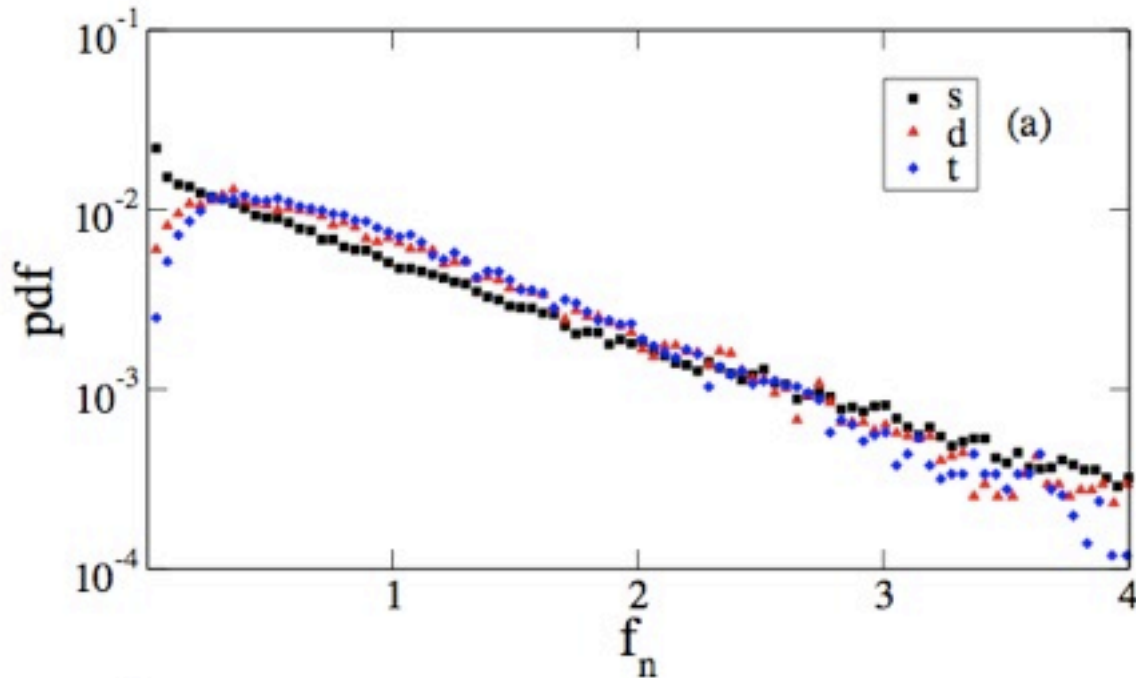




# Polyhedral particles (S1) vs. spherical particles (S2)



Azéma et al. (2009)

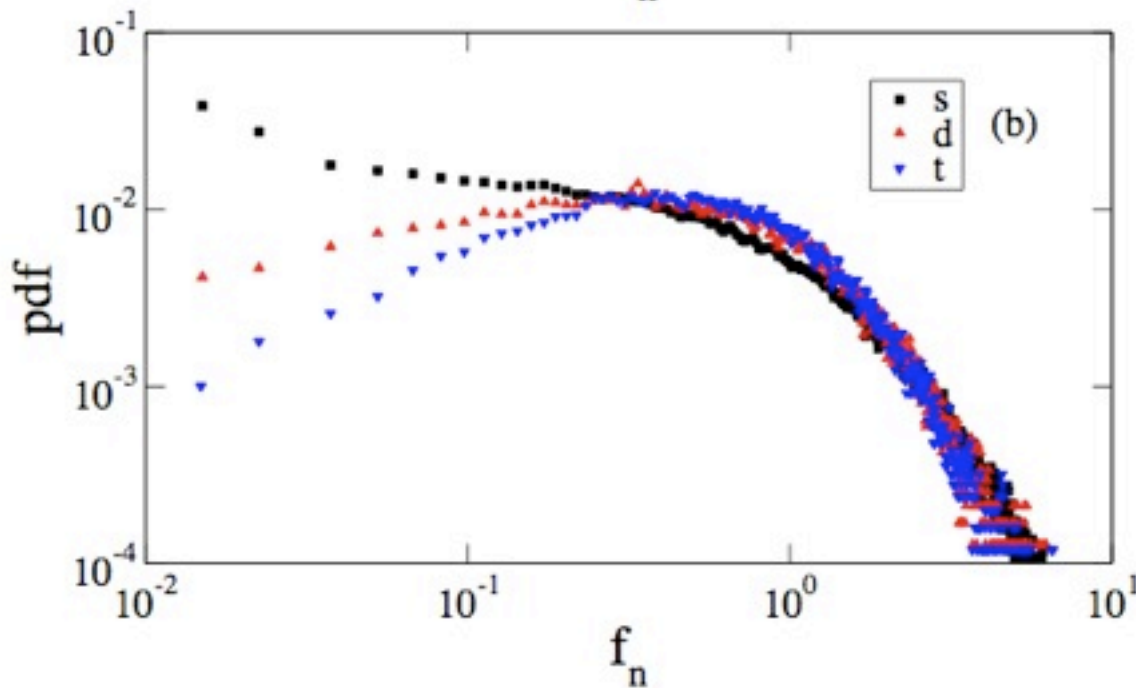


Force pdf's for different types of contacts between the polyhedra:

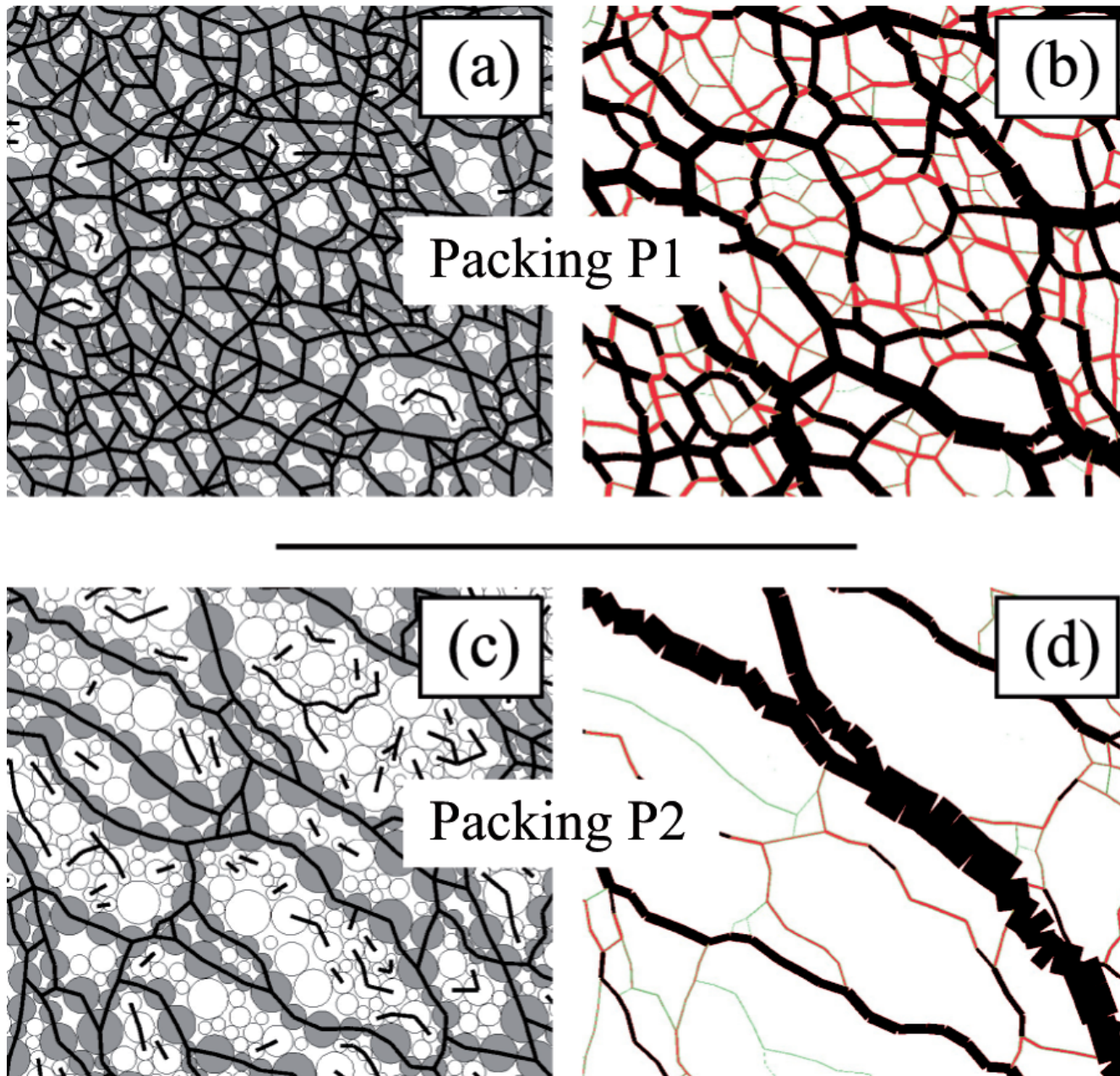
$s$  = simple contact = vertex/face or edge/edge

$d$  = double contact = edge/face

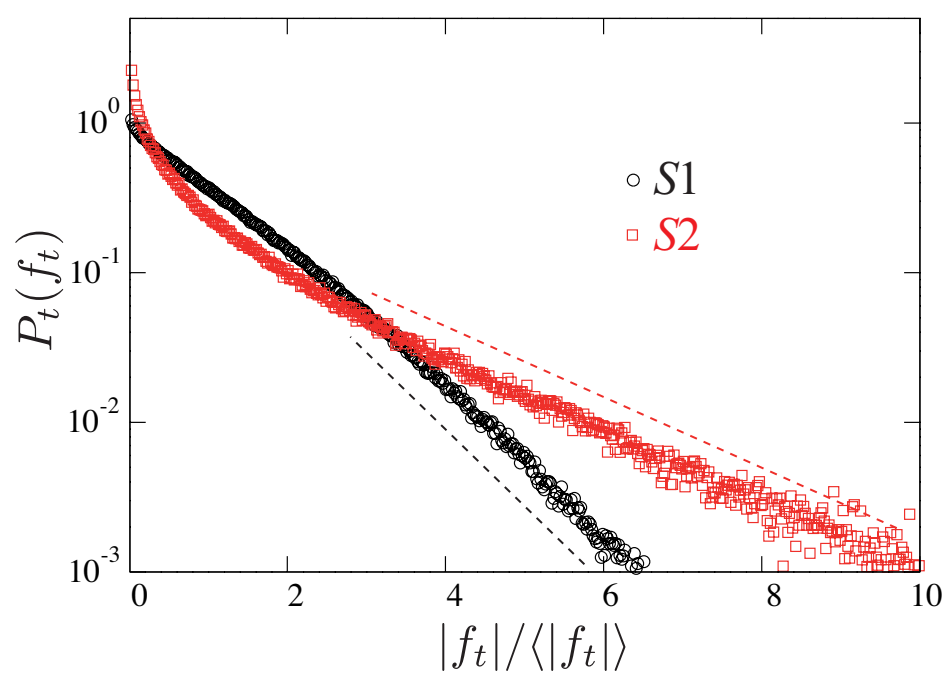
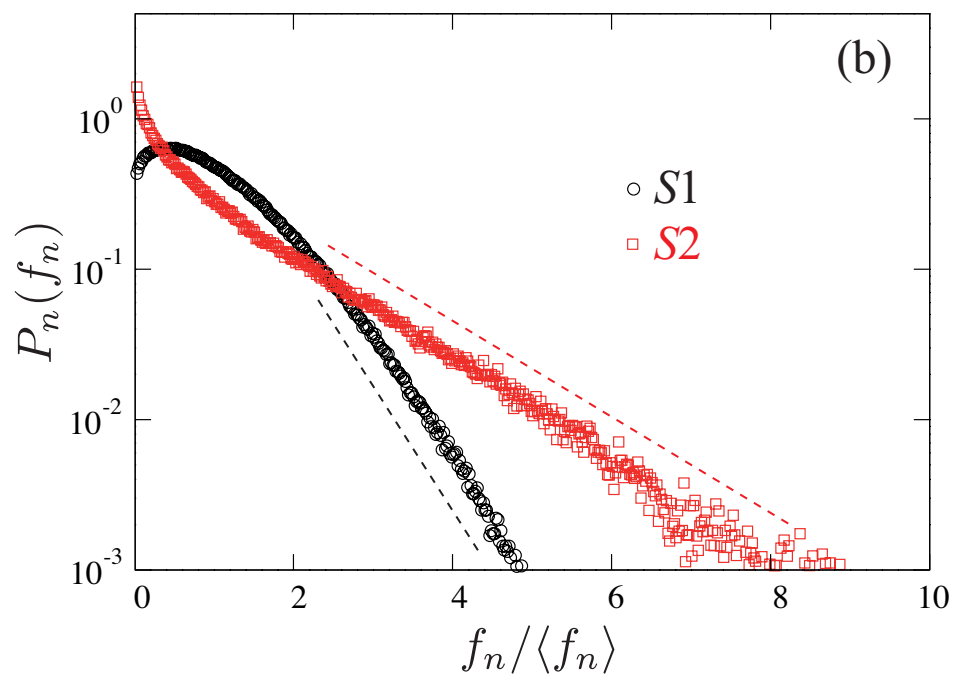
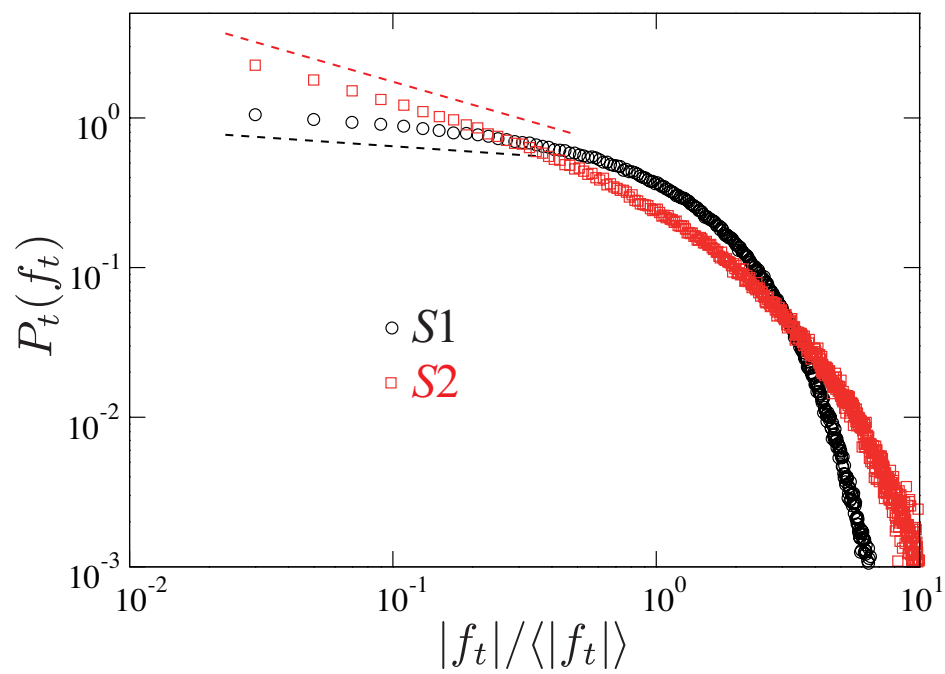
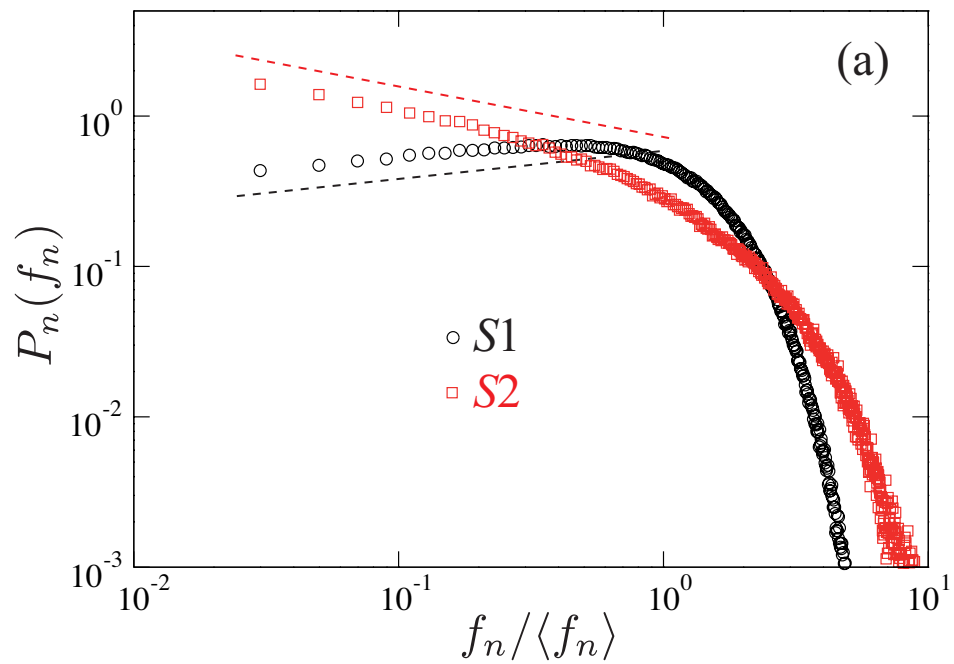
$t$  = triple contact = face/face



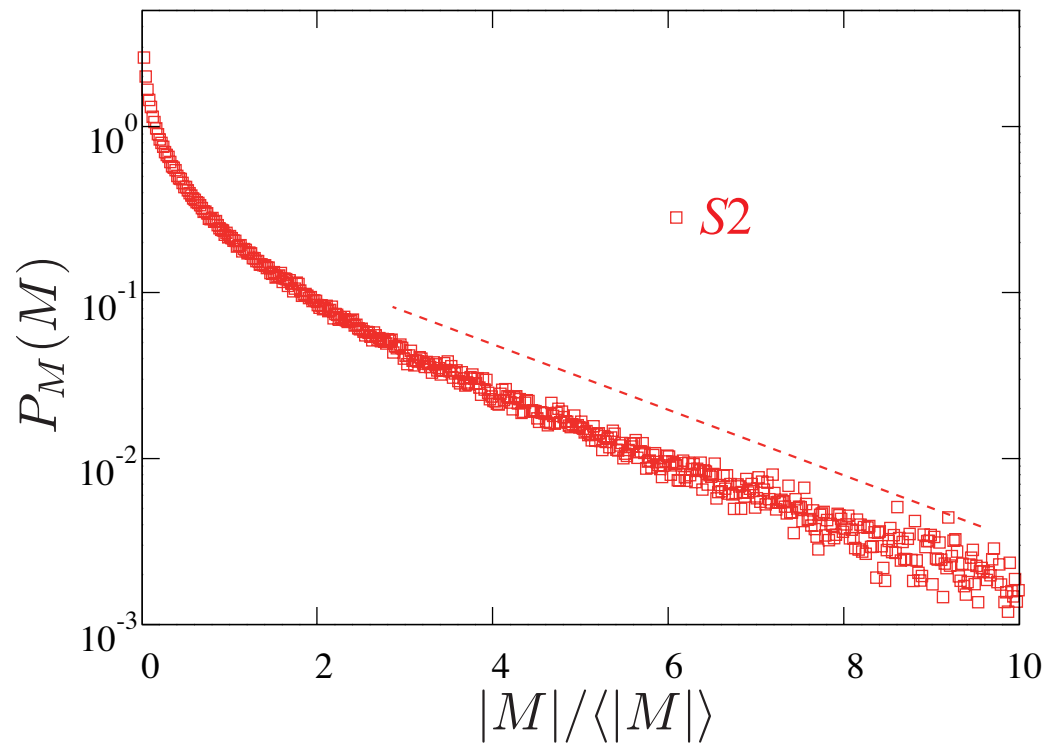
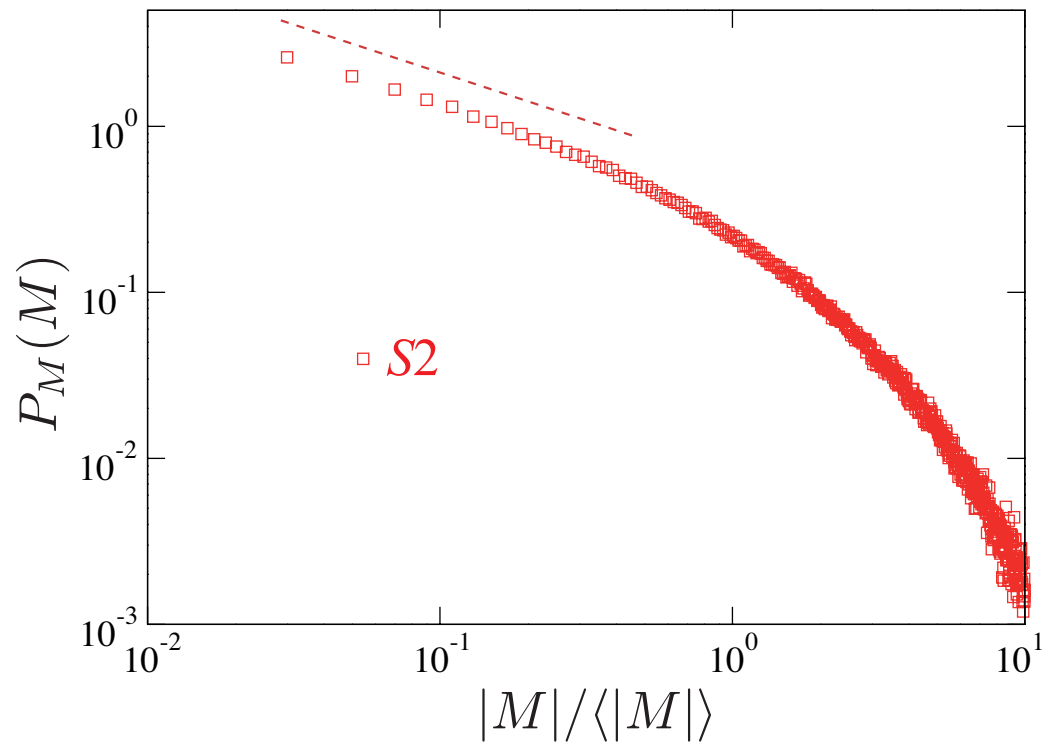
## Effect of rolling friction

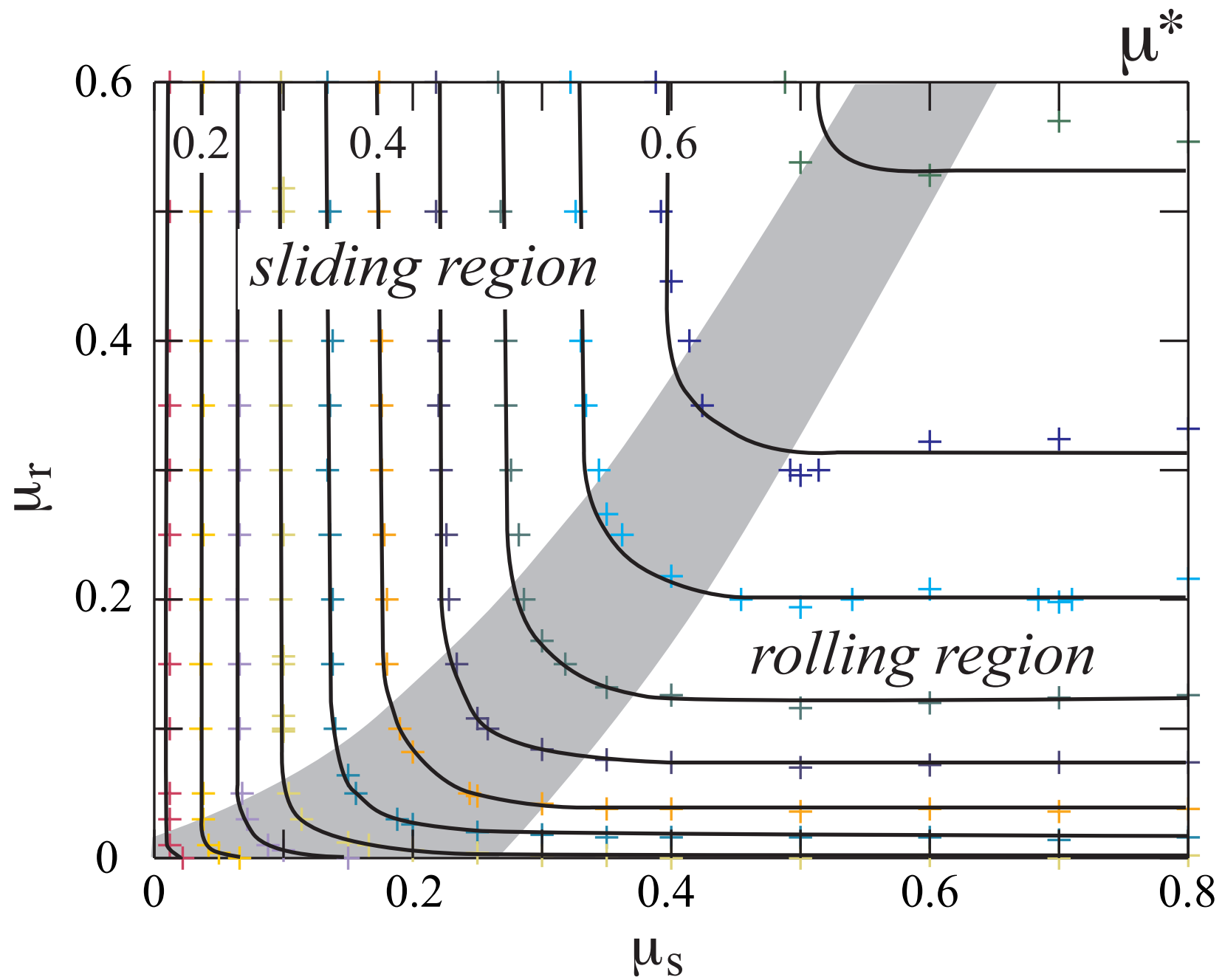


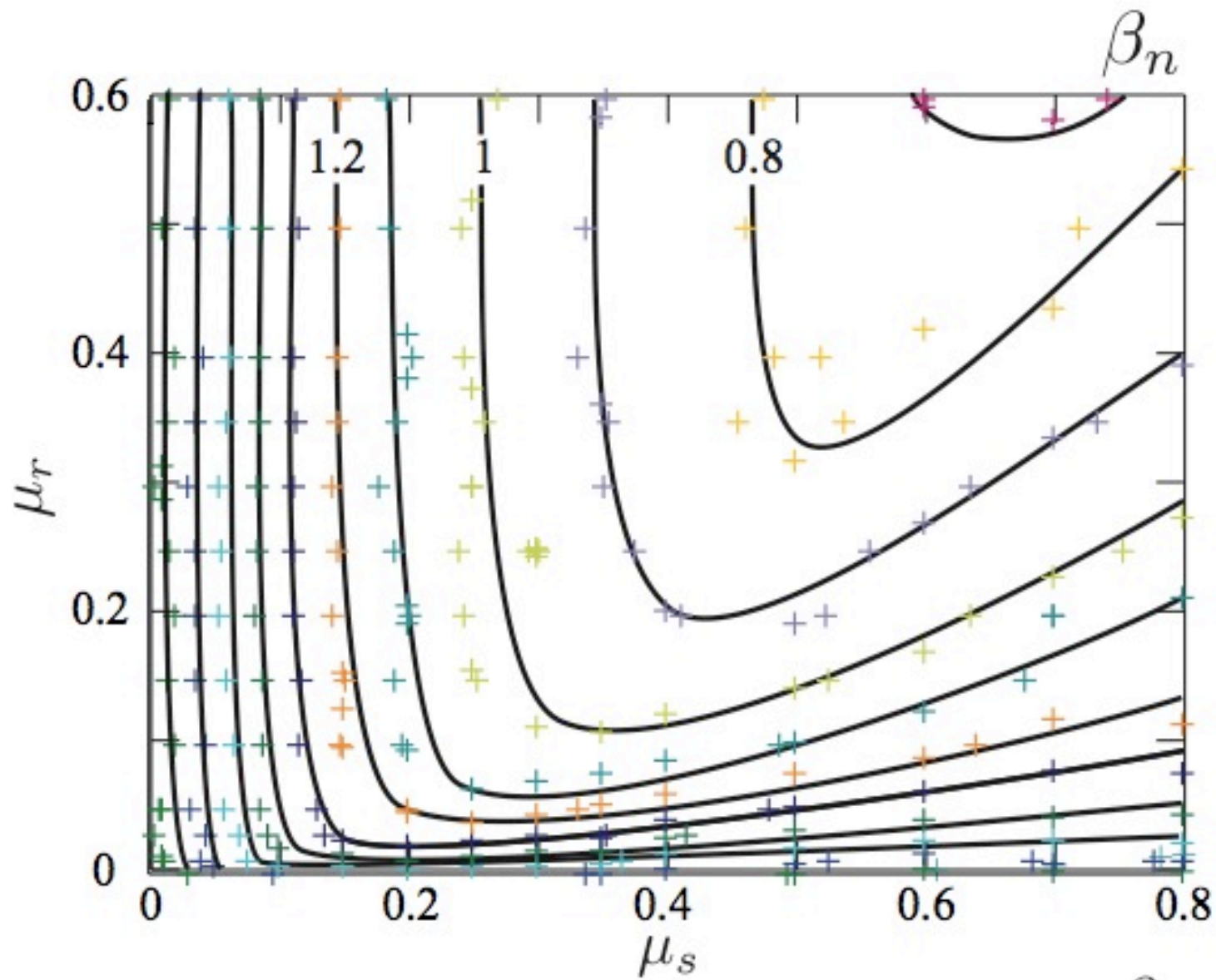
Estrada et al. (2008)





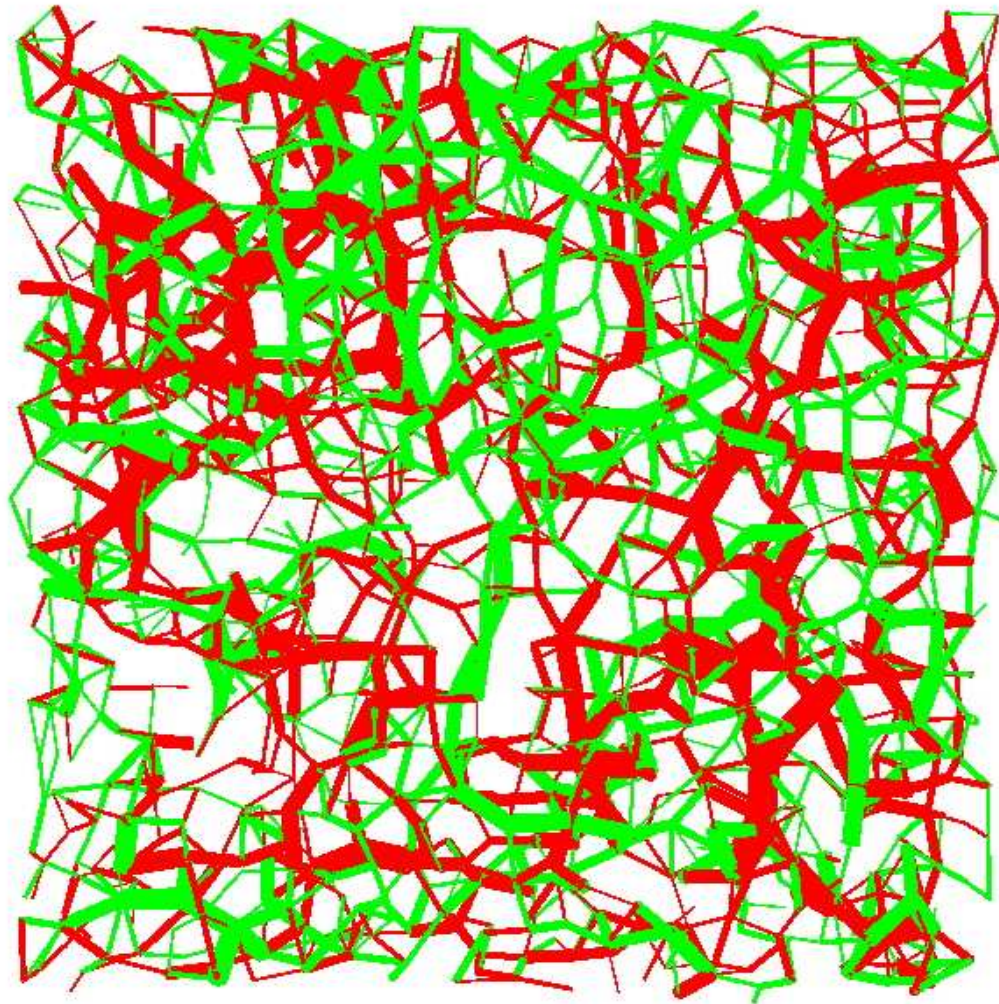




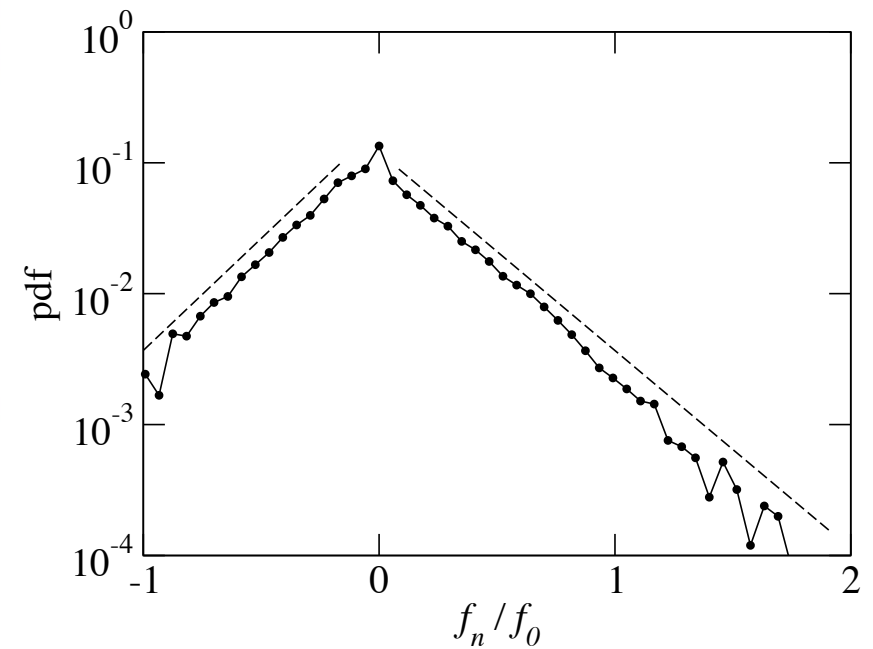
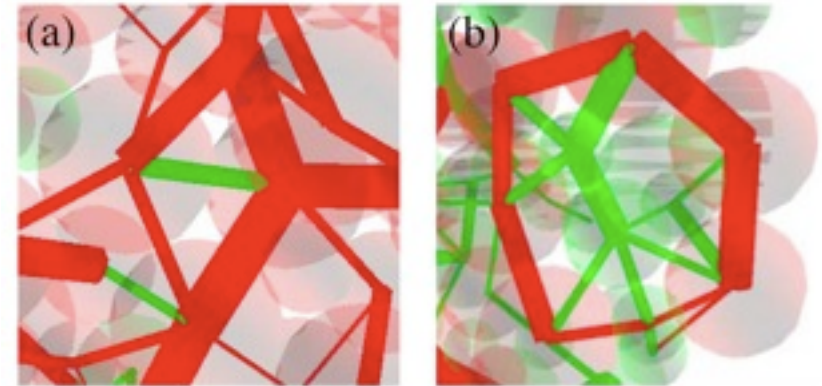


$$h(x; \alpha, \beta) = A \begin{cases} x^{-\alpha} & x < 1 \\ e^{\beta(1-x)} & x > 1 \end{cases}$$

## Effect of capillary bonding

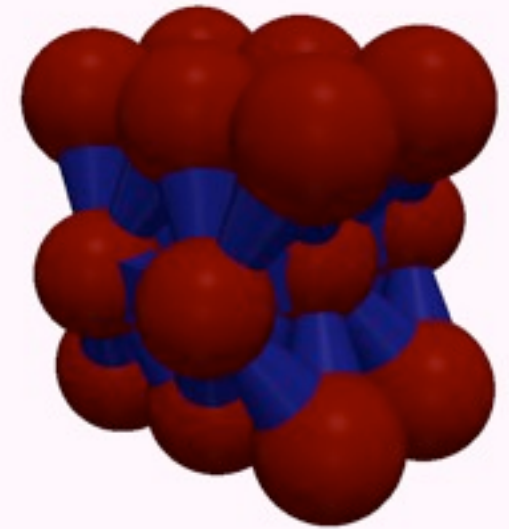
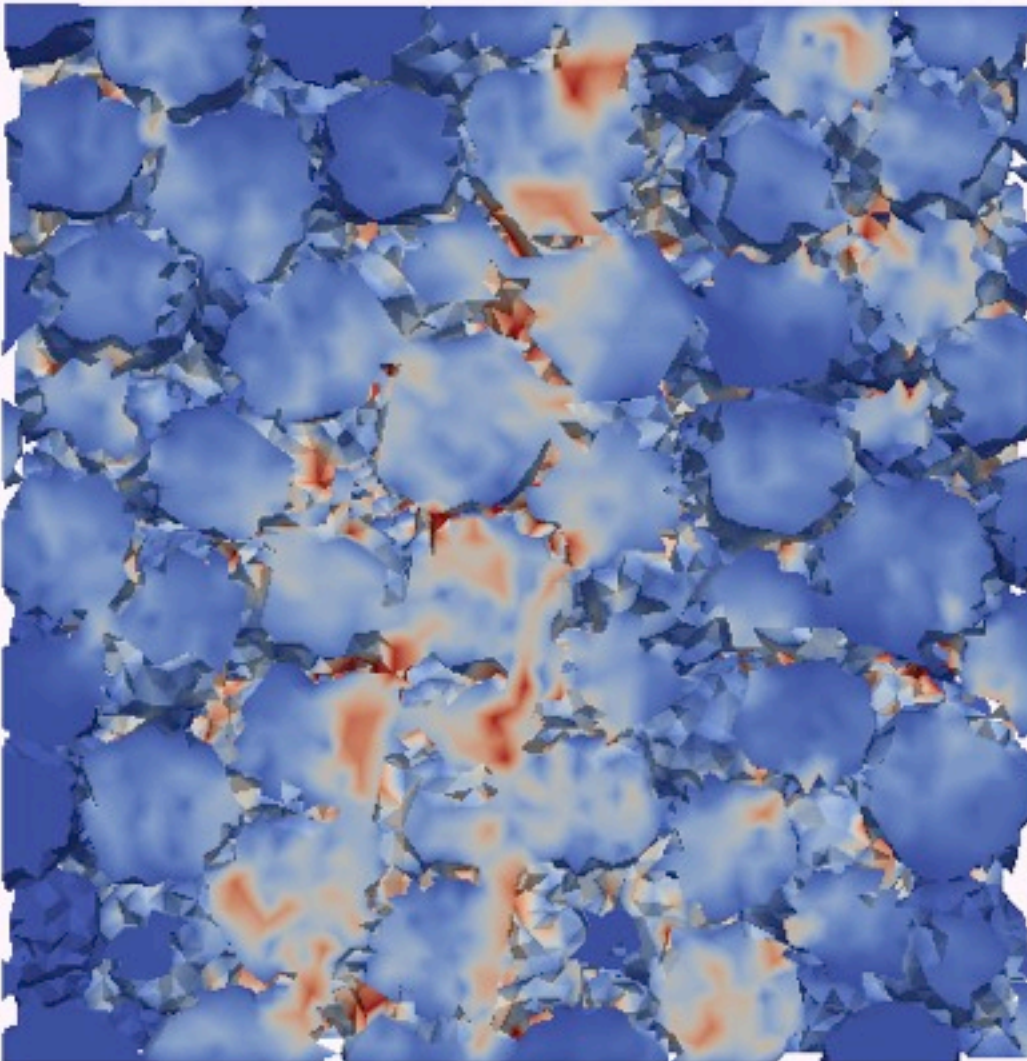


Richefeu et al. (2008)



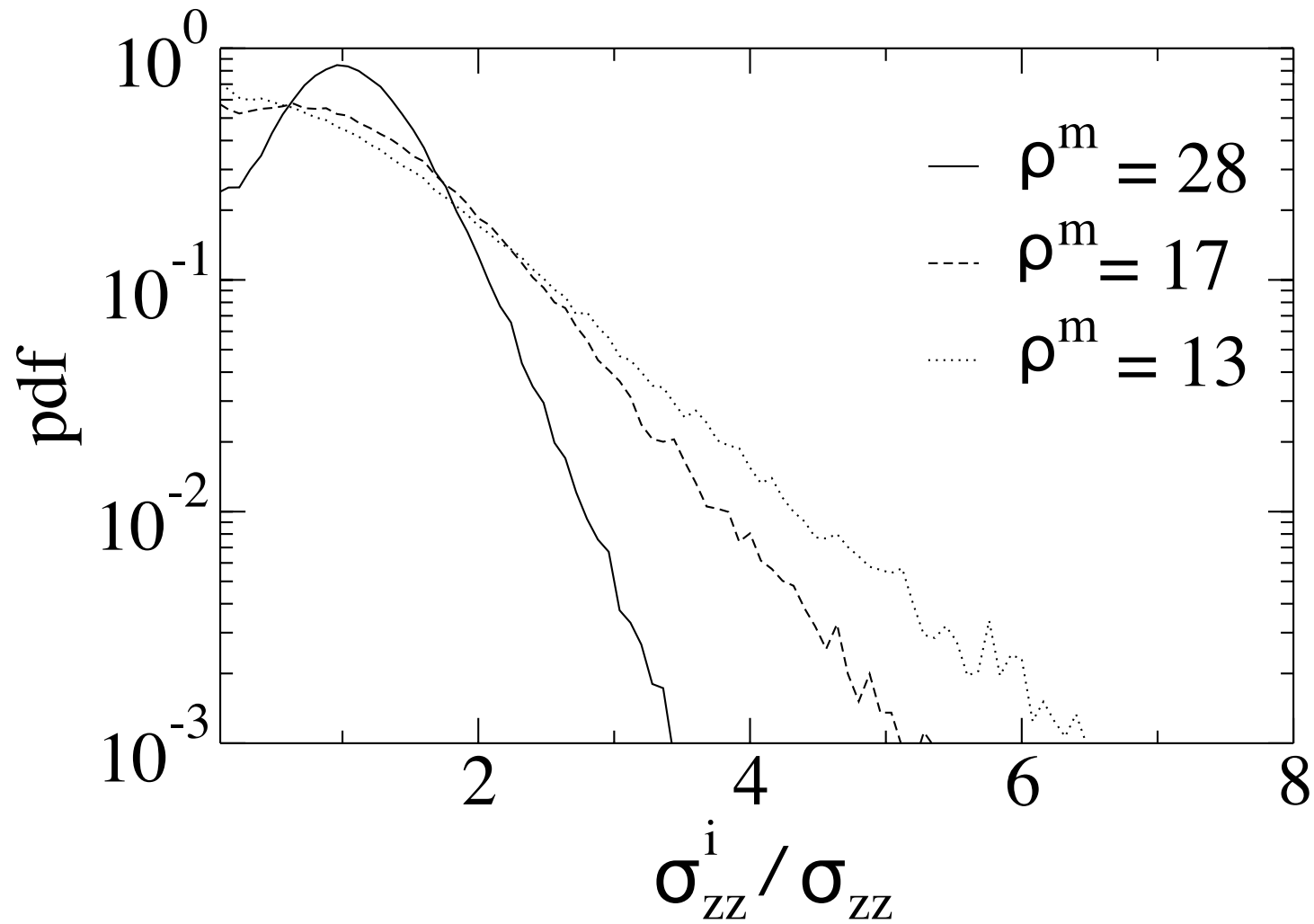
Network of self-equilibrated tensile and compressive forces in a thin layer inside a wet material.

## Cemented granular materials



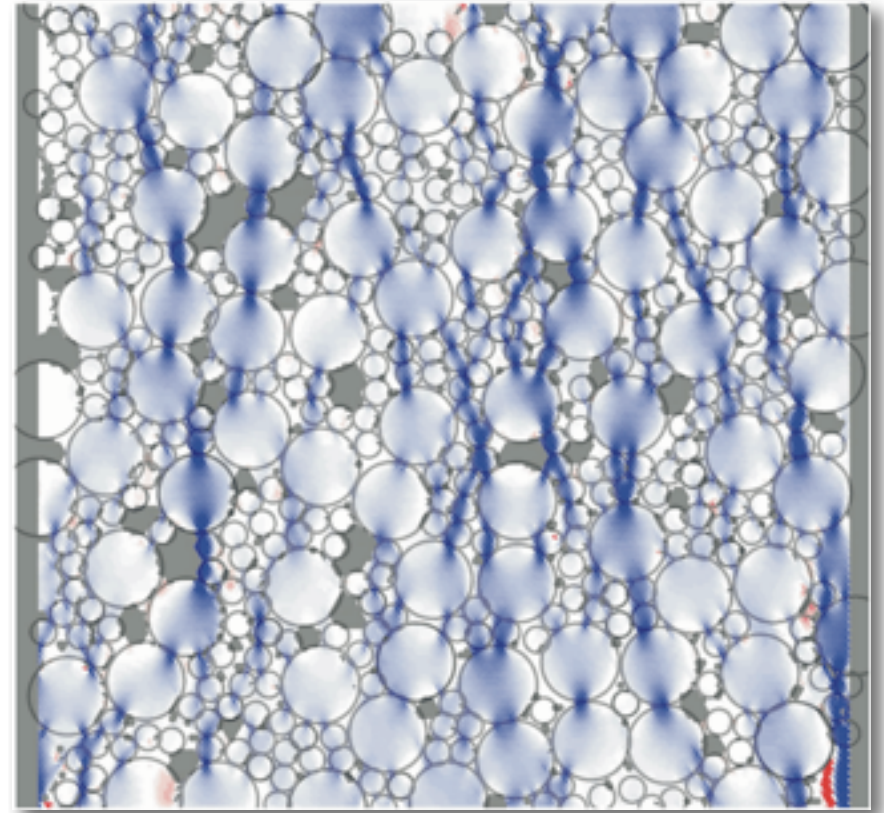
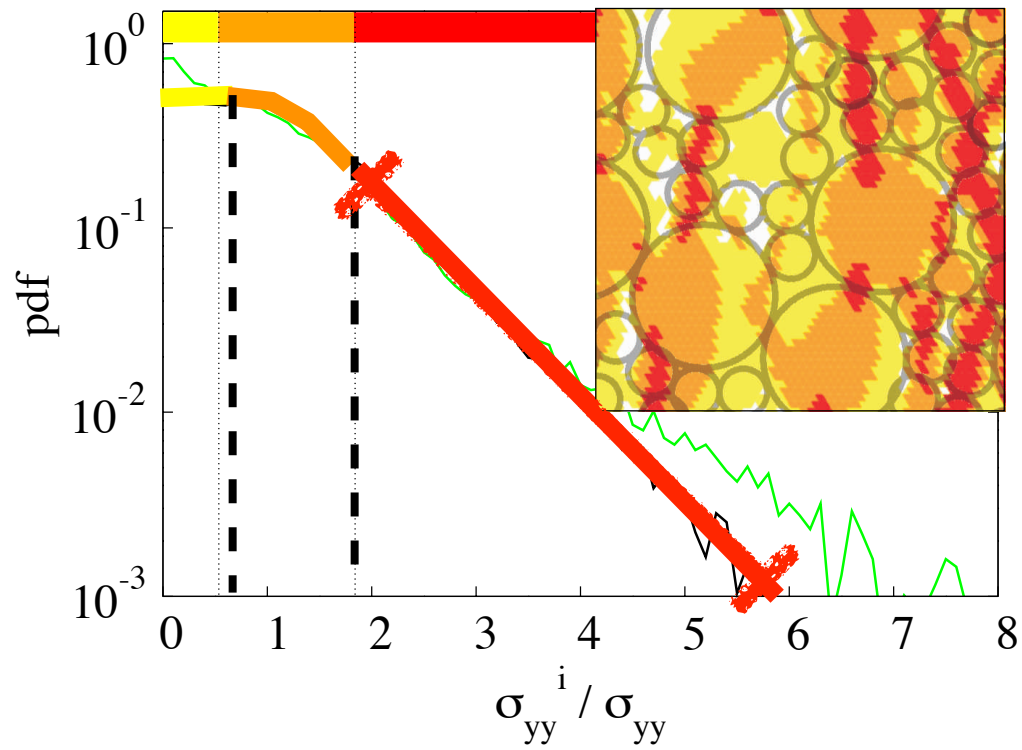
3D

Afes et al. (2011)



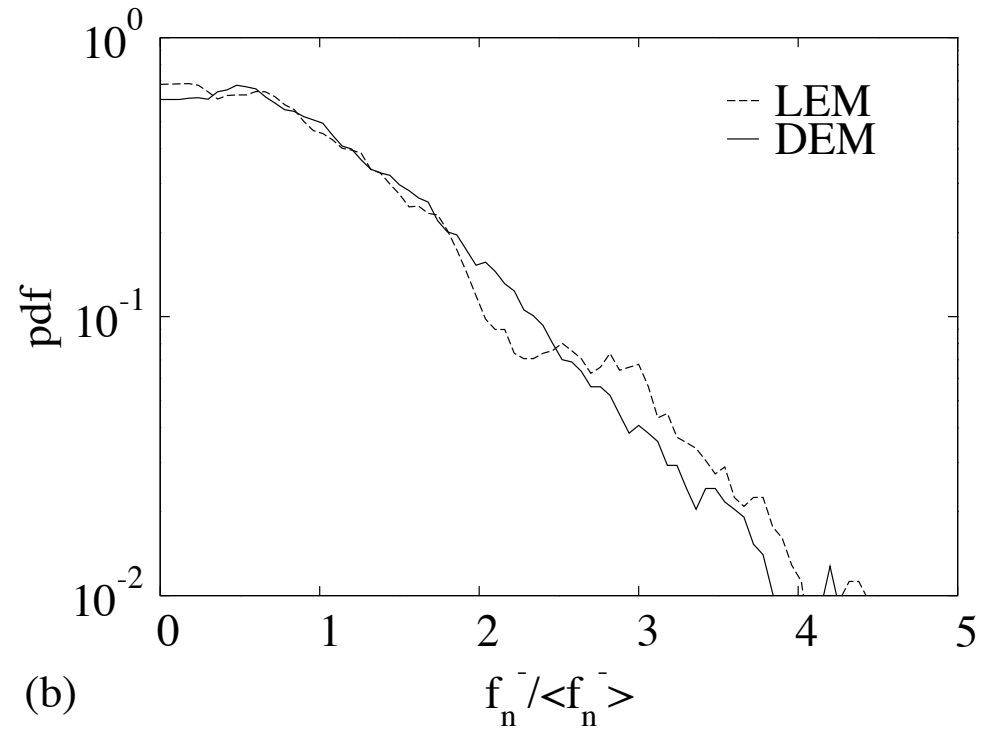
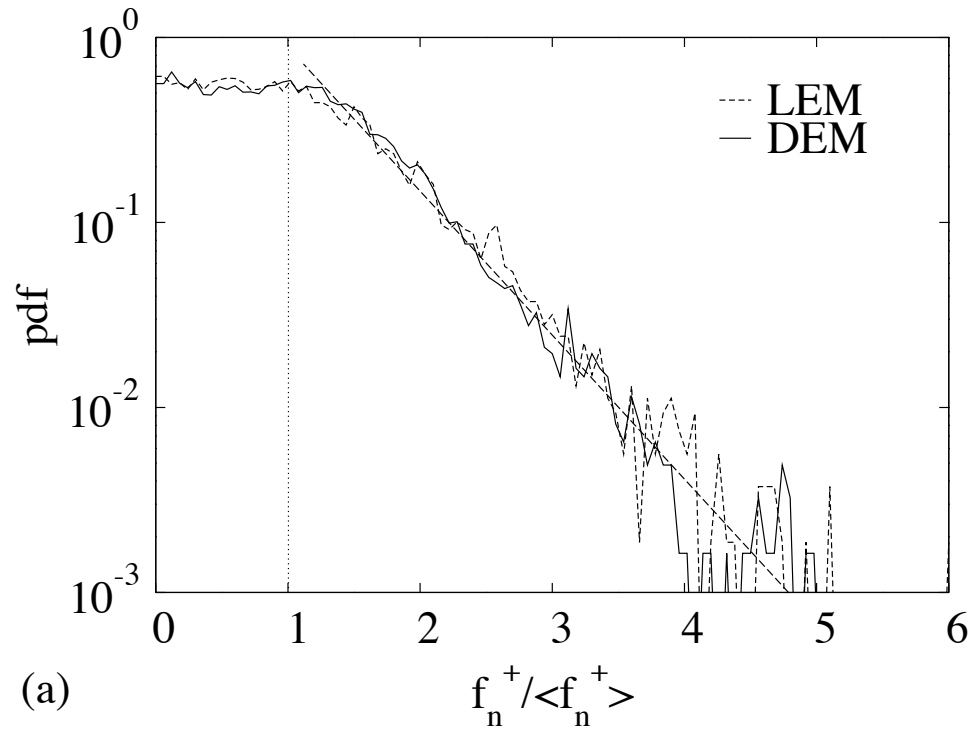
Distribution of vertical stresses for three different values of the matrix volume fraction.

2D

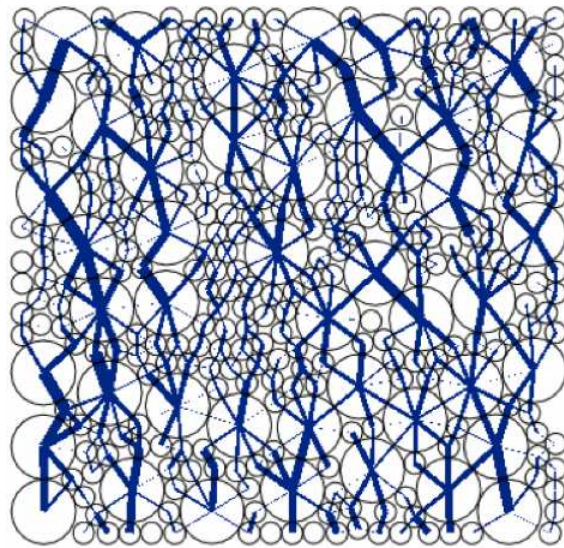


Topin et al. (2007)

# Contact forces

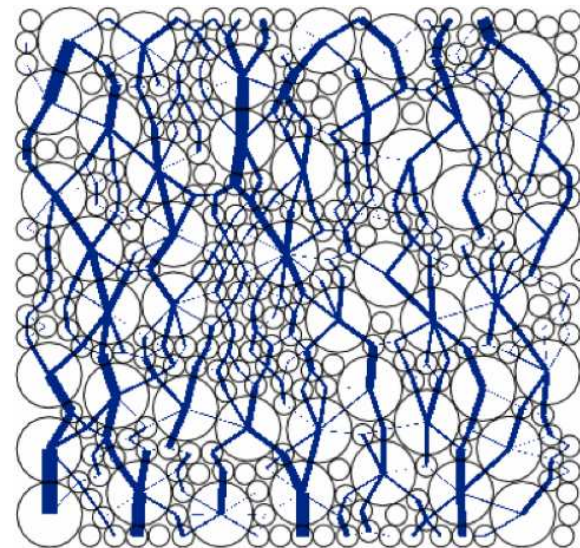


DEM



(a)

LEM



(b)



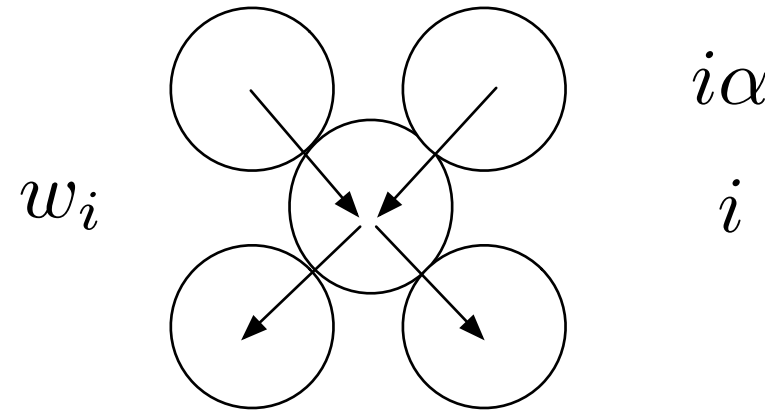
# Statistical models

**q-model** The forces are assumed to be a scalar quantity «propagating» along successive layers of particles.

$$q_{i\alpha} \quad \sum_{\alpha} q_{i\alpha} = 1$$

$$w_i = \sum_{\alpha} q_{i\alpha} w_{i\alpha} \quad \text{stress}$$

$$f_{i\alpha} = q_{i\alpha} w_{i\alpha} \quad \text{force}$$



Coppersmith et al. (1998)

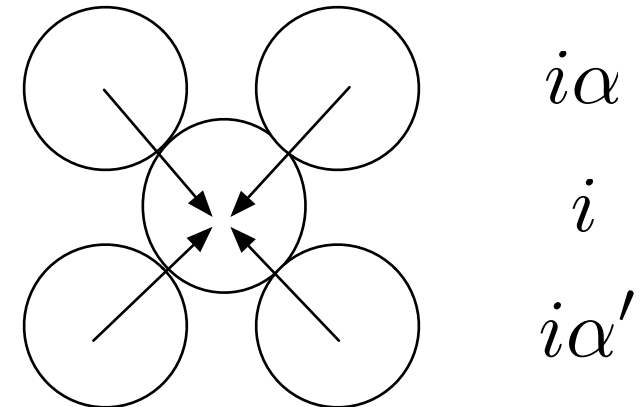
$$\Rightarrow P(w) = n^n \frac{w^{n-1}}{(n-1)!} e^{-nw} \quad \Rightarrow \quad P(f) = 2 e^{-2f}$$

$$n = 2$$

## A more general scalar model

$$\sum_{\alpha} f_{i\alpha} = \sum'_{\alpha} f_{i\alpha'} \quad \text{Equilibrium}$$

$\Rightarrow f$  additively conserved



$$P_n(f_{1\alpha}, \dots, f_{n\alpha}) = P_n(f_{1\alpha'}, \dots, f_{n\alpha'}) \quad \text{Invariance by force reversal}$$

$$P_n(f_{1\alpha}, \dots, f_{n\alpha}) = P(f_{1\alpha}), \dots, P(f_{n\alpha}) \quad \text{Decorrelation (molecular chaos)}$$

$\Rightarrow \ln[P(f)]$  additively conserved

$$\Rightarrow \ln[P(f)] = a + b f \quad \Rightarrow P(f) = \beta e^{-\beta f}$$

# Stress tensor

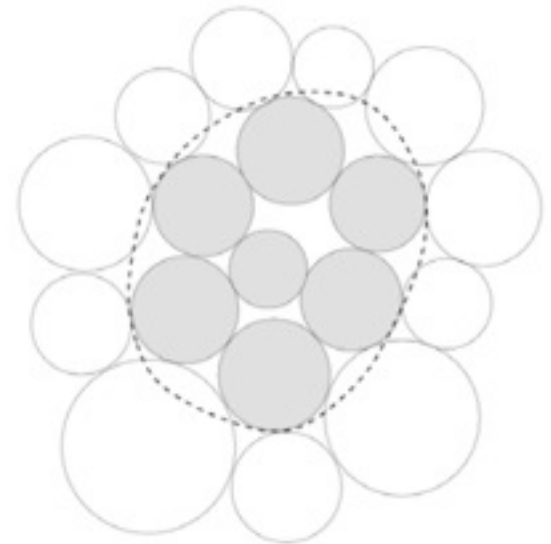
The Cauchy stress tensor in a granular material at the RVE scale is an average over the particle stresses. The particle stresses can be obtained from the contact forces by means of **internal moment tensors**.

Consider a domain and the forces acting at its boundary. We assume that the particle move according to an affine virtual velocity field:

$$v_{\alpha} = b_{\alpha\beta} r_{\beta}$$

The total power is a sum of internal and external powers and it vanishes when the particles are in equilibrium:

$$\mathcal{P} = \mathcal{P}_{int} + \mathcal{P}_{ext} = 0$$



$$\Rightarrow \mathcal{P}_{int} = -\mathcal{P}_{ext} = \sum_c v_\alpha^c f_\alpha^c = b_{\alpha\beta} \sum_c r_\alpha^c f_\beta^c$$

We set  $M_{\alpha\beta} = \sum_c r_\alpha^c f_\beta^c$       Internal moment tensor  
Moreau (1998)

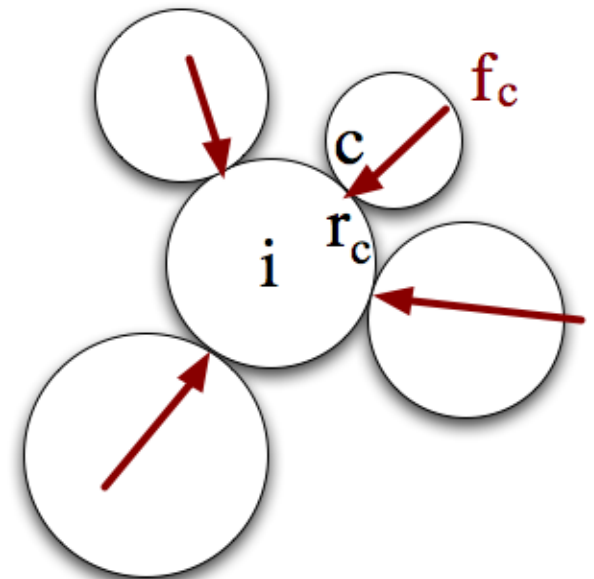
For a rigid motion,  $b_{\alpha\beta}$  is anti-symmetric and  $\mathcal{P}_{int} = 0$

$\Rightarrow M_{\alpha\beta}$  is a symmetric tensor.

Properties:

- 1) Symmetric
- 2) Independent of the origin of coordinates
- 3) Additive due to the action/reaction law

$$M_{\alpha\beta}^{i \cup j} = M_{\alpha\beta}^i + M_{\alpha\beta}^j$$



4) The density of internal moments tends to the Cauchy stress tensor as the number density of the particles increases:

$$\frac{1}{V} \sum_{i \in V} M_{\alpha\beta}^i \rightarrow \sigma_{\alpha\beta}$$

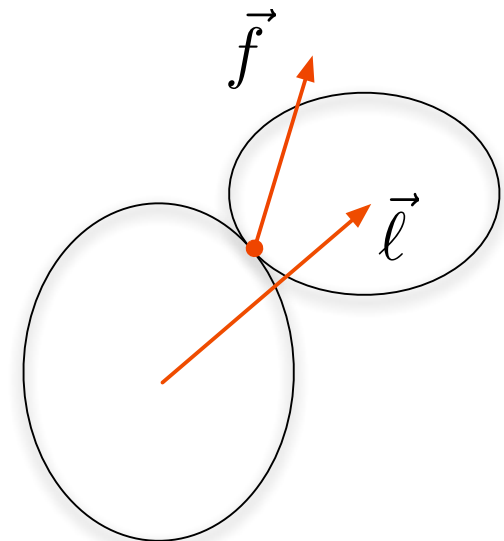
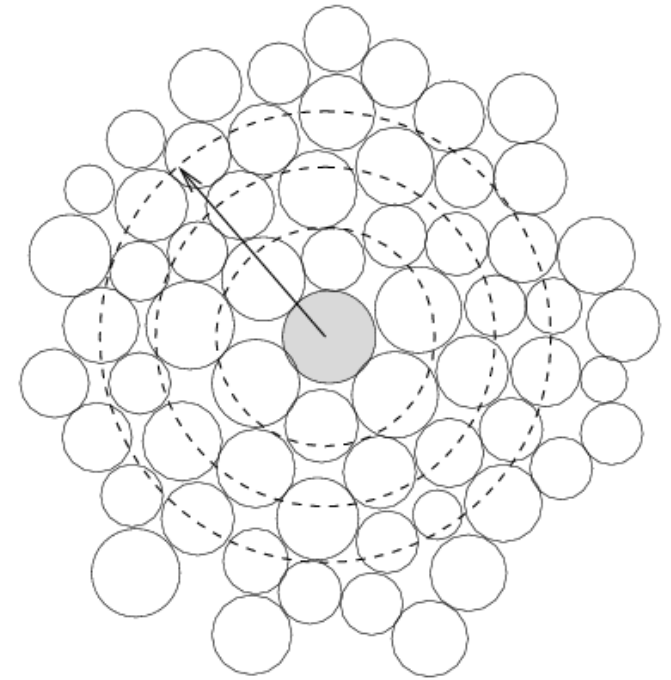
$$N_p \rightarrow \infty$$

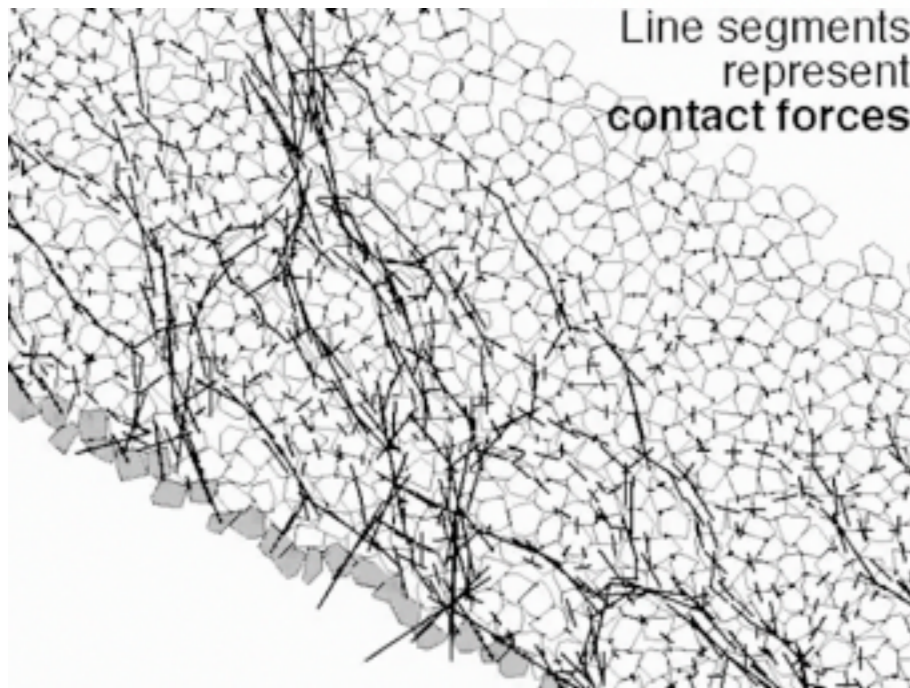
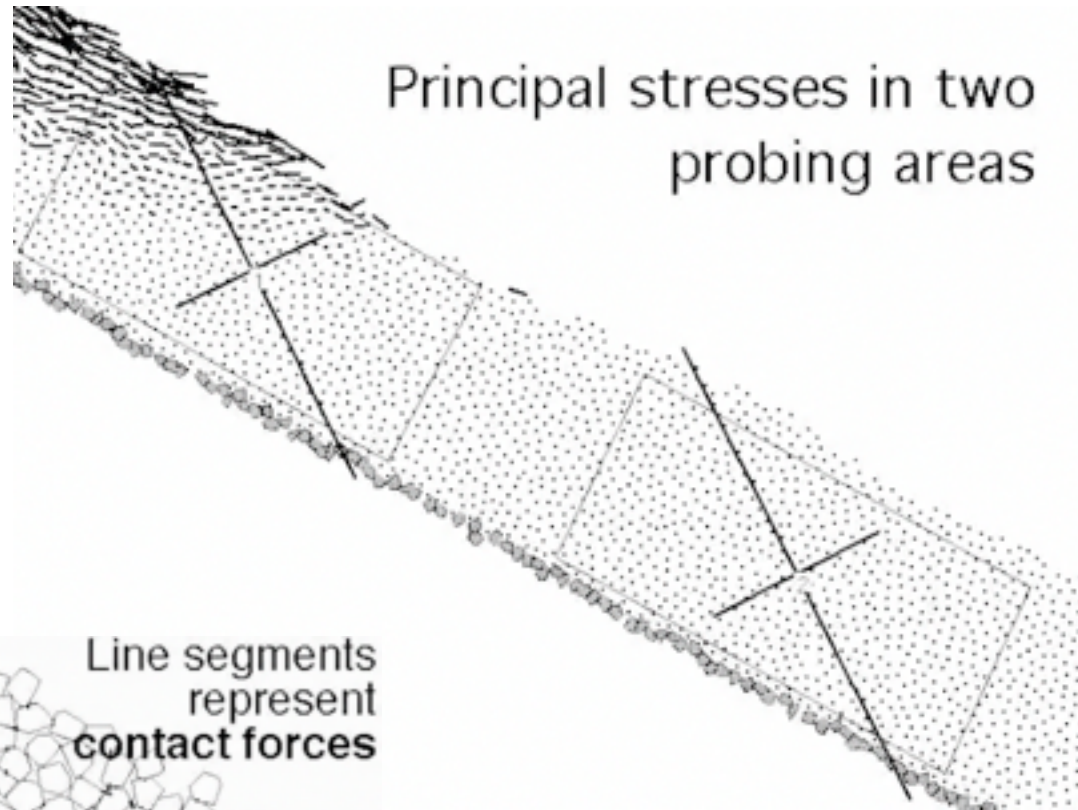
By taking the origin for each particle at its center of mass, we get

$$\sigma_{\alpha\beta} = \frac{1}{V} \sum_{i \in V} M^i = \frac{1}{V} \sum_{c \in V} f_{\alpha}^c \ell_{\beta}^c$$

$$\Rightarrow \sigma_{\alpha\beta} = n_c \langle f_{\alpha} \ell_{\beta} \rangle$$

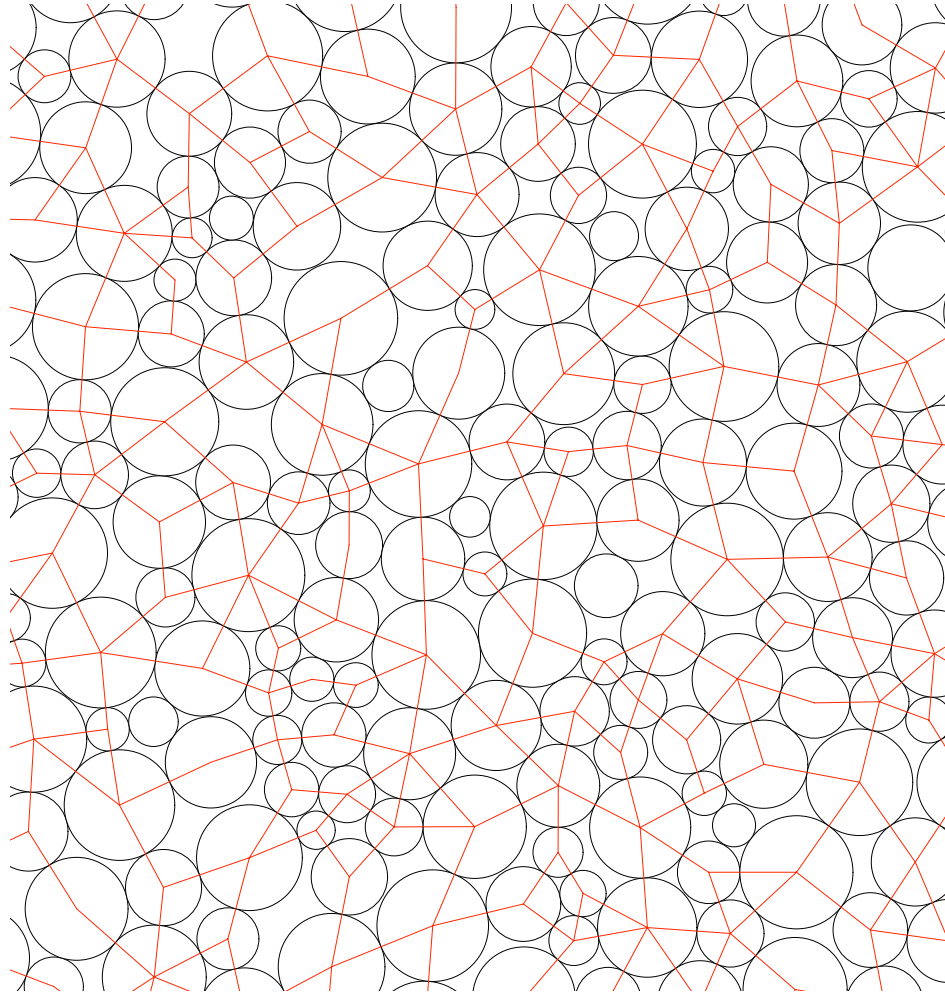
$n_c$  number density of contacts





Moreau (1998)

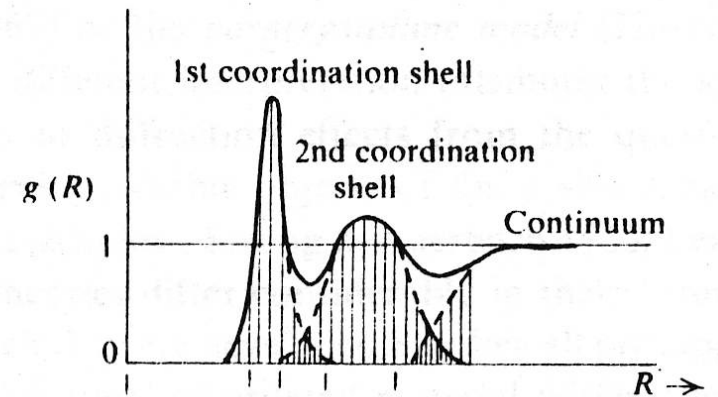
# Fabric variables



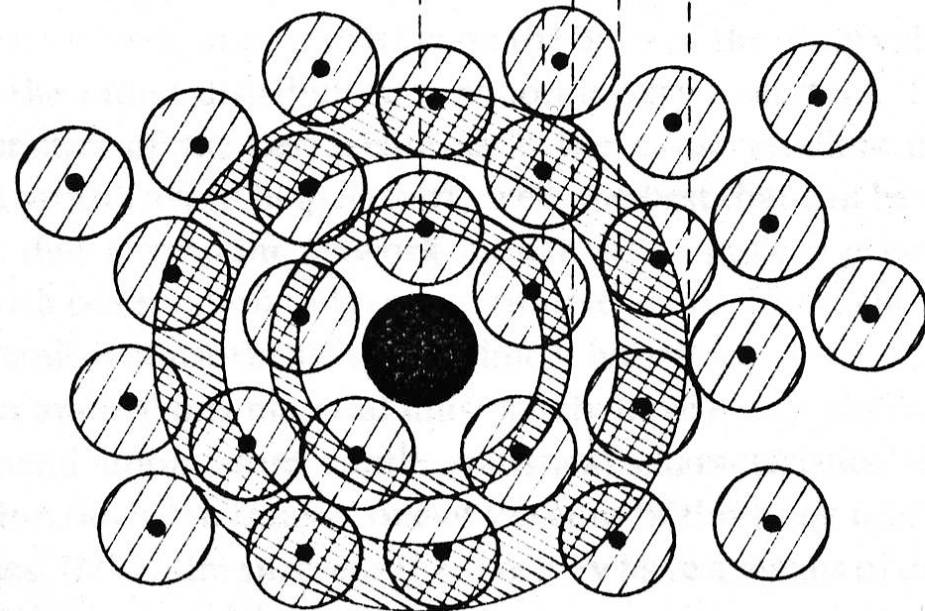
Classically, amorphous materials are described by the correlation functions of the particle positions.

**Radial distribution function:**  
number density of particles as a function of the distance from a particle, averaged over all particles:

$$g(r) = \frac{n(r)}{n}$$

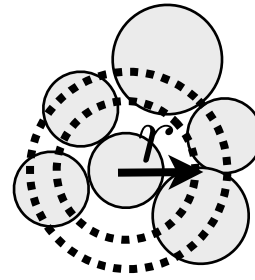


Short-range order

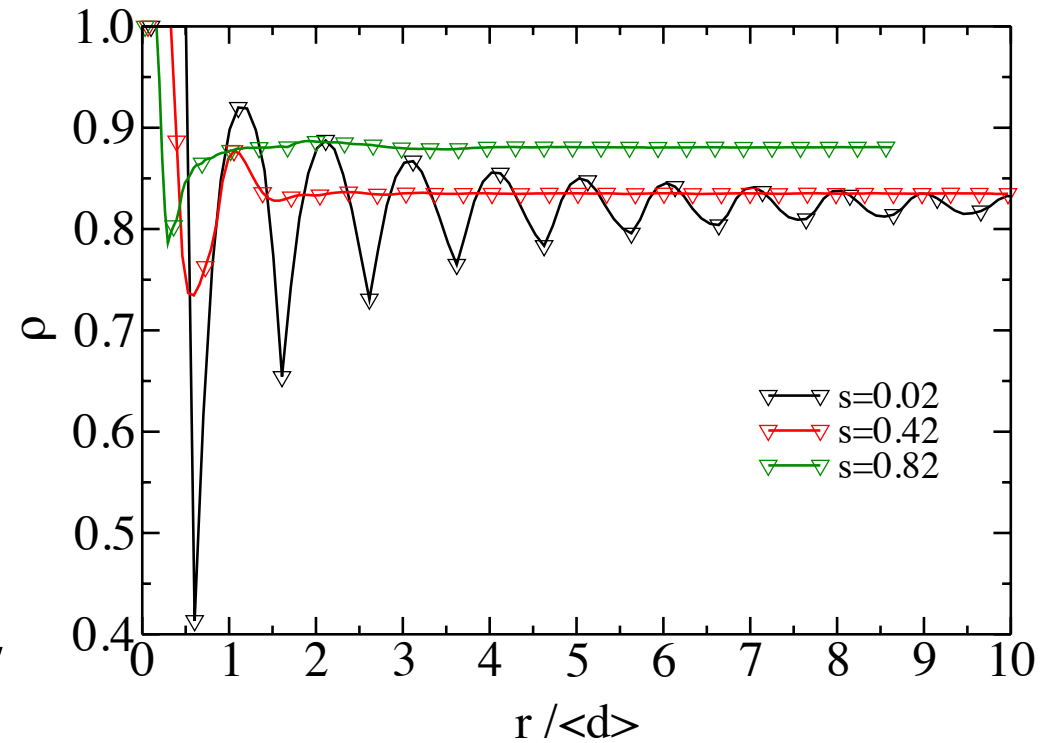
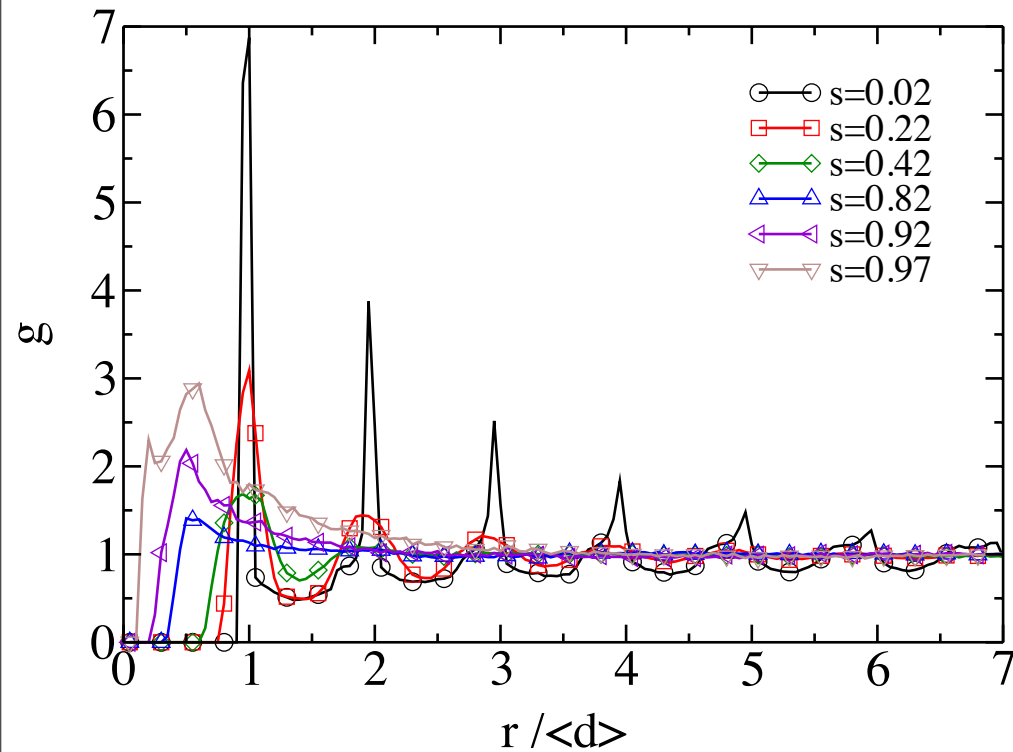




$$g(r) = \frac{n(r)}{n}$$



$$\rho(r)$$



Radial distribution function of granular packings for different particle size spans (Voivret et al., 2007).

But the radial distribution function describes only the **metric disorder**. It may be used for the space-filling properties of the grains.

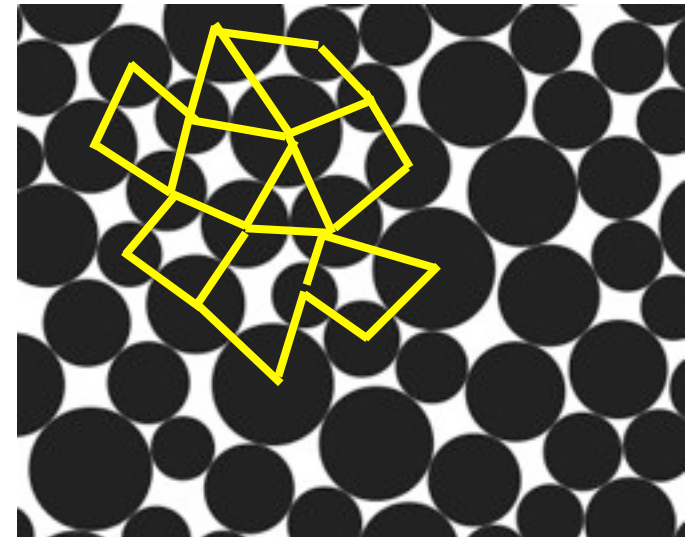
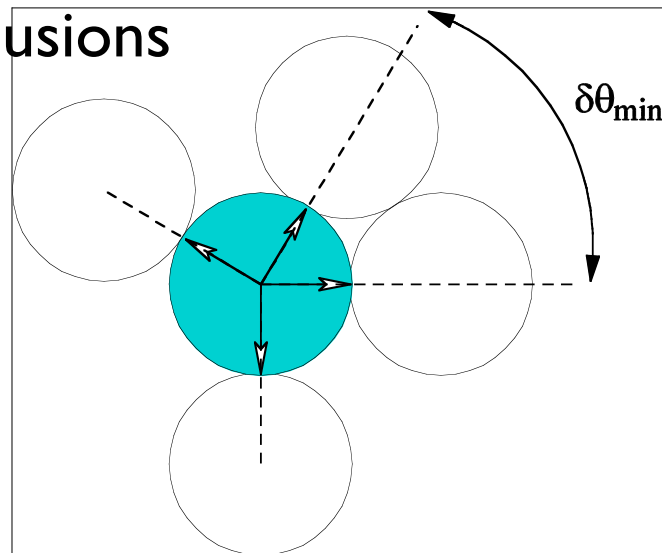
Most relevant fabric variables are those related to the **contact network** and its disorder as a result of contact interactions between particles.

The contact network is characterized by:

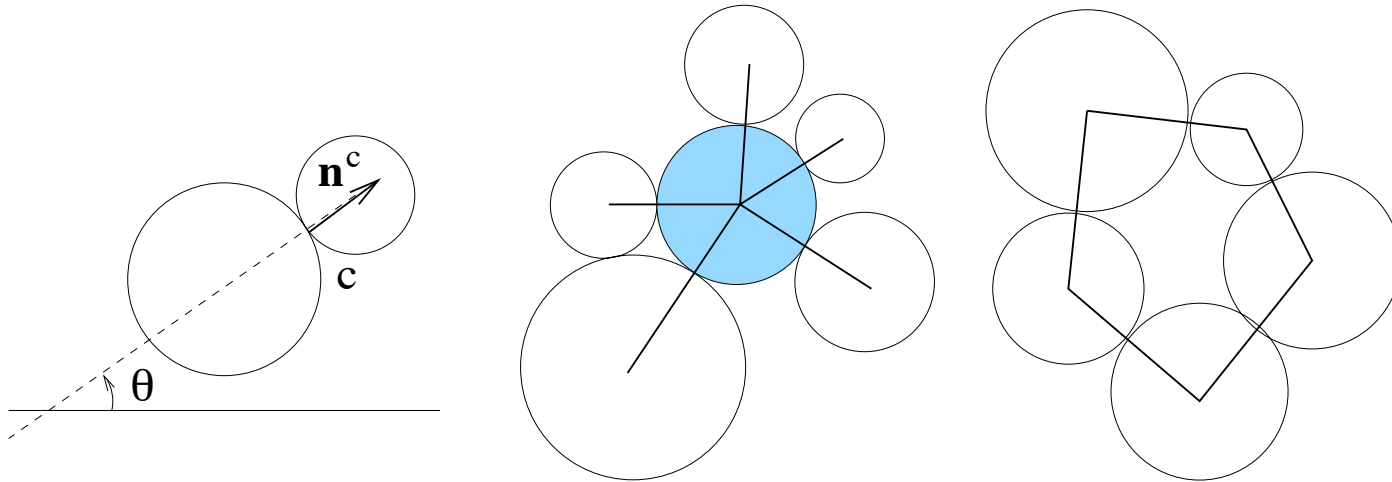
Topological disorder

Anisotropy

Steric exclusions



The topological disorder is best described by the variation of the local environments of particles and cells (cycles).



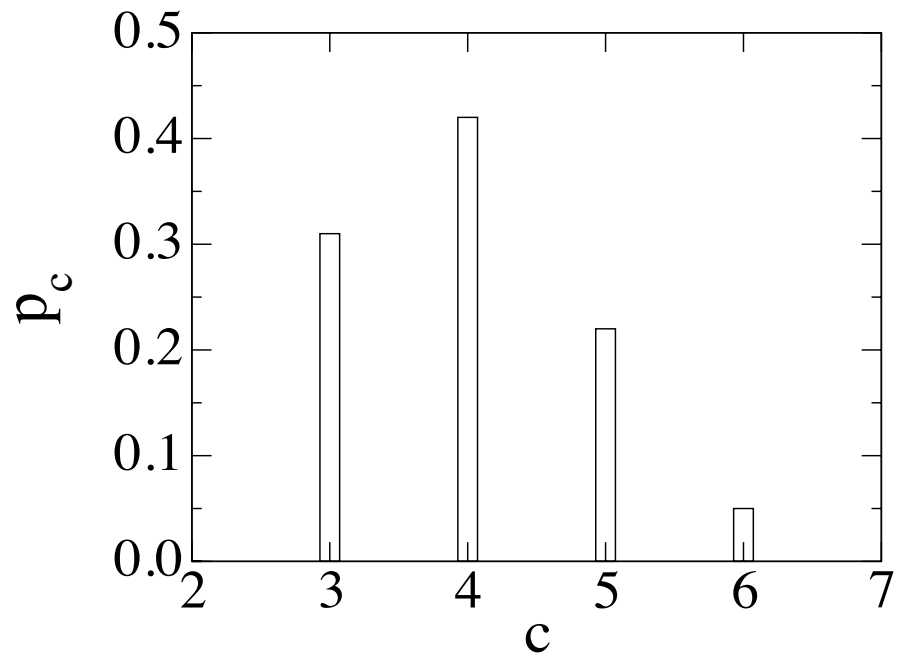
$z$  coordination number

$m$  valence  $m = 2 + \frac{4}{z - 2}$

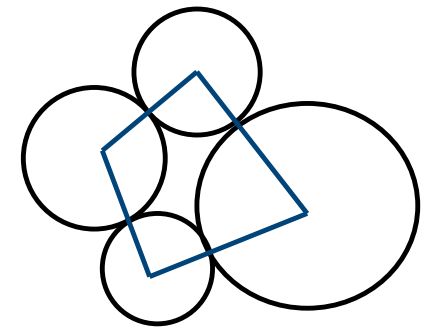
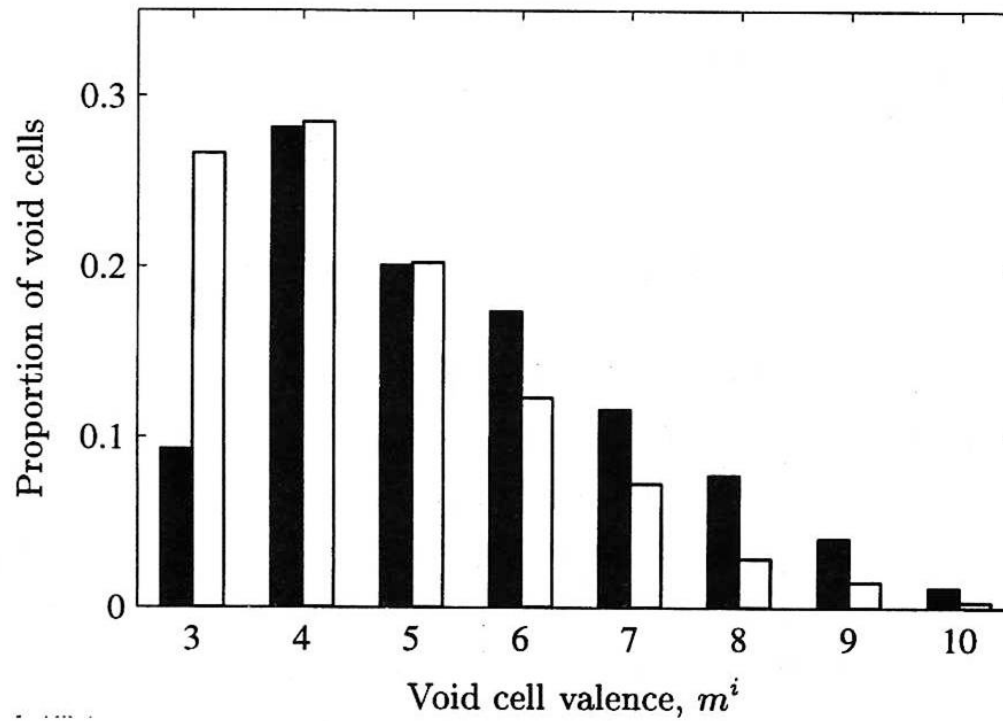
$P_c(c)$  fraction of particles with  $c$  contacts

$$z = \sum_{k=1}^{\infty} k P_c(k)$$

$P_m(m)$  fraction of cells composed of  $m$  sides



A weakly polydisperse packing of disks

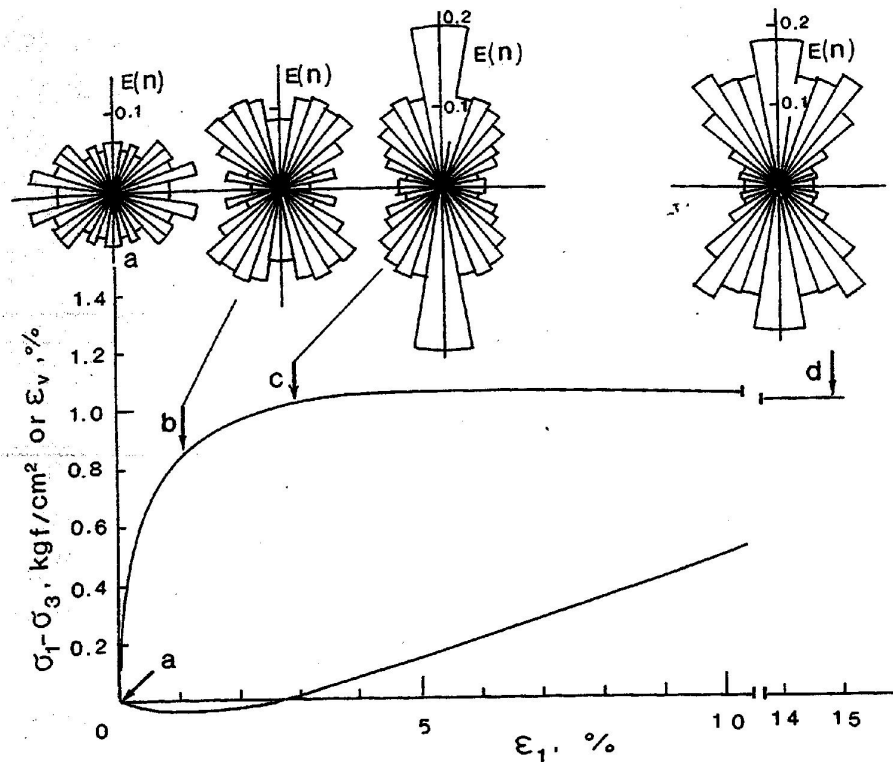


Yang et al. (2002)

Distribution of valence numbers in a sheared 3D packing of spheres.

## Fabric anisotropy

Contact orientations are not isotropically distributed.



Polar diagram of contact orientations

$$P(\vec{n})$$

Oda (1972)

This is a periodic function and may be expanded on a base of Fourier functions (2D) or spherical harmonics (3D):

$$P(\vec{n}) = P_0 + P_{ij}e_{ij}(\vec{n}) + P_{ijkl}e_{ijkl}(\vec{n}) + \dots$$

$P_{ij}$      $P_{ijkl}$     **fabric tensors** of increasing order

$e_{ij}$      $e_{ijkl}$     a base of orthonormal functions

$$e_{ij} = n_i n_j \quad e_{ijkl} = n_i n_j n_k n_l$$

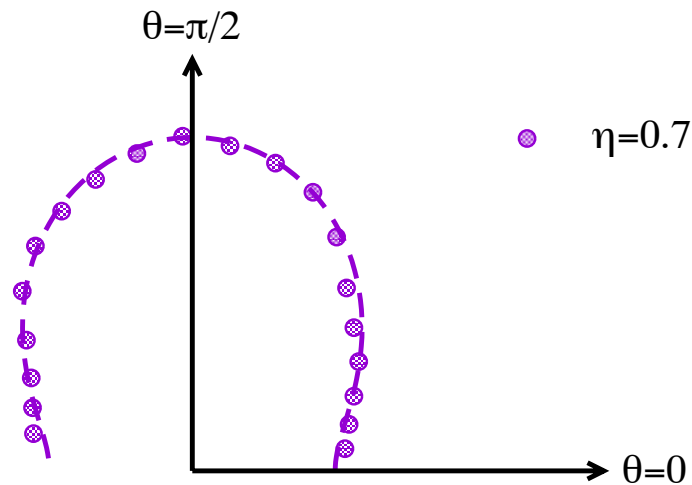
$$P_{ij} = \int_{\Omega} P(\vec{n}) e_{ij} d\vec{n} = \langle e_{ij} \rangle$$

2D example     $P(\theta)$      $\vec{n} = (\cos \theta, \sin \theta)$

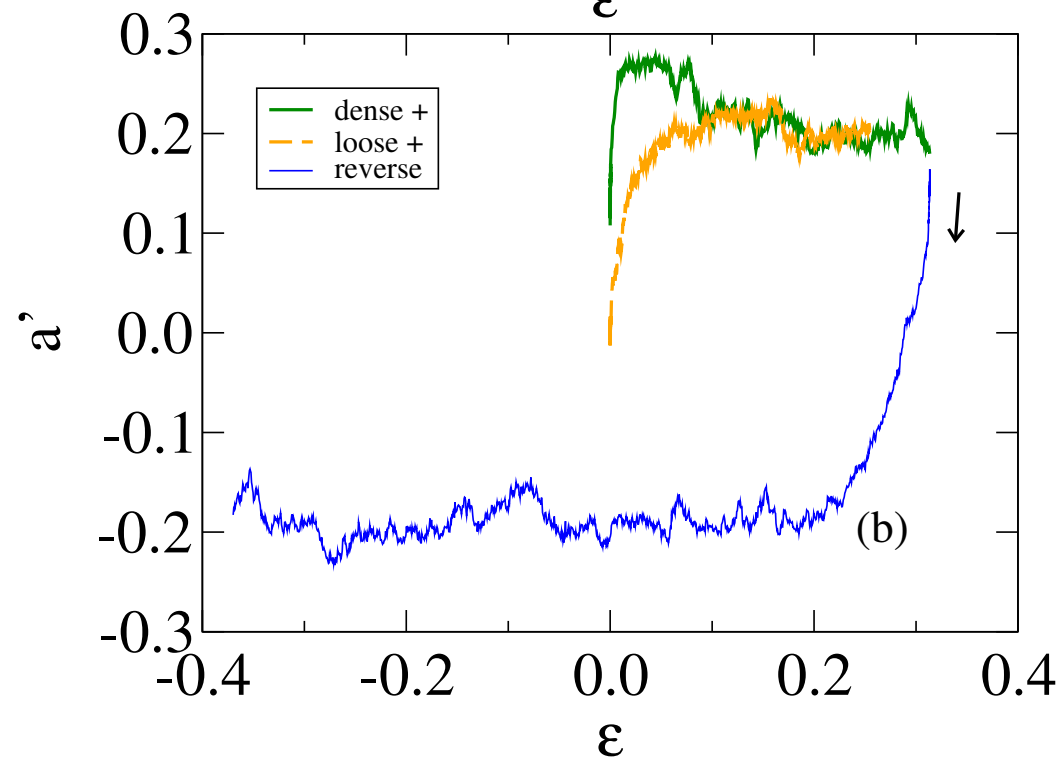
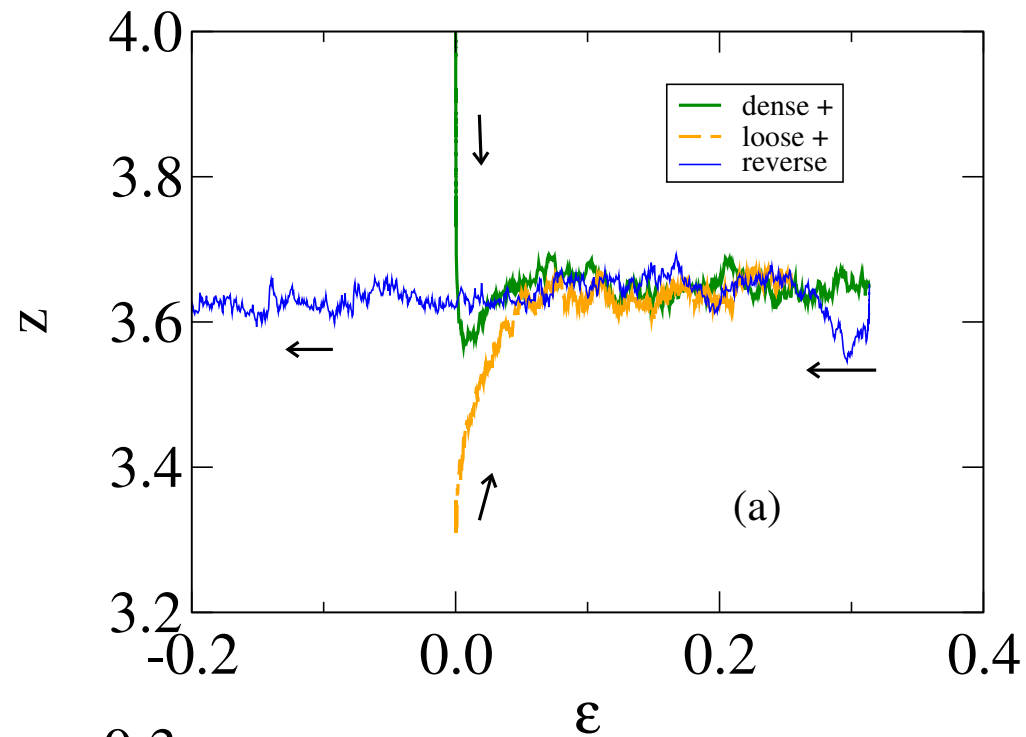
$$P(\theta) = \frac{1}{\pi} \{ 1 + a \cos 2(\theta - \theta_c) + \dots \}$$

$$F_{ij} = \langle n_i n_j \rangle = \int_0^\pi n_i n_j P(\theta) d\theta$$

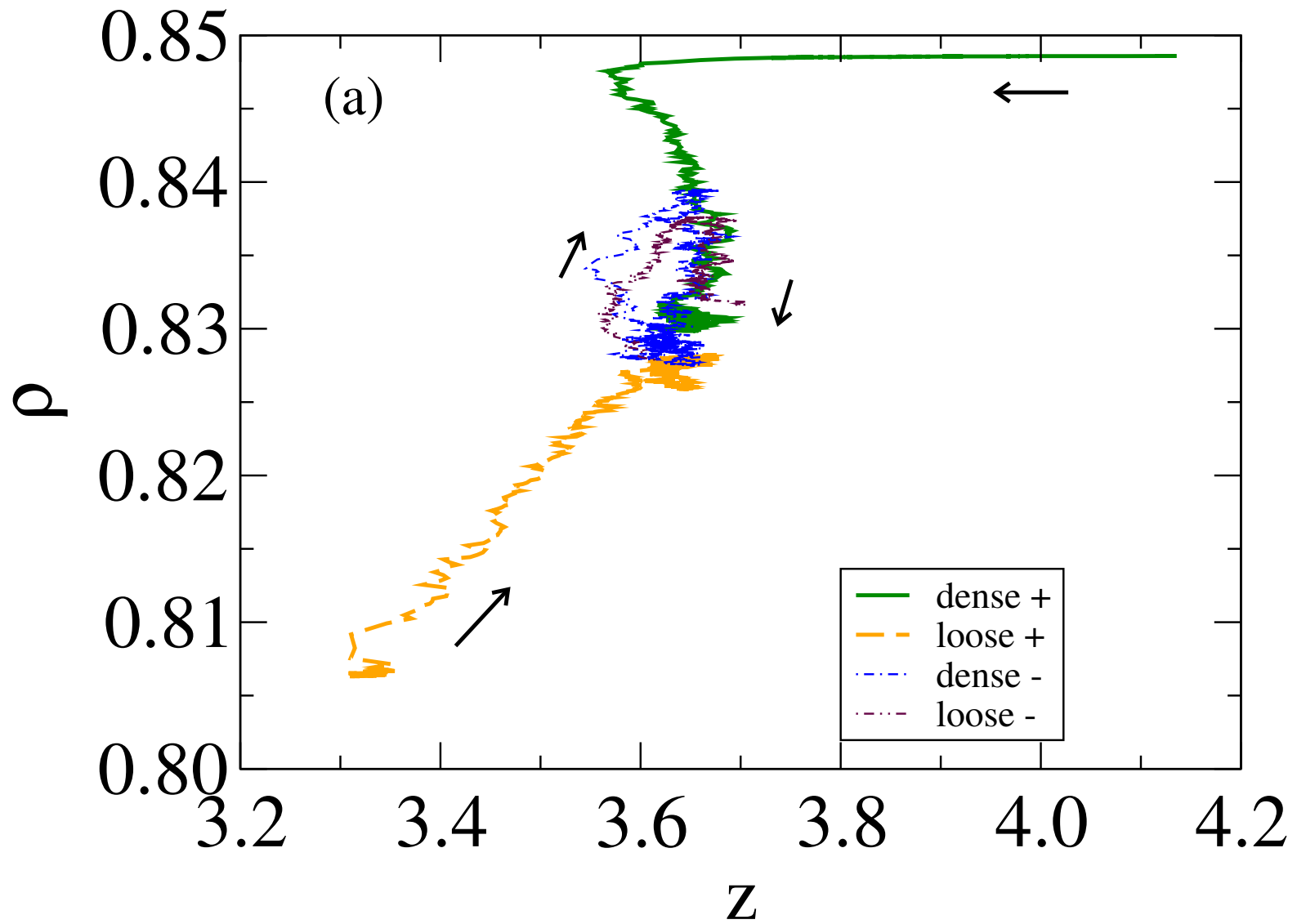
$\Rightarrow$      $a = 2(F_1 - F_2)$     lowest-order anisotropy







Radjai and Roux (2003)



During shear reversal, the solid fraction is anti-correlated with coordination number.

# Harmonic decomposition

$$\sigma_{ij} = n_b \langle l_i^\alpha f_j^\alpha \rangle_\alpha$$

The stress tensor is a state function if the internal state is represented by the discrete set:

$$\{ \vec{f}^\alpha, \vec{l}^\alpha \}$$

A statistical description requires the joint probability density function:

$$P_{\ell f}(\vec{\ell}, \vec{f})$$

$$\Rightarrow \sigma_{ij} = n_b \int_{\mathcal{A}_\ell} \int_{\mathcal{A}_f} l_i f_j P_{\ell f}(\vec{\ell}, \vec{f}) d\vec{\ell} d\vec{f}$$

$$\vec{\ell} = \ell \vec{n} \quad \vec{f} = f_n \vec{n} + f_t \vec{t}$$

We may keep only the angular information by integrating over the forces and branch vector lengths:

$$\sigma_{ij} = n_b \int_{\Omega} \langle \ell \rangle(\vec{n}) P(\vec{n}) \{ \langle f_n \rangle(\vec{n}) n_i(\vec{n}) n_j(\vec{n}) + \langle f_t \rangle(\vec{n}) n_i(\vec{n}) t_j(\vec{n}) \} d\vec{n}$$

with 
$$P(\vec{n}) = \int_{\ell=0}^{\infty} \int_{\mathcal{A}_f} P_{\ell f}(\vec{\ell}, \vec{f}) d\ell d\vec{f}$$

$$\langle \ell \rangle(\vec{n}) P(\vec{n}) = \int_{\mathcal{A}_f} \ell P_{\ell f}(\vec{\ell}, \vec{f}) d\vec{f}$$

$$\langle f_n \rangle(\vec{n}) P(\vec{n}) = \int_{\ell=0}^{\infty} \int_{\mathcal{A}_f} f_n P_{\ell f}(\vec{\ell}, \vec{f}) d\ell d\vec{f}$$

$$\langle f_t \rangle(\vec{n}) P(\vec{n}) = \int_{\ell=0}^{\infty} \int_{\mathcal{A}_f} f_t P_{\ell f}(\vec{\ell}, \vec{f}) d\ell d\vec{f}$$

## Harmonic approximation at leading order (here in 2D)

$$P(\theta) \simeq \frac{1}{2\pi} \{1 + a_b \cos 2(\theta - \theta_b)\}$$

$$\langle \ell \rangle(\theta) \simeq \ell_m \{1 + a_\ell \cos 2(\theta - \theta_b)\}$$

$$\langle f_n \rangle(\theta) \simeq f_m \{1 + a_n \cos 2(\theta - \theta_f)\}$$

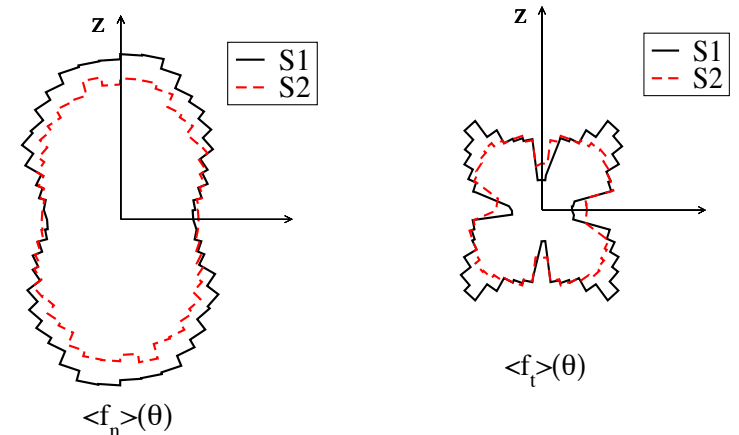
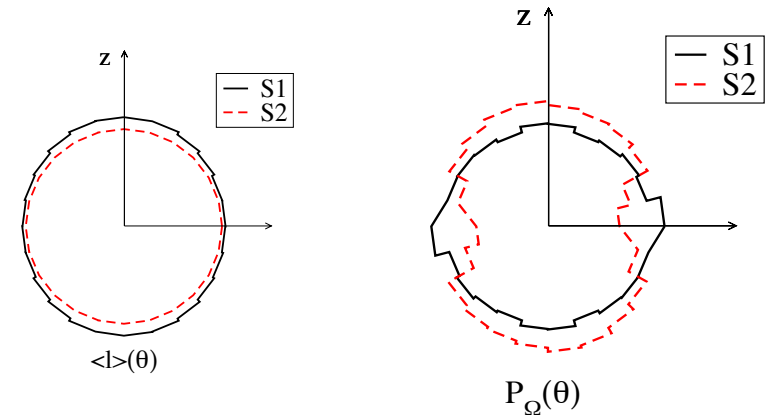
$$\langle f_t \rangle(\theta) \simeq f_m a_t \sin 2(\theta - \theta_f)$$

The last relation is imposed by the requirement of the balance of force moments:

$$\int P(\theta) \langle f_t \rangle(\theta) d\theta = 0$$

State parameters:

$$\{n_b, \ell_m, f_m, a_b, a_\ell, a_n, a_t, \theta_b, \theta_f\}$$



Examples of fabric and force functions in two triaxially compressed granular samples (Azéma et al., 2009)

Within the harmonic representation of fabric and force states, and keeping only the linear terms in anisotropies, the expression of the stress tensor leads to two state functions:

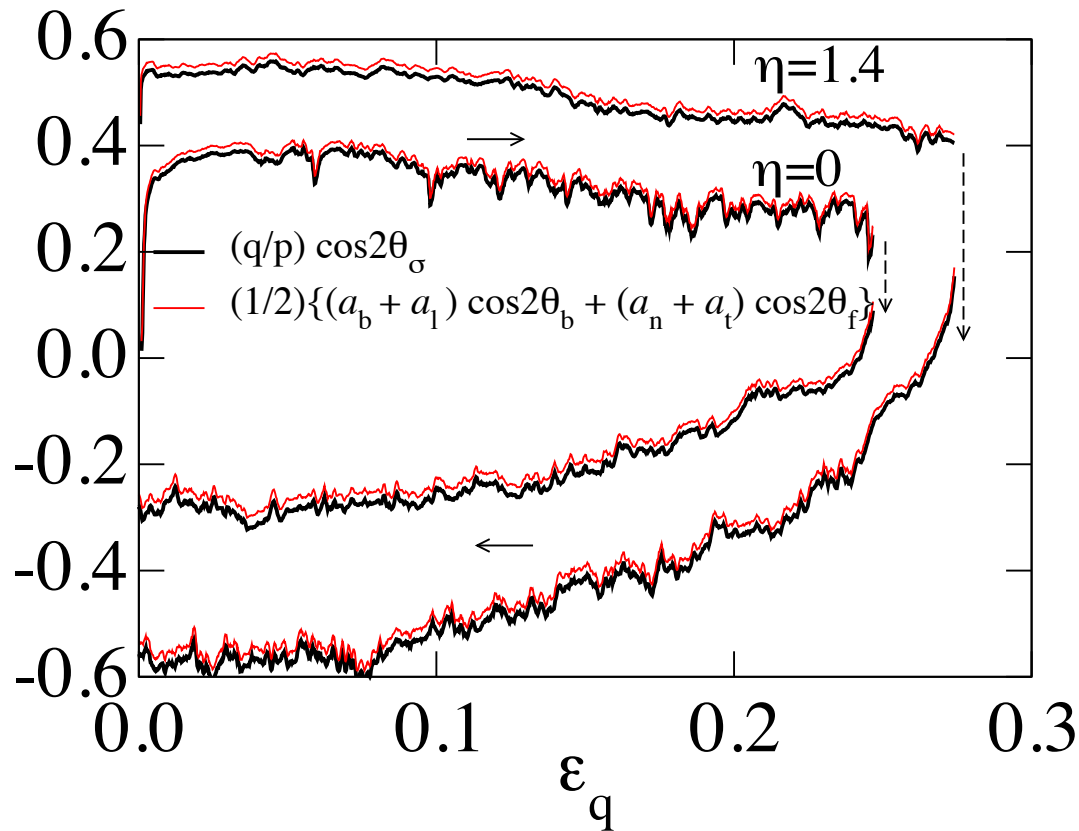
$$p \simeq \frac{1}{2} n_b \ell_m f_m$$

$$\frac{q}{p} \cos 2\theta_\sigma \simeq \frac{1}{2} \{ (a_b + a_\ell) \cos 2\theta_b + (a_n + a_t) \cos 2\theta_f \}$$

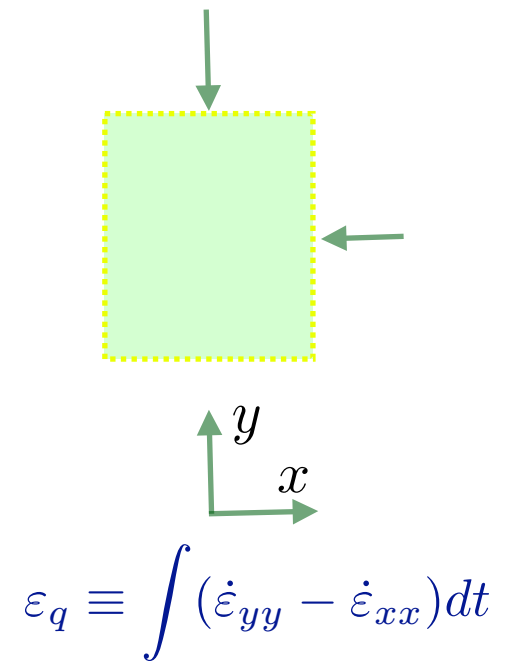
The first equation is the static analog of the ideal gas law for kinetic pressure. The second equation reveals that the stress deviator is controlled by the force and fabric anisotropies and their privileged directions.

$$\frac{q}{p} \cos 2\theta_\sigma \simeq \frac{1}{2} \{ (a_b + a_\ell) \cos 2\theta_b + (a_n + a_t) \cos 2\theta_f \}$$

Simulations by the contact dynamics method (biaxial compression, 5000 particles, initially isotropic, compression followed by extension):



Radjai et Richefeu (2009)



The shear strength reflects the ability of a granular material to build up force and fabric anisotropies, but is strongly modulated by phase factors.

## Fragile behavior

The phase differences are responsible for the fragile behavior.

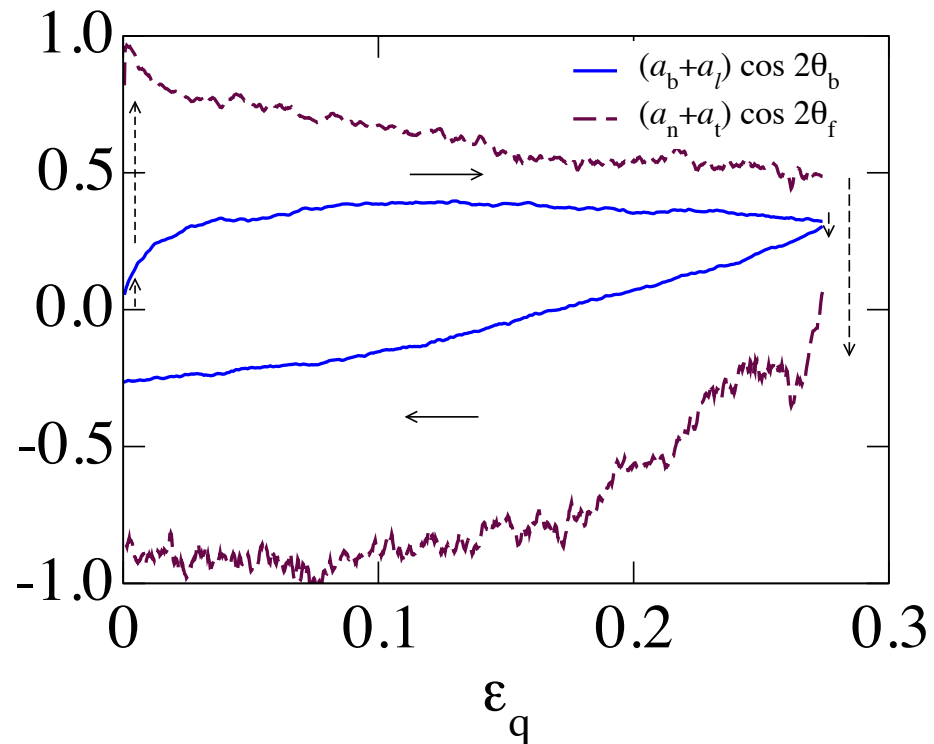
Weak formulation: The shear strength is largest along the loading path that conducted the system to its present state.

$$\theta_b = \theta_f = \theta_\sigma \quad \Rightarrow \quad \frac{q}{p} \simeq \frac{1}{2}(a_b + a_\ell + a_n + a_t)$$

$$\theta_\sigma = \theta_f = \theta_b + \frac{\pi}{2} \quad \Rightarrow \quad \frac{q}{p} \simeq \frac{1}{2}(-a_b - a_\ell + a_n + a_t)$$

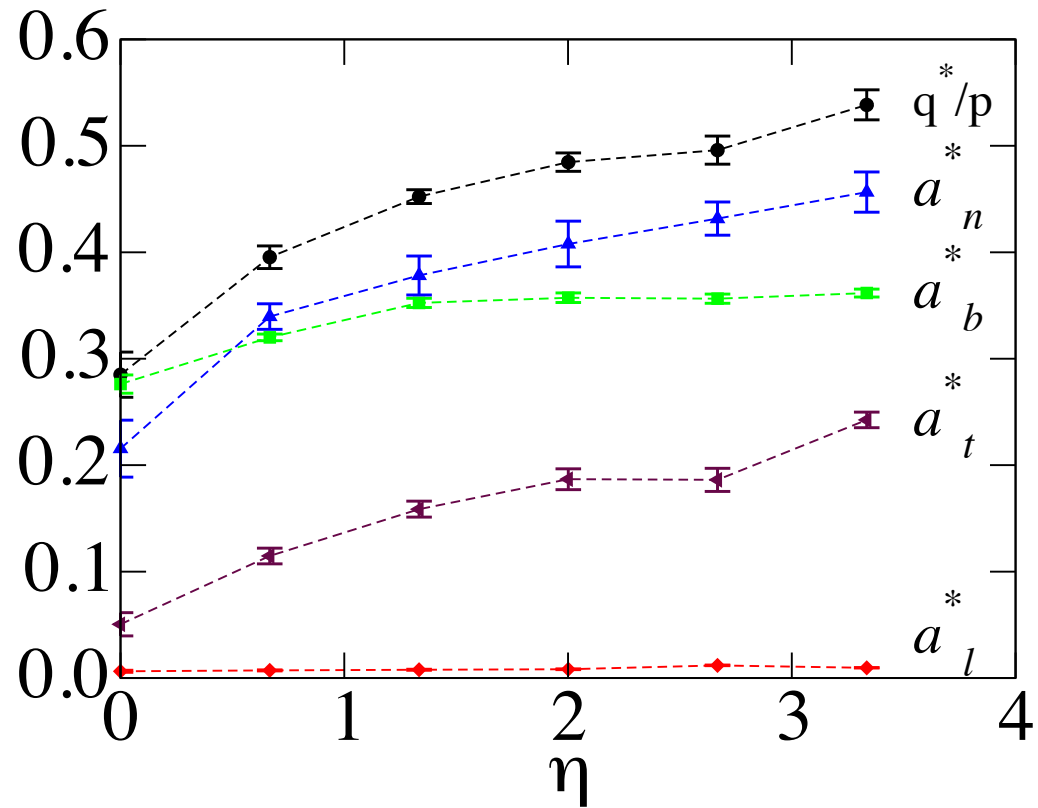
$$\frac{\Delta q}{p} = a_b + a_\ell$$

shear stress jump





The fragile character is influenced by adhesion only in the range  $\eta < 2$

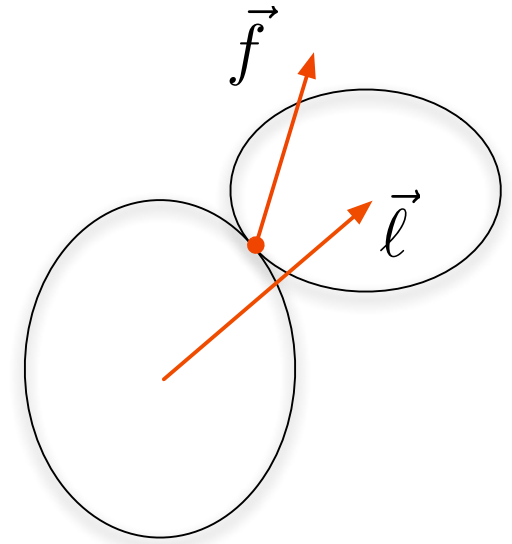


### 3D

$$P_{\Omega f \ell}(\vec{n}, \vec{f}, \ell)$$

$$\vec{\ell} = \ell \vec{n}$$

$$\vec{f} = f_n \vec{n} + f_t \vec{t}$$



**Fabric:**

$$P_{\Omega}(\Omega) = \frac{N_b(\Omega)}{N_b}$$

$$\langle \ell \rangle(\Omega) = \frac{1}{N_b(\Omega)} \sum_{c \in \mathcal{A}(\Omega)} \ell^c$$

**Force:**

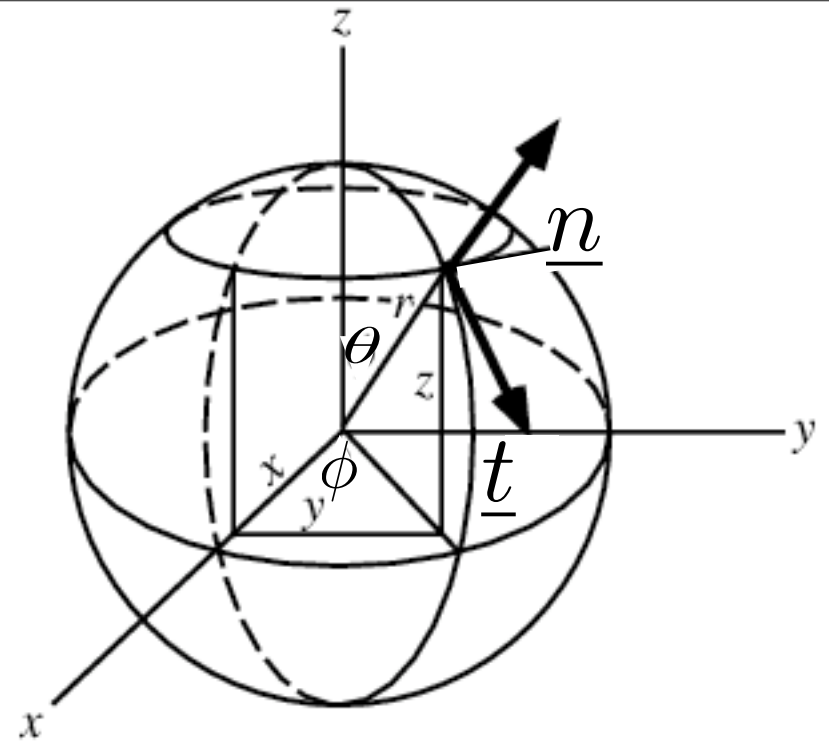
$$\langle f_n \rangle(\Omega) = \frac{1}{N_b(\Omega)} \sum_{c \in \mathcal{A}(\Omega)} f_n^c$$

$$\langle f_t \rangle(\Omega) = \frac{1}{N_b(\Omega)} \sum_{c \in \mathcal{A}(\Omega)} f_t^c$$

$$Y_m^l(\theta, \phi)$$

Under axisymmetric conditions:

$$Y_0^0 = 1 \quad Y_2^0 = 3 \cos^2 \theta - 1$$



$$P_\Omega(\theta) = \frac{1}{4\pi} \{1 + a (3 \cos^2 \theta - 1)\}$$

$$\Rightarrow \langle \ell \rangle(\theta) = \ell_0 \{1 + a_\ell (3 \cos^2 \theta - 1)\}$$

$$\langle f_n \rangle(\theta) = f_0 \{1 + a_n (3 \cos^2 \theta - 1)\}$$

$$\langle f_t \rangle(\theta) = f_0 a_t \sin 2\theta$$

## Expression of stress ratio within harmonic approximation

$$\sigma_{\alpha\beta} = n_b \langle \ell_\alpha f_\beta \rangle$$

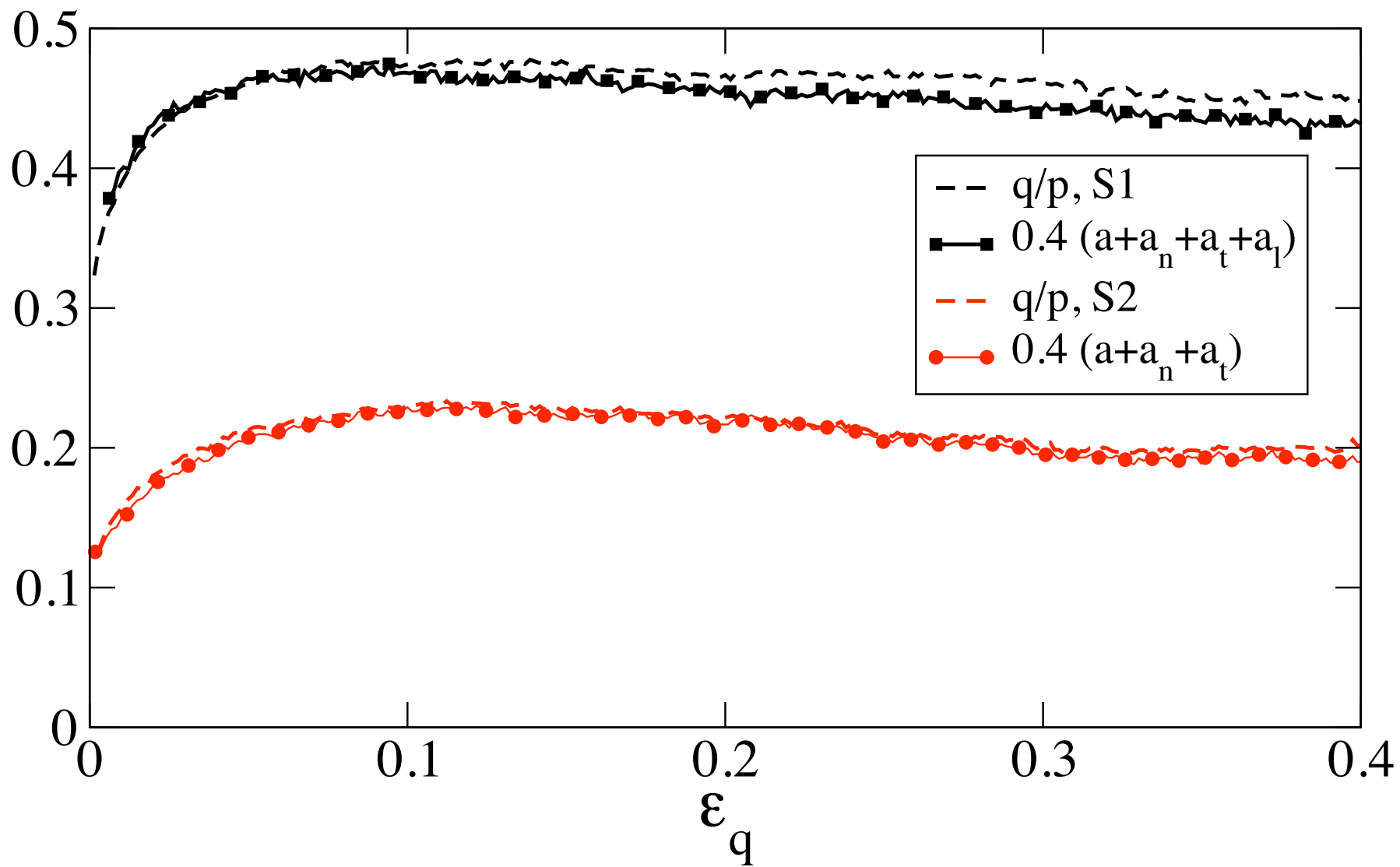
$$\sigma_{\alpha\beta} = n_b \int P_{\Omega f \ell}(\vec{n}, \vec{f}, \ell) \ell(\vec{n}) f_\beta(\vec{n}, \ell) n_\alpha d\Omega d\vec{f} d\ell$$

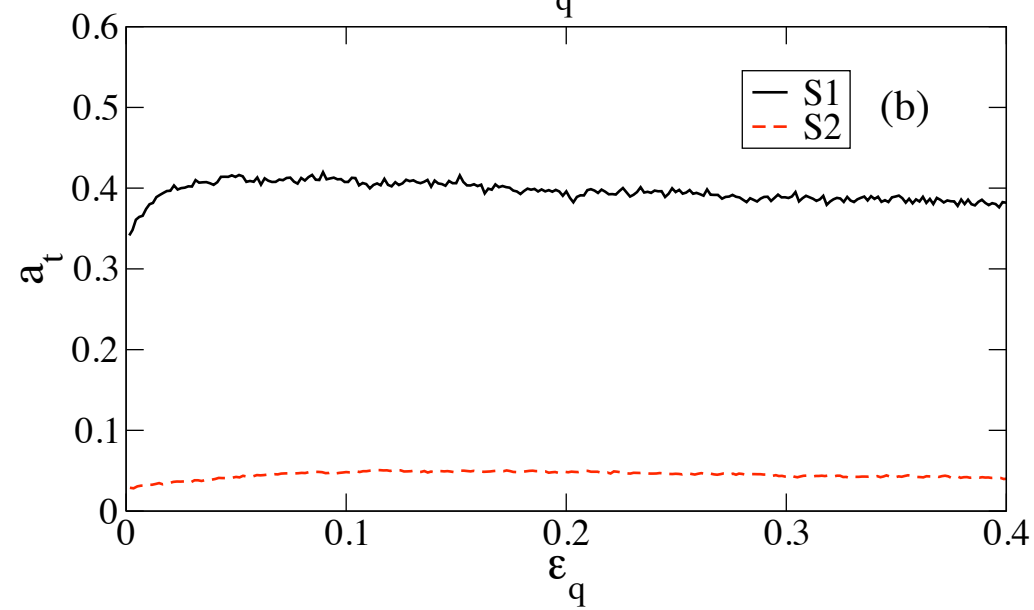
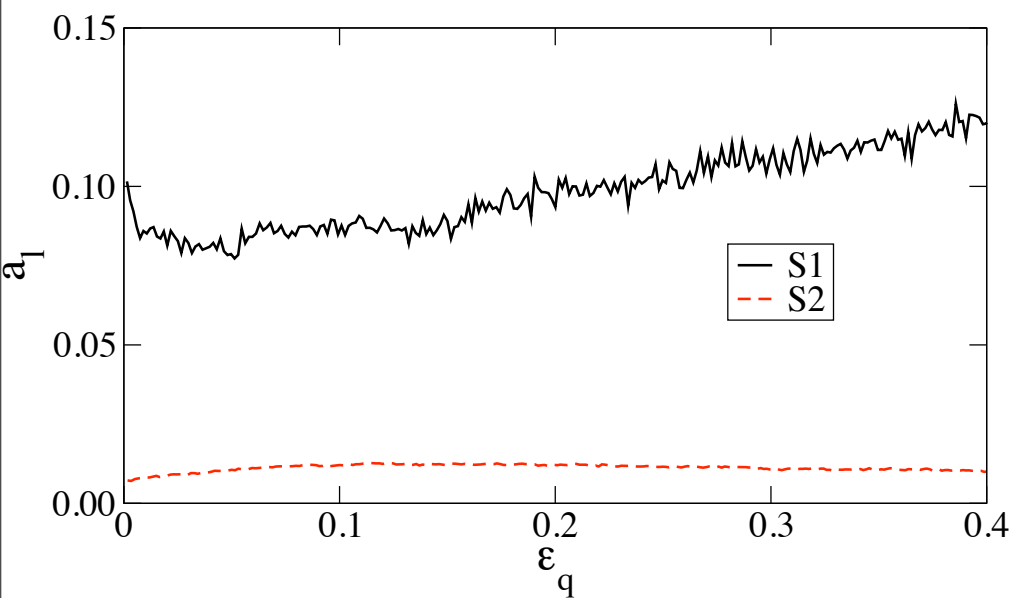
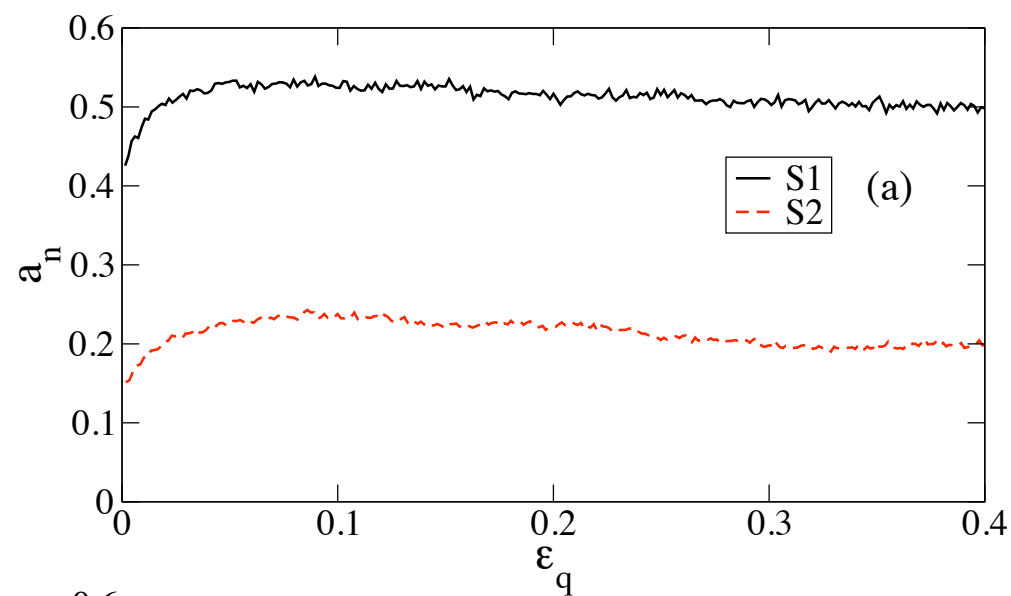
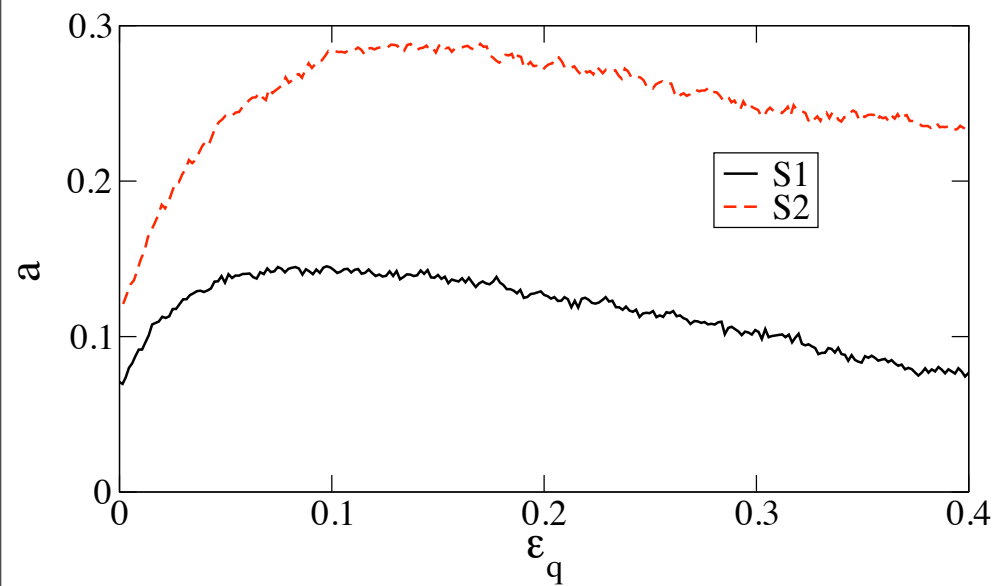
$$\text{with } d\Omega = \sin \theta d\theta d\phi$$

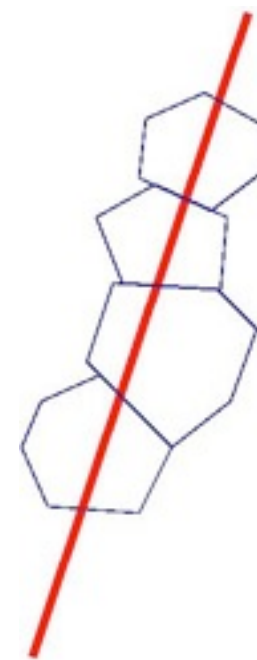
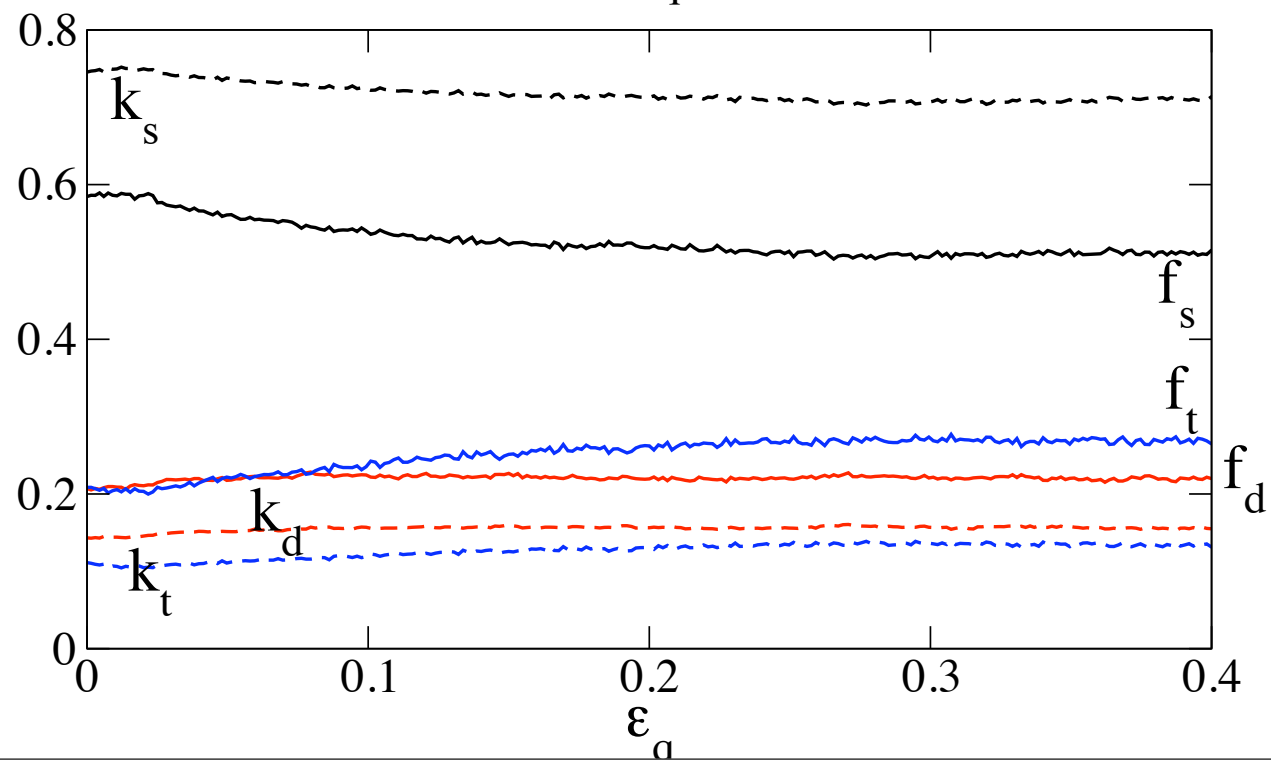
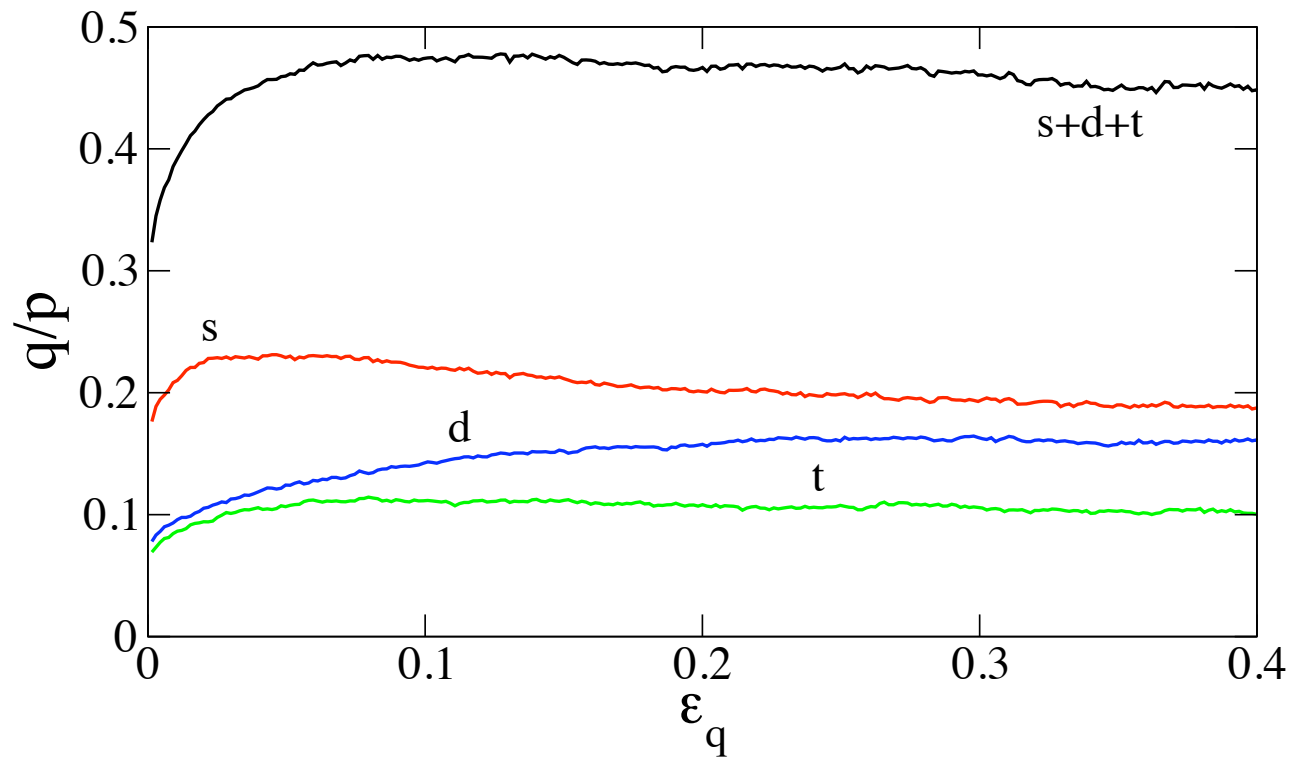
$$\Rightarrow \sigma_{\alpha\beta} = n_b \int P_{\Omega f}(\vec{n}, \vec{f}) \langle \ell \rangle(\vec{n}) f_\beta(\vec{n}) n_\alpha d\Omega d\vec{f}$$

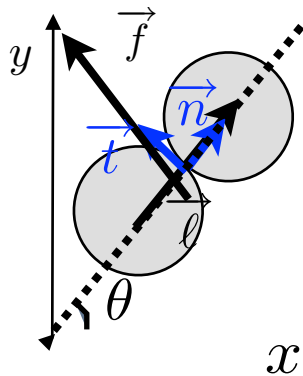
$$\Rightarrow \sigma_{\alpha\beta} = n_b \int P_{\Omega}(\vec{n}) \langle \ell \rangle(\vec{n}) n_\alpha \langle f_\beta \rangle(\vec{n}) d\Omega$$

$$\Rightarrow \frac{q}{p} \simeq \frac{2}{5} (a + a_l + a_n + a_t) \quad p \simeq n_b \ell_0 f_0$$









$$\langle f_n \rangle(\theta) \simeq \frac{\langle f \rangle}{\pi} \{1 + a_n \cos(2(\theta - \theta_n))\}$$

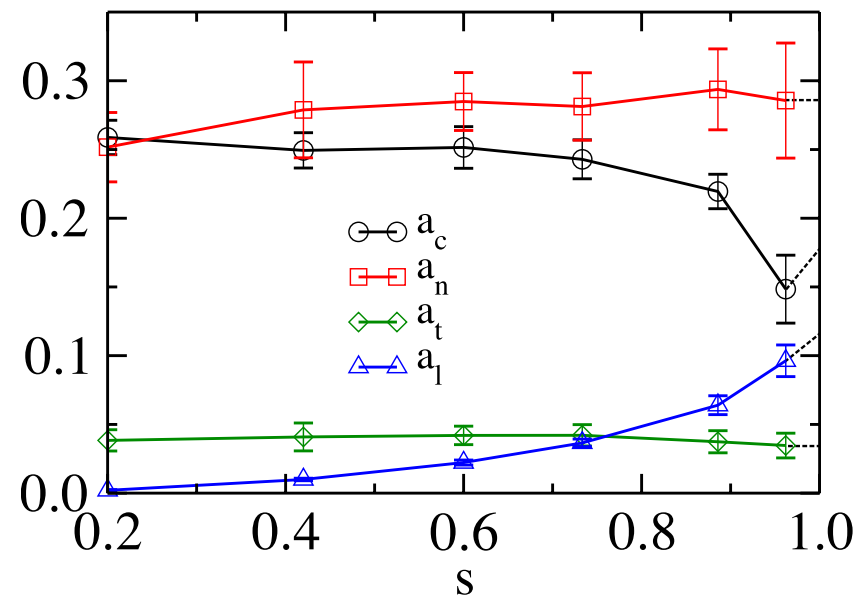
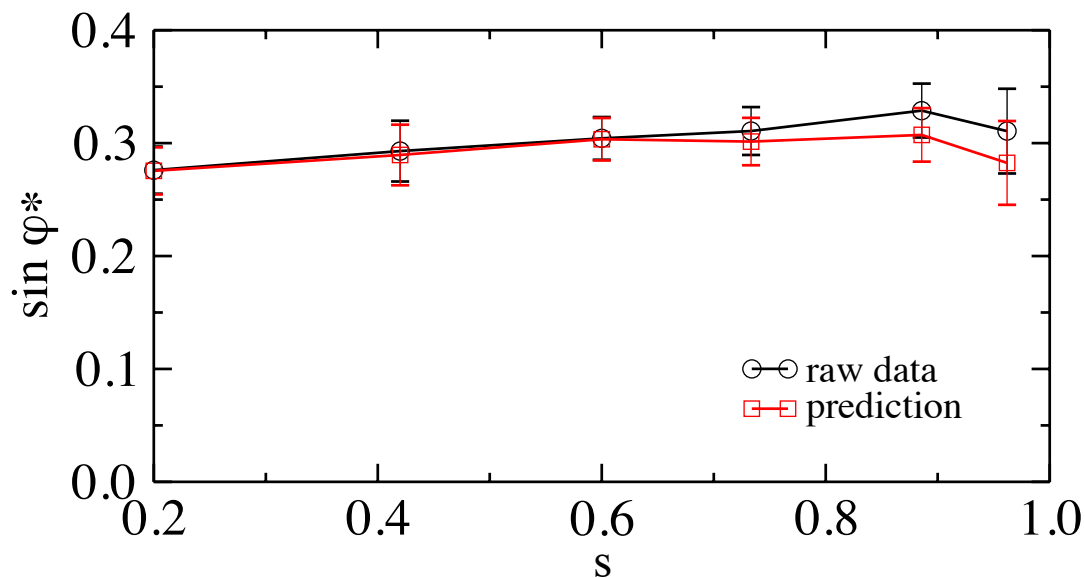
$$P(\theta) \simeq \frac{1}{\pi} [1 + a_c \cos(2(\theta - \theta_c))]$$

$$\langle \ell \rangle(\theta) \simeq \frac{\langle \ell \rangle}{\pi} \{1 + a_\ell \cos(2(\theta - \theta_\ell))\}$$

$$\langle f_t \rangle(\theta) \simeq \frac{\langle f \rangle}{\pi} \{-a_t \sin(2(\theta - \theta_t))\}$$

$$\frac{q}{p} = cte \simeq \frac{1}{2} (a_c + a_l + a_n + a_t)$$

Voivret et al. (2009)



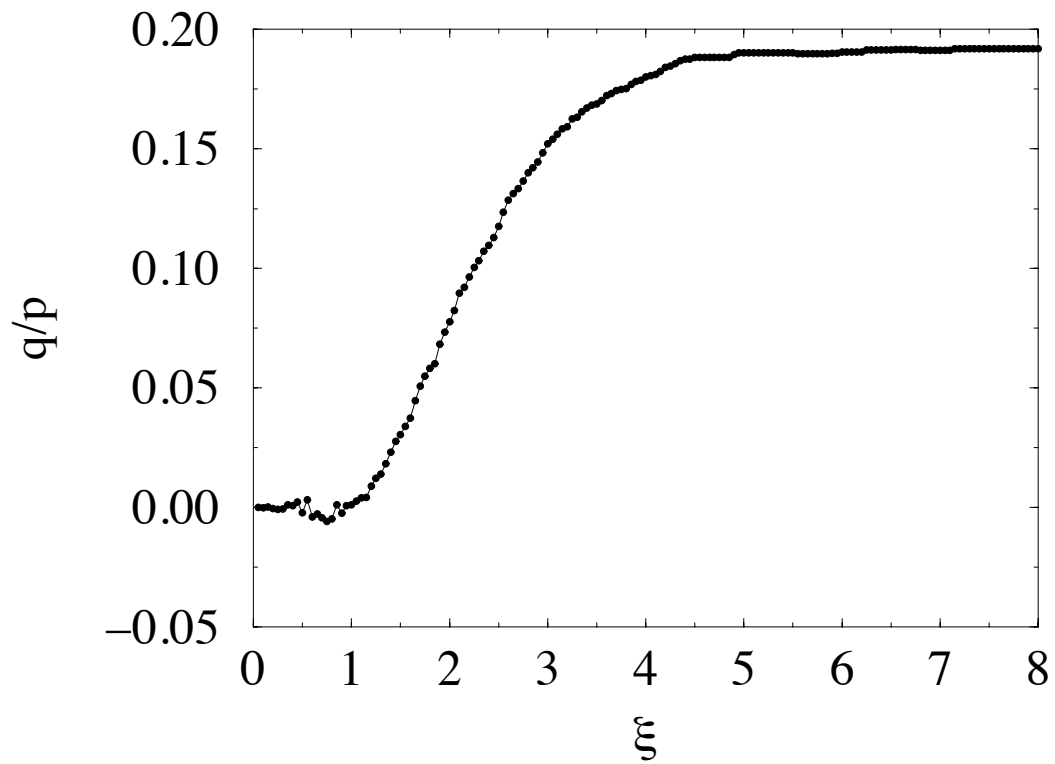


# Bimodal nature of force networks

The expression of the stress tensor can be used to evaluate the shear stress sustained by contact sub-networks. We consider the set of contacts carrying a force below a given threshold:

$$\mathcal{S}(\xi) \equiv \{f_n \mid f_n < \xi \langle f_n \rangle\}$$

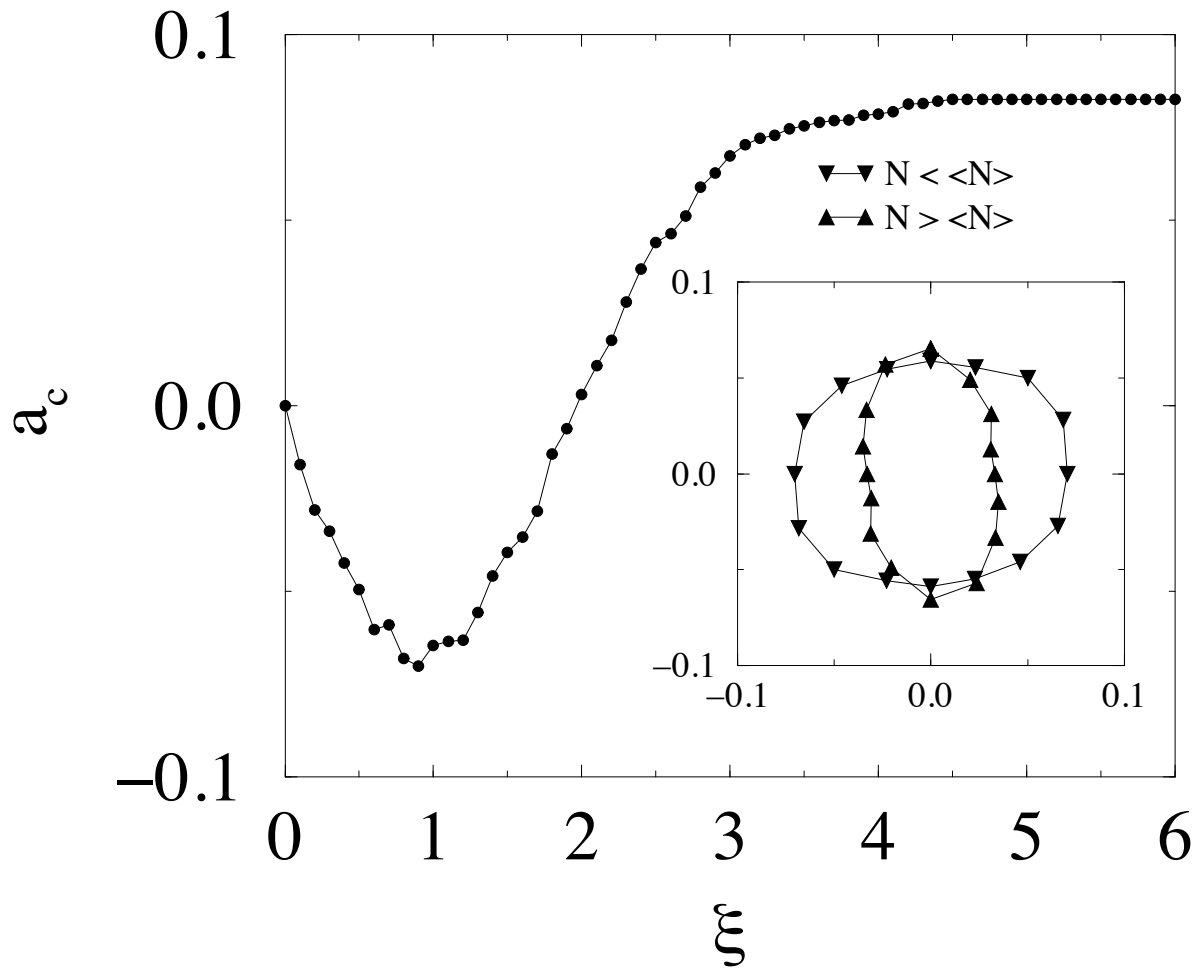
The fabric and force anisotropies can be evaluated for the same sub-networks.



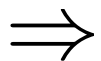
$$\boldsymbol{\sigma} = p_w \mathbf{I} + \boldsymbol{\sigma}_s$$

The shear stress is sustained by the strong force network.

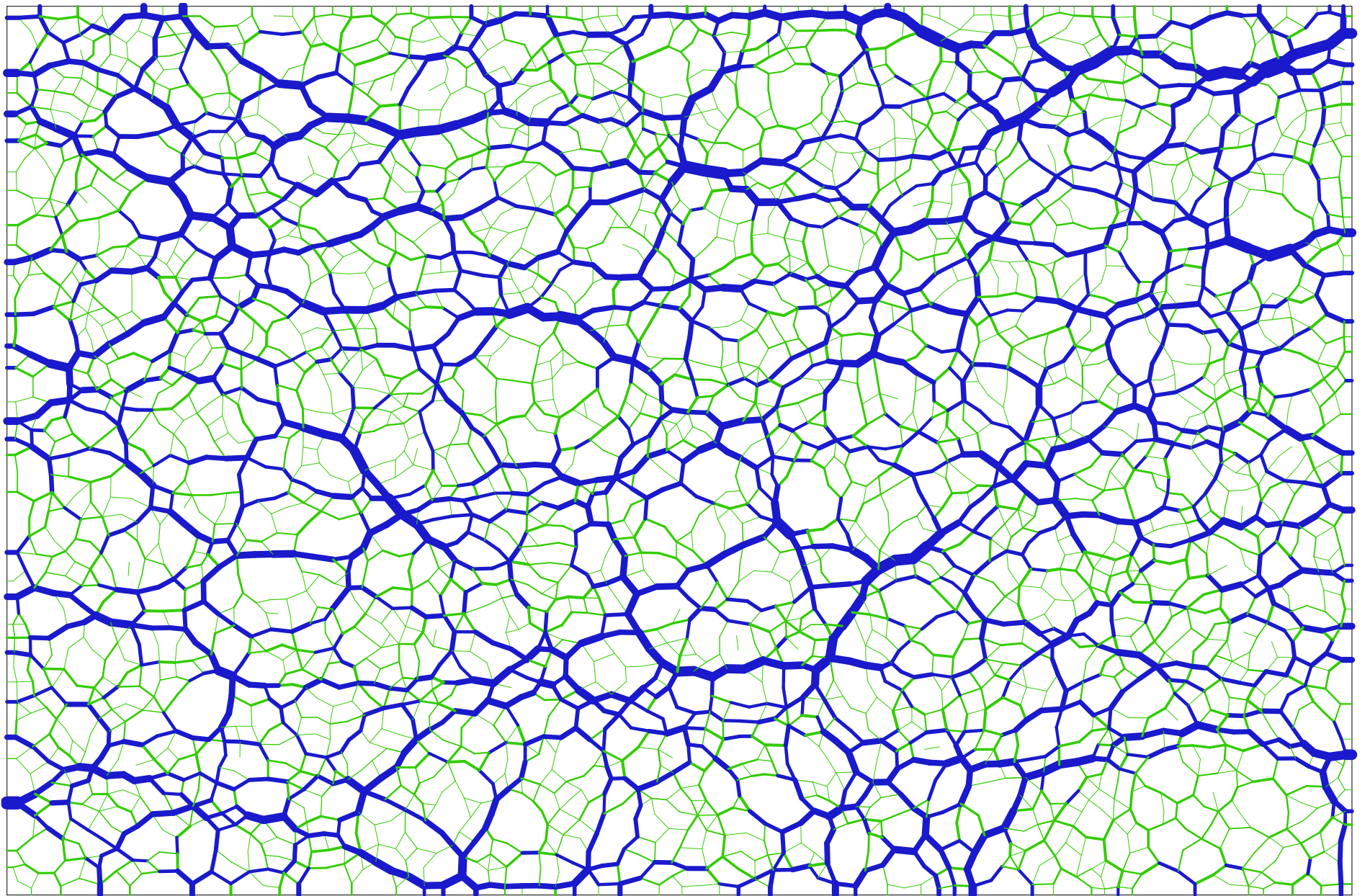
# Fabric anisotropy of contact sub-networks:



Weak contacts tend to be along the minor principal stress direction.



**Tensorial arching effect:** sequences of strong force chains are balanced by side-wise weak forces.



The critical contacts (where friction is fully mobilized) belong essentially to the weak network.

